

ISSN 0236-2945

LIGHT & ENGINEERING

Volume 24, Number 4, 2016

LLC “Editorial of Journal “Light Technik”, Moscow




*Dear Colleagues,
Authors and Co-authors!
Dear Friends!*

*We wish you a Year
that is filled with all the
Fragrance of Roses,
Illuminated with all the LIGHTS
of the world and be blessed with
all the Smiles on the Planet.*

*We wish you all the best,
great work to reach your fondest goals,
and when you're done, sweet rest.
We hope this year will be the year
when all your dreams come true!*

*Warmest wishes for a
Happy holiday season
and a wonderful New Year!
Happy New Year 2017!*



LIGHT & ENGINEERING

(Svetotekhnika)

Editor-in-Chief: **Julian B. Aizenberg**, Dr. of Sc., Prof., Academician of AESc.RF

Deputy Chief Editor: **Raisa I. Stolyarevskaya**, Dr. of Sc., LLC "Editorial of Journal "Light Technik"

Editorial Board Chairman: **George V. Boos**, Ph.D., Moscow Power University

Editorial Board:

Sergey G. Ashurkov, Ph.D., LLC "Editorial of Journal "Light Technik"

Vladimir P. Budak, Dr. of Sc., Prof. Moscow Power University

Vladislav E. Bugrov, Dr., Prof., ITMO University rector, S. – Petersburg

Natalya V. Bystryantseva, Ph.D., ITMO University, S. – Petersburg

Alexei A. Korobko, Ph.D., BL Group, Moscow

Alexander T. Ovcharov, Dr. of Sc., Prof., Tomsk State Arch. – Building University, Tomsk

Leonid B. Prikupets, Ph.D., VNISI named by S.I. Vavilov, Moscow

Vladimir M. Pyatigorsky, Ph.D., VNISI named by S.I. Vavilov, Moscow

Anna G. Shakhparunyants, Ph.D., General Director of VNISI named by S.I. Vavilov, Moscow

Nikolay I. Shchepetkov, Dr. of Arch., prof. of SA MARchi, Moscow

Alexei K. Solovyov, Dr. of Sc., Prof., State Building University, Moscow

Konstantin A. Tomsky, Dr. of Sc., Prof., St.-Petersburg State University of Film and Television

Leonid P. Varfolomeev, Ph.D., Moscow

Pavel P. Zak, Dr. of Biol. Sc., Prof., Emanuel Institute of Biochemical Physics of Russian Academy of Science (IBCP RAS)

International Editorial Advisory Board:

Lou Bedocs, Thorn Lighting Limited, United Kingdom

Wout van Bommel, Philips Lighting, the Netherlands

Peter R. Boyce, Lighting Research Center, the USA

Lars Bylund, Bergen's School of Architecture, Norway

Stanislav Darula, Academy Institute of Construction and Architecture, Bratislava, Slovakia

Peter Dehoff, Zumtobel Lighting, Dornbirn, Austria

Marc Fontoynt, Ecole Nationale des Travaux Publics de l'Etat (ENTPE), France

Franz Hengstberger, National Metrology Institute of South Africa

Warren G. Julian, University of Sydney, Australia

Zeya Krasko, OSRAM Sylvania, USA

Evan Mills, Lawrence Berkeley Laboratory, the USA

Lucia R. Ronchi, Higher School of Specialization for Optics, University of Florence, Italy

Nicolay Vassilev, Sofia Technical University, Bulgaria

Jennifer Veitch, National Research Council of Canada



Moscow, 2016

Editorial Office:

VNISI, Rooms 327 and 334
106 Prospekt Mira, Moscow 129626,
Russia
Tel: +7.495.682.26.54
Tel./Fax: +7.495.682.58.46
E-mail: lights-nr@inbox.ru
<http://www.sveto-tehnika.ru>

Scientific Editors:
Sergey G. Ashurkov
Evgeny I. Rozovsky
Raisa I. Stolyarevskaya
Style Editor
Marsha Vinogradova
Art and CAD Editor
Andrei M. Bogdanov

Light & Engineering" is an international scientific Journal subscribed to by readers in many different countries. It is the English edition of the journal "Svetotekhnika" the oldest scientific publication in Russia, established in 1932.

Establishing the English edition "Light and Engineering" in 1993 allowed Russian illumination science to be presented the colleagues abroad. It attracted the attention of experts and a new generation of scientists from different countries to Russian domestic achievements in light and engineering science. It also introduced the results of international research and their industrial application on the Russian lighting market.

The scope of our publication is to present the most current results of fundamental research in the field of illumination science. This includes theoretical bases of light

source development, physiological optics, lighting technology, photometry, colorimetry, radiometry and metrology, visual perception, health and hazard, energy efficiency, semiconductor sources of light and many others related directions. The journal also aims to cover the application illumination science in technology of light sources, lighting devices, lighting installations, control systems, standards, lighting art and design, and so on.

"Light & Engineering" is well known by its brand and design in the field of light and illumination. Each annual volume has four issues, with about 80–140 pages per issue. Each paper is reviewed by recognized world experts.

To promote the work of the Journal, the editorial staff is in active communication with Thomson Scientific (Citation index) and other international publishing houses and agencies, such as Elsevier and EBSCO Publishing.

CONTENTS

VOLUME 24

NUMBER 4

2016

LIGHT & ENGINEERING

Julian B. Aizenberg, Gennadiy B. Bukhman, Alexei A. Korobko, and Vladimir M. Pyatigorskiy Several not embodied concepts of optical schemes and lighting systems with hollow light guides	4
Nicolai I. Shchepetkov Topical Light Design for Classical Architecture	14
Roger Narboni From Light Urbanism to Nocturnal Urbanism	19
Elena V. Barchugova and Nataliya A. Rochegova Video Mapping from Presentation to Architecture	25
Vladimir P. Budak and Tatyana V. Meshkova Models of Visual Discomfort from Sources of Glare	31
Egor E. Nilov and Vitaly N. Stepanov Illumination Design: Problems of Translation and Criteria of Evaluation	38
Giovanni Ciampi, Antonio Rosato, Michelangelo Scorpio, and Sergio Sibilio Basic System for the Preliminary Experimental Photometric Characterization of a LED Based Luminaire	47
Burcu Büyükkınacı, Sermin Onaygil, Önder Güler, and M. Berker Yurtseven Comparison of Road Lighting Calculations with Measurements Using Conventional and Camera Luminance Meters	56
Aysel Ersoy Yilmaz Artificial Neural Network Modeling of Colour Temperature Variations with Different Types of Armatures and Light Sources	64
Nikolai N. Bespalov, Sergei S. Kapitonov, and Anastasiya V. Kapitonova Research of Processes in the LEDs Luminaire in Case of the Voltage Temperature Coefficient of Separate LEDs Variation	72
K. Furkan Sökmen, Nurettin Yamankaradeniz, and Salih Coşkun Investigation of Heat Transfer Types in an Automobile Fog Lamp with Computational Fluid Dynamic Analysis	76
Lev M. Kogan, Alexander N. Kolesnikov, and Andrei N. Turkin New Powerful Ultra-Violet and Violet Emmiting Diodes	87
Andrzej Pawlak Comparison of Results of Computer Simulations for the Escape Route Lighting Installation	91
Vladimir N. Kuzmin and Sergei E. Nikolaev Methods and Devices for Quick Evaluation of Optical Radiation Energy Efficiency under Photoculture Conditions	99
Sergei A. Golubin, Alexei N. Lomanov, Vladimir S. Nikitin, Valery M. Komarov, and Ernst I. Semenov Experimental Study of How Lighting Patterns Affect Optical Ministicks Characteristics	105
Sergei A. Golubin, Alexei N. Lomanov, Vladimir S. Nikitin, Valery M. Komarov, and Ernst I. Semenov Study of Characteristics of VCSEL-based Optical Ministicks	111
Contents 2016	
#1	117
#2	118
#3	119

Founder of Light & Engineering Journal Julian Aizenberg at 85!



Doctor of Technical Science, Professor Julian Aizenberg is well known in Russia and around the world as a lighting scientist and engineer; a lighting industry leader; an inventor and developer of lighting devices and systems; an author and editor of multiple books and pamphlets; a lighting knowledge leader and communicator; and, a respected educator and public figure. The shortest list of his major achievements:

- 62 years of continuous work at VNISI of S.I. Vavilov;
- 47 years as Editor-in-Chief of Svetotekhnika Journal;
- Founder of Moscow "Light House" and leader of its activities over 20 years;
- Developer (together with Gennadiy Bukhman) of the new field of lighting engineering – light transportation and redistribution in space by means of hollow light guides: their development, research, manufacture, and application in a wide range of illumination projects, as well as securing their protection via patents in several leading world countries;
- Publication of the monograph "Bases of Designing of Light Devices";
- Preparation and release of three editions of "The handbook on lighting engineering";
- Management of development of about 40 series of luminaires for industry and public buildings and their implementation for mass production, amounting to over 110 million pieces.

The Journal's editorial team and board would like to express their warmest wishes and regards to Julian Aizenberg on the occasion of his 85th birthday, wishing him health and all the best for the future.

SEVERAL NOT EMBODIED CONCEPTS OF OPTICAL SCHEMES AND LIGHTING SYSTEMS WITH HOLLOW LIGHT GUIDES

Julian B. Aizenberg, Gennadiy B. Bukhman, Aleksei A. Korobko,
and Vladimir M. Pyatigorskiy

VNISI by S.I. Vavilov
E-mail: lights-nr@inbox.ru

ABSTRACT

Options of use of hollow light guides for illumination of various objects are given in article: arch inflatable constructions, buildings, pools, tunnels, mines of elevators, rooms with eaves, and also a number of constructive decisions with hollow light guides.

Keywords: light guide, hollow light guide, slot-hole light guide, integrated system of lighting

1. INTRODUCTION

Beforehand, it should be noted that everything presented in this chapter belongs to the creative team including the author, G.B. Bukhman, Koro-

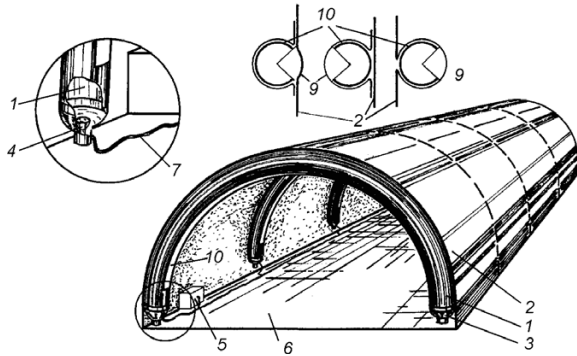


Fig. 1. Arched cylindrical inflated light guide: 1 – slit light guide; 2 – construction shell; 3 – input device; 4 – light source; 5 – electrical unit; 6 – illuminated surface; 10 – optical slit; 12 – reflecting layer

bro, and V.M. Pyatigorskiy. The most part of design concepts is patented in Russia and several Western Europe countries. Some of the given below systems are based on lighting calculations that proved their efficiency.

Unfortunately, the changing economical conditions in Russia had prevented us from accomplishing the work. Our team had broken, and its members had switched to other tasks in other companies. Nevertheless, the ideas, which were being generated and discussed, are still actual and they may be supported by other devotees who will continue to develop this interesting and promising branch of lighting engineering.

2. ARCHED INFLATED LIGHT GUIDES

Recently, the inflated structures have come into wide use in constructions of sports halls, industrial workshops, stores, field hospitals, etc.. The elastic shell of inflated building retains its shape due to overpressure inside. The in door illumination of such constructions is a real problem, since it is not easy and safe to attach wires to and suspend luminaires inside the shell. In this case, it is possible to employ arched inflated slit light guides (integrated into a shell) as load bearing and shaping structures [1]. The system has the following advantages: the light guides act as load carrying structure of the construction; the electrical wires do not run in the shell (they can be put in the ground); the input devices are located below, hence the maintenance and relamping can be easily done. The light guide may be a part of the shell.

Figs.1 and 2 show the examples of constructions with cylindrical and semi spherical shapes: 1 – light

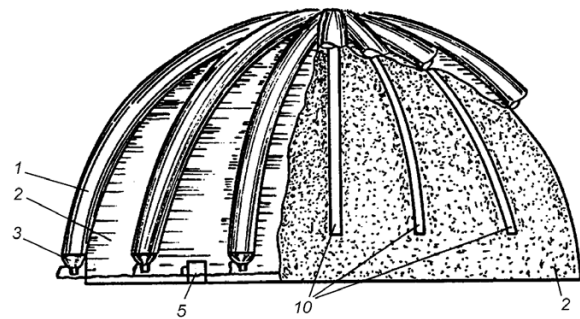


Fig. 2. Semispherical construction with arched inflated light guides

guide, 2 – shell, 3 – input device, 4 – lamp, 5 – ballast, 6 – floor (ground), 7 – cable, 9 – optical slit, 10 – light guide reflector. When using light guides, it is not necessary to make a transfer sluice with compressor in order to provide over pressure in the whole volume.

3. AIR DISTRIBUTING LIGHT GUIDE

Since essentially a HLG is a tube of appreciable diameter (up to 1 m), it can be used as well for conveying purified air, i.e. it may operate both as

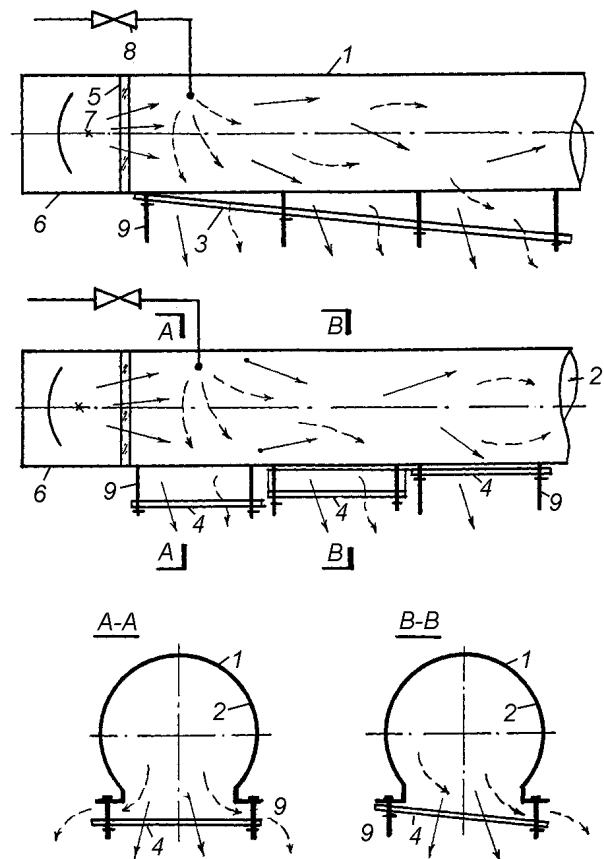


Fig.3. Air distributing light guide

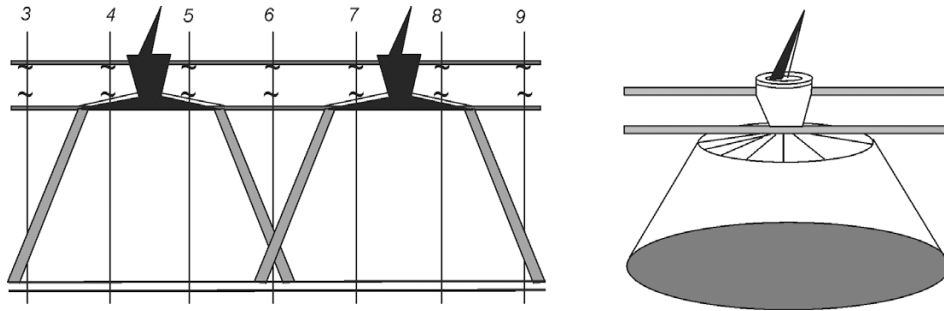


Fig. 4. Integral lighting system for high one storey building

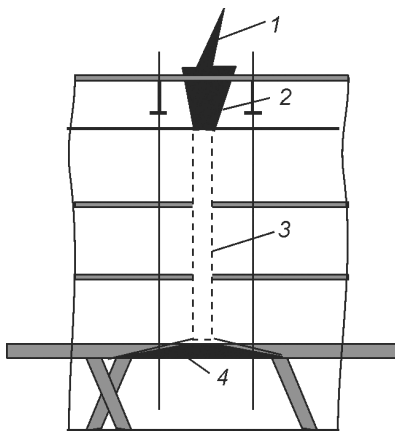


Fig.5. Integral lighting system for underground spaces

a light guide and an air conduit. Experimental installation was made in a factory near Moscow. The applications of the combined engineering system can be very interesting and promising. The system comprises the following parts, Fig.3: 1 – envelope of rigid slit light guide, 2 – light guide, 3 – optical slit, 4 – part of optical slit with adjustable gap to direct air jet, 5 – transparent protective glass, 6 – input device housing, 7 – light source, 8 – air purifier, 9 – screws for adjusting position of optical slit.

4. INJECTION OF DAYLIGHT INTO A BUILDING

Three integral systems are suggested below for the following objects: high one storey building, underground spaces, and deep open spaces in a building with perimeter glazing. The following requirements shall be met:

- The most simple sealed heliostat shall be used;
- The unified units shall be used for transportation and distribution of solar and electrical light;
- The number of “nodes”, where optical transformation of light takes place, shall be reduced to minimum;

- The electrical parts and the units that require maintenance shall be taken out of the room;
- The heat dissipated by Sun or electrical lamps shall be eliminated;
- The openings, where light enters room, shall be reduced to minimum.

Figs.4 and 5 show the optical schemes of the suggested systems. Fig.4 gives the integral system for a high one storey building. The system comprises heliostats, transitional units (with light sources) passing through the walls, and HLGs with distributing devices having shapes of luminous disks, rectangles, or bands (see bottom view). The calculations prove that in a 8–10 m high building located in the Central Europe the system is able to provide the illuminance level of 300–400 lx on the area of 150–250 m², depending on the heliostat size and the number of light sources.

To illuminate underground rooms, the system shall be completed with a vertical light guide with definite height and diameter (see Fig. 5, dotted line).

Fig.6 exposes the lighting system designed to illuminate the open space rooms, where the back walls are located at 10–20 m distance from the windows. The calculations show that the HLG system provides the illuminance level of 300 lx in the 17 m deep office with low height [2].

5. SWIMMING POOL LIGHTING

In conventional practice the luminaires are arranged above the bath and sometimes the lighting system comprises under water fixtures recessed into the side walls of a bath to illuminate water from inside. The maintenance of luminaires is difficult. In order to reach a luminaire to replace a lamp, one has to pour off water from the pool. The design of sealed water proof fixtures for underwater lighting is complicated as well.

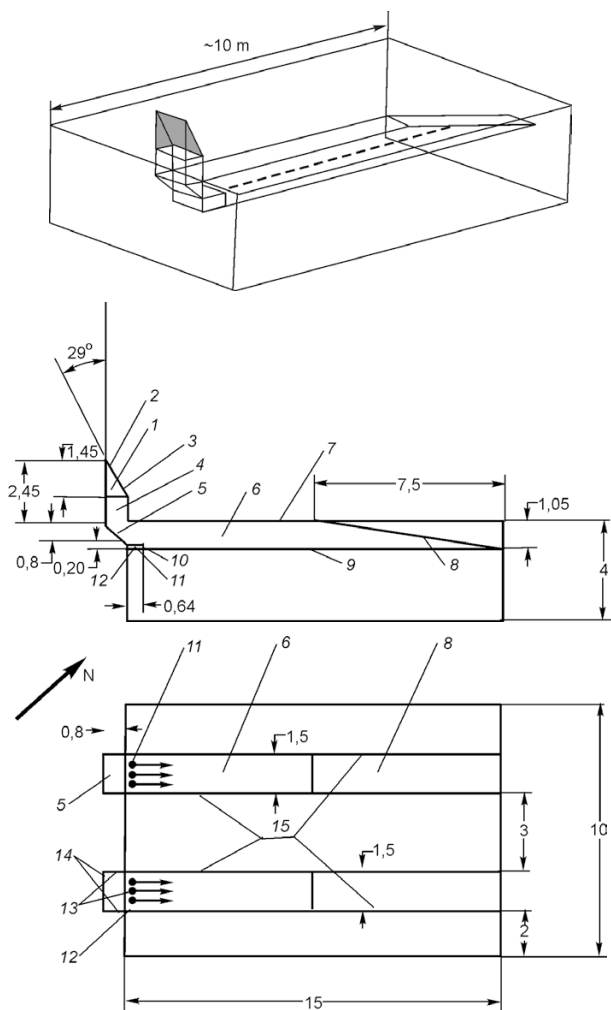


Fig. 6. Integral lighting system for open space rooms (with back walls located at 10 m distance from windows). All dimensions in m

We suggest a lighting system which is capable to do the following:

- A dynamic colour changing of under water illumination;
- An easy maintenance of lighting fixtures;
- A new look of swimming pool lighting system.

The input devices 3 and 4 (Figs.7, 8) may be located behind the end walls of a bath, in adjacent rooms 8, or in the start pedestals 9. In the latter case, the angle connecting light guides 10 are used. The light colour may be constant or variable. It may be provided by using either control system, or colour lamps, or color light guide envelope, or colour glasses in side wall niches, or colour filters 11 between input devices and light guide entrances. The light injected into opposite sides of a light guide may have different colours as well. In some cases, the inner volume of a light guide may be filled with transparent liquid, e.g. the water.

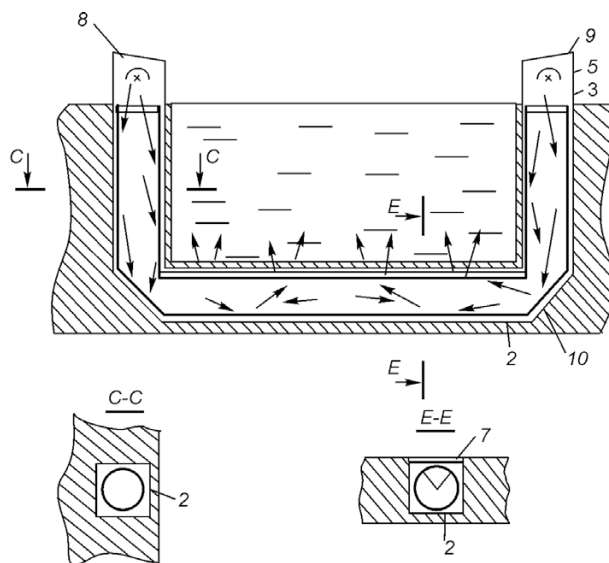


Fig.7. Under water illumination in swimming pool: 1 – niche in a bath wall; 2 – slit light guide; 3 – cavity for input device; 4 – input device; 5 – reflector; 6, 7 – protective glasses; 8, 9 – start pedestals; 10 – angle mirror

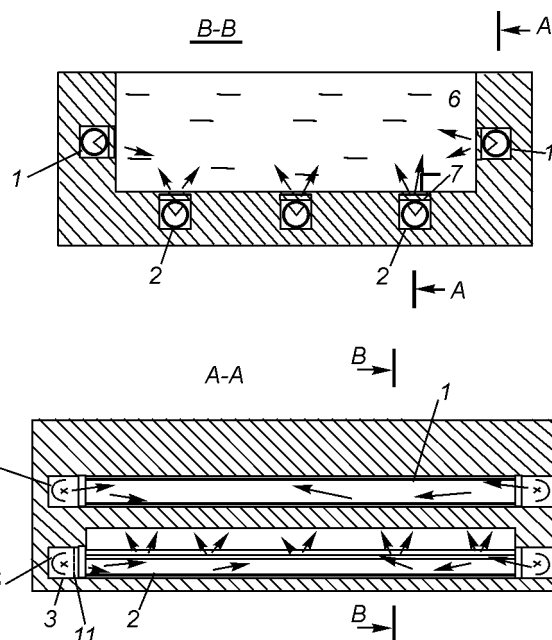


Fig.8. Under water illumination in swimming pool

6. TUNNEL LIGHTING

The lighting system may comprise wedge shape HLGs that form luminous arches across the tunnel (Figs. 9, 10). Prismatic film may be used

Fig. 9. Arch light guide for escalator tunnels cover the inner surface of a light guide. The application of the system for illumination of the escalator tunnel is illustrated in Figs.10, 11.

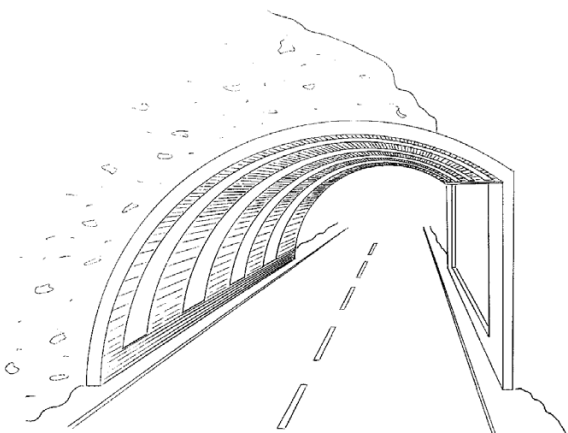


Fig. 10. Arch HLG open tunnel

7. LIGHTING SYSTEM FOR SLOPING ESCALATOR TUNNEL IN THE METRO

The cylindrical HLGs may be mounted above the escalator spacing bars and form continuous luminous lines having the same inclination angle as the sloping tunnel itself. The lines, as well as input devices, rest on vertical sup ports fixed on spacing bars. The supports shall have a sufficient height to provide uniform illumination of escalator stairways. The supports may be constructed as hollow light guides as well with light sources located at the support bases (Figs.12, 13).

8. ILLUMINATION OF A LIFT SHAFT

The task is to create a dynamic lighting which is related to the movement of lift cabin (Fig.14). The lift cabin acts as a light plunger. When the

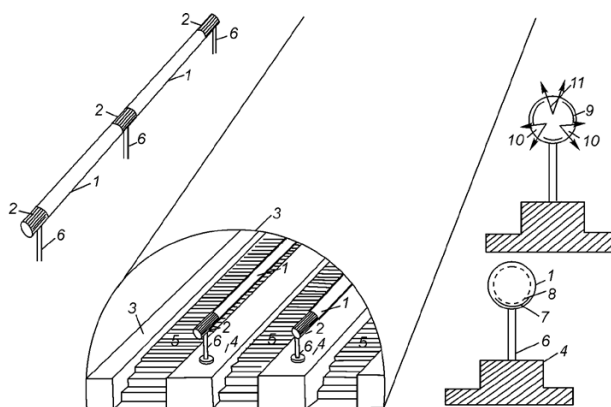


Fig. 12. Lighting system of sloping escalator tunnel: 1 – hollow light guide; 2 – input devices; 3,4 – escalator sides; 5 – escalator step; 6 – light guide support; 7 – light diffusing envelope of light guide; 8 – SOLF film; 9 – inner reflectors; 10 – side exit openings; 11 – upper exit opening

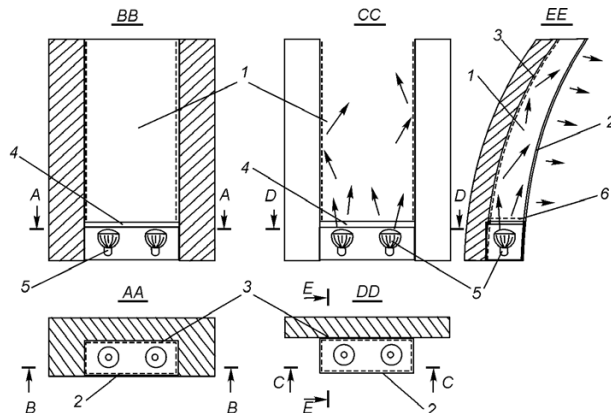


Fig. 11. Design of HLG for tunnel: 1 – hollow light guide; 2 – light diffusing glass; 3 – reflecting surface with high reflectance factor (0.98); 4 – transparent glass isolating input device; 5 – reflector metal halide lamps providing narrow light beam; 6 – colour filter

cabin is approaching some part of light transmitting wall of a shaft, the luminance of the latter is increasing. And vice versa, when the cabin is moving away from the surface, the luminance of the latter is reducing. Being at the lift hall or at the stairs, an observer gets information whether the lift cabin is approaching or moving away.

To enhance lighting effect, one can use different colours for radiation at the upper and lower sections of a shaft. For this purpose, the light sources with different spectrums or colour filters mounted at exit apertures of luminaires can be used. For example, if red radiation is taken for the upper shaft part, and green – for the lower, then the shaft space above the lift cabin, and consequently, the corresponding lift hall and stairs will be illuminated in red, while halls and stairs below the cabin – in green. When the cabin passes an arbitrary floor, e.g. moving downward, the lift hall at this floor will be illuminated by increasing green light when the

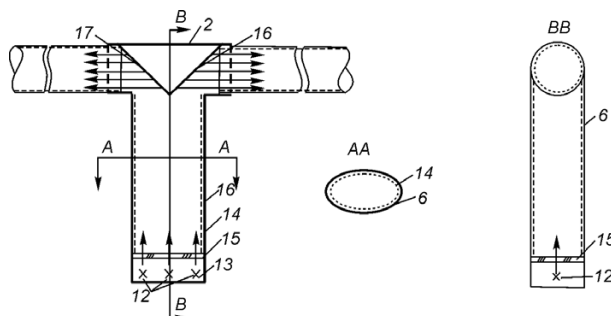


Fig. 13. Light carrying support for light guides: 12 – light sources; 13 – lamp for emergency lighting; 14 – end lighting light guide (metal support); 15 – protective glass, 16 – SOLF film; 17 – light distributing mirror

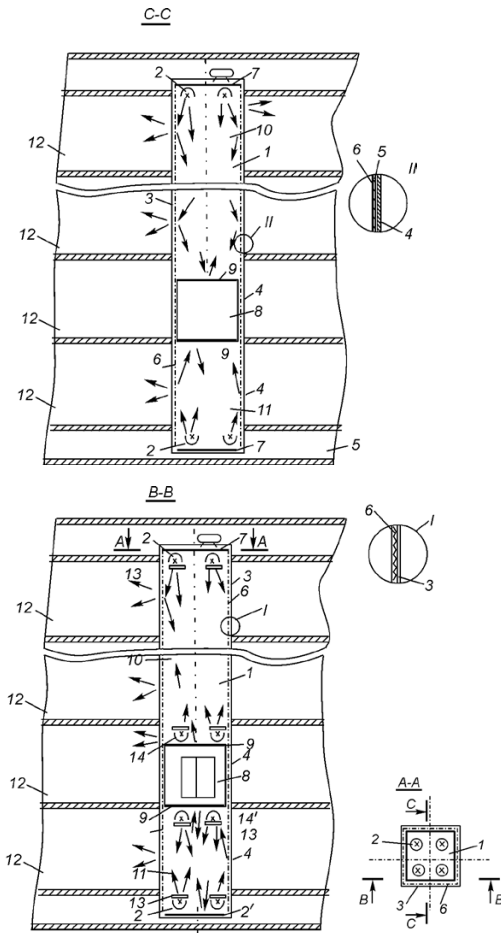


Fig. 14. Decorative illuminatin in a lift shaft: 1 – lift shaft; 2 – luminaires with narrow light beams; 3 – protective grid; 4 – transparent acrylic glass; 5 – cellar; 6 – SOLF film; 7 – mirror; 8 – lift cabin; 9 – mirror; 10 and 11 – upper and lower parts of lift shaft; 12 – floors of stairwell. The same designations: 13 – colour filters

cabin was approaching, and by fainting red after the cabin has gone.

To increase the intensity of light in the shaft, additional light sources should be mounted over and under the lift cabin. In this case, when colour effects are applied, the light sources in every shaft section should have similar colour spectrums.

9. INJECTION OF “COOL” LIGHT INTO A LIGHT GUIDE AND UTILIZATION OF HEAT

To inject a “cool” light into a flat light guide and utilize a heat generated by high power light sources, the system shown in Fig.15 is proposed. The system comprises the following parts: specular reflector 4 having the shape of elliptical cylinder [8.3]; the linear gas discharge lamps 3 are located along the first

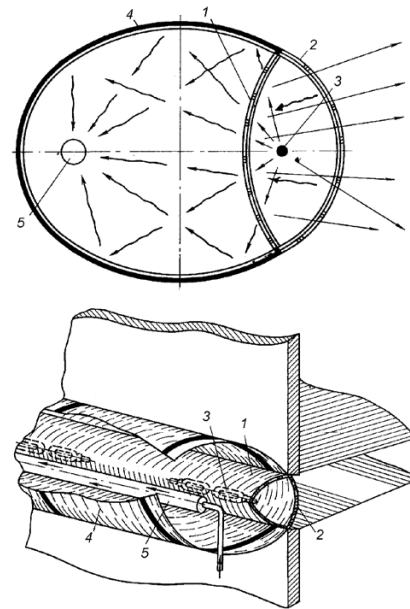


Fig. 15. Input device for injection of “cool” light into light guide and utilization of heat

focal line of the reflector; the heat exchanger 5 is located along the second focal line; the exit domelike opening 2 is covered by the glass with multi layer interference coating which transmits the “cool” light and reflects the IR radiation back; the glass partition 1 with multi layer interference coating that transmits the IR radiation reflected by the dome 2 from outside and “cool” light from inside. Thus, the IR radiation generated by lamps is concentrated along the second focal line and heat the pipe with running water. Only UV and visible radiation enter the light guide and illuminate the space [3].

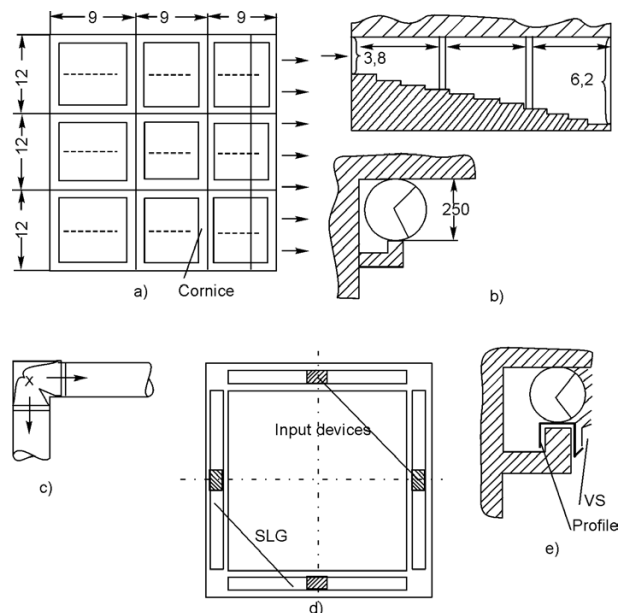


Fig. 8. 16. Cornice lighting with HLG

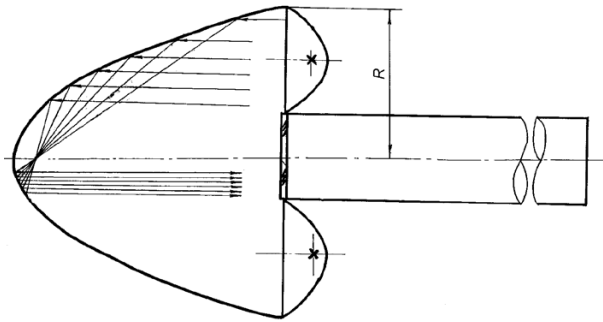


Fig. 17. Optical scheme for injecting luminous flux of several light sources into light guide with relatively small diameter (with deep parabolic reflector)

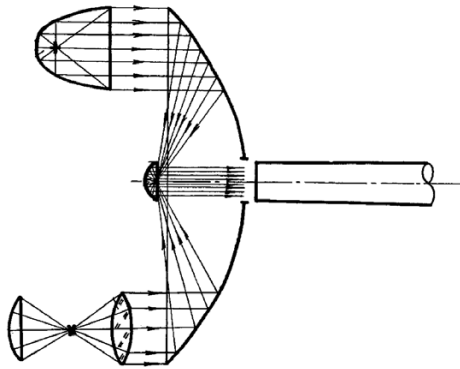


Fig. 18. Optical scheme for injecting luminous flux of several light sources into light guide with relatively small diameter (with shallow parabolic reflector)

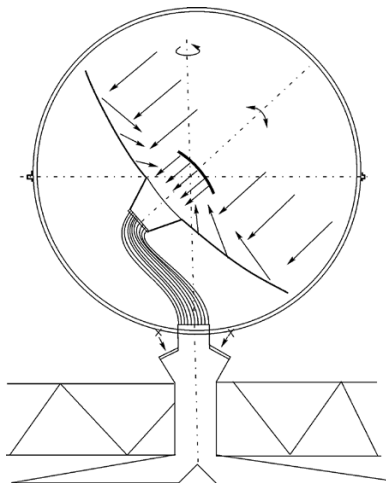


Fig. 19. Heliostat with Cassegrain optical systems (version 1)

10. CORNICE LIGHTING

Application of HLGs enables to change the conventional cornice lighting. Instead of recessing numerous fluorescent lamps into a cornice, thus spoiling the appearance of the system (different colour hues, dark spots at the joints of lamps), it is rea-

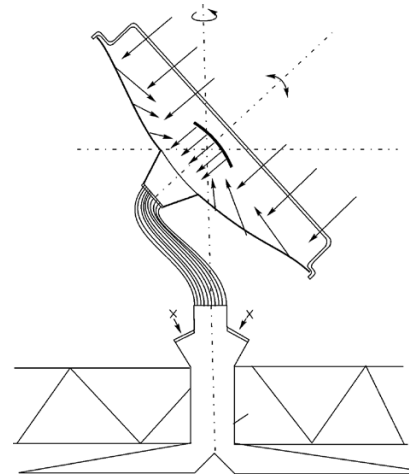


Fig. 20. Heliostat with Cassegrain optical systems (version 2)

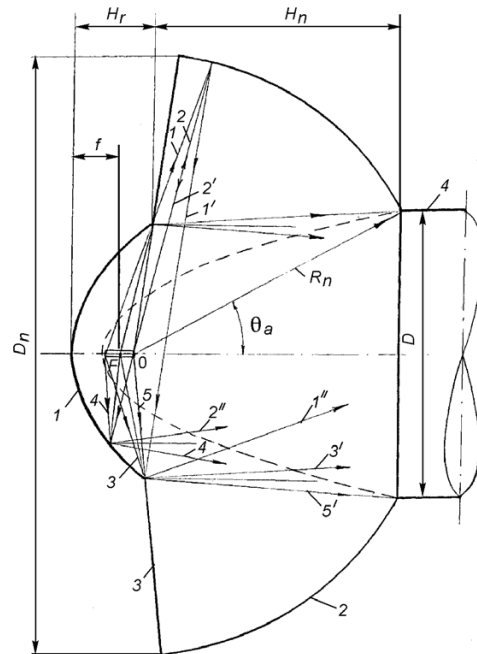


Fig. 21. Optical system with parabolic reflector and spherical attachment

sonable to use light guides, 6m or 12m long, with diameter of 250 mm. The light guide dimensions should correspond to the size of construction module. Fig.16 give two examples of input devices with different lamp powers.

11. USE OF MULTI LAMPS PROJECTOR IN AN INPUT DEVICE

It is very important to increase the volume of luminous flux injected into a light guide and keep the diameter of the latter as small as possible. Figs.17

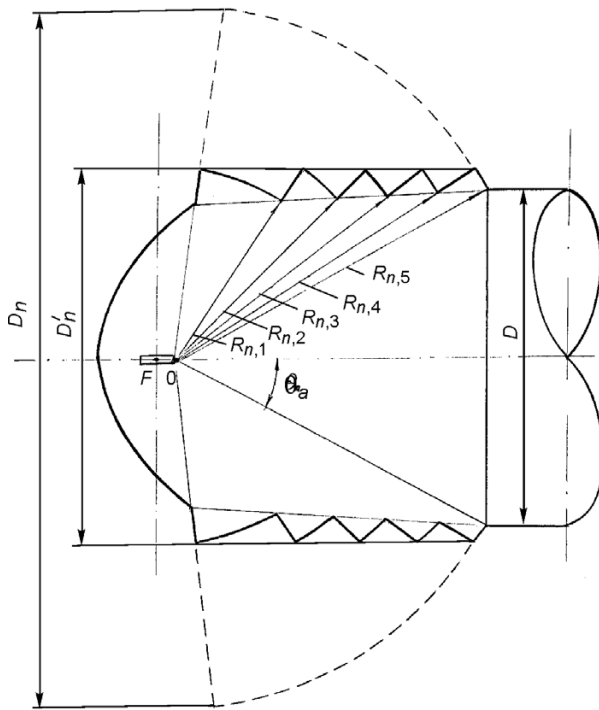


Fig.22. Optical system with parabolic reflector and attachment as a set of several spherical bands

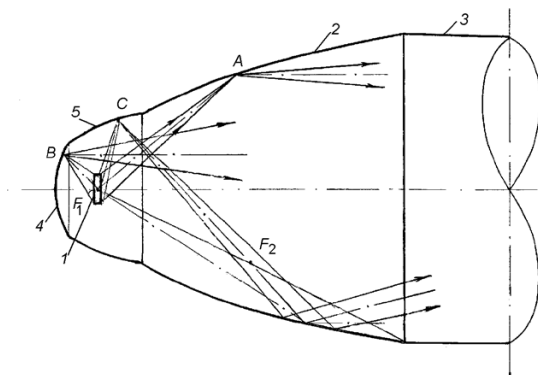


Fig.23. Ray paths in optical system with two parabolic reflectors and elliptical phocone the luminous flux utilization factor with respect to the entrance end 3 of a light guide. Besides, the input beam is well shaped

and 18 give examples of solving the problem. The concept is based on the use of large (with diameter much larger than the light guide), either deep (Fig.17) or shallow (Fig. 18) parabolic specular reflector that collects the light beams from several projectors and directs the accumulated luminous flux into the entrance aperture of a light guide. The deep parabolic reflector has short focal length, and the shallow reflector has long focal length. The optical scheme given in Fig. 8.18 is known by the name of Cassegrain with additional parabolic reflector 9 and central opening in the larger reflector.

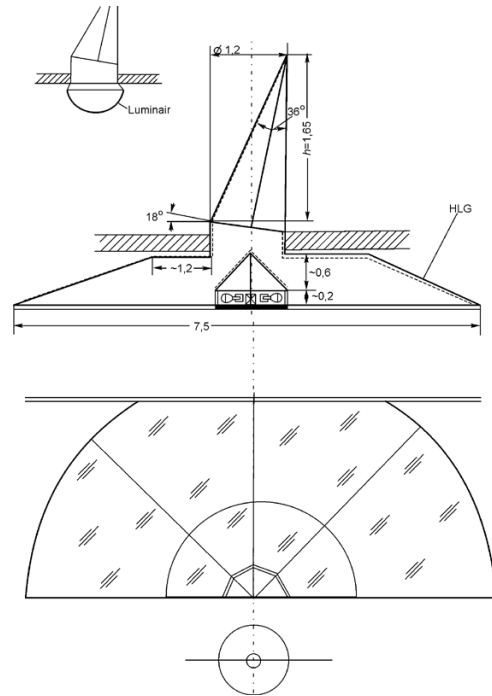


Fig.24. Heliostat system for department store

11. HELIOSTATS WITH CASSEGRAIN OPTICAL SYSTEMS

Figs.19 and 20 show the schemes for heliostats based on Cassegrain principle. The optical system comprises a large parabolic mirror 2, protective transparent envelope 1 having spherical or flat shape, secondary specular re flector 3, harness of fiber light guides 4, end lighting light guide 7, light sources 5 and input windows, flat light guide with a lower surface having a shape of luminous disk or two (or four) rectangles.

12. OPTICAL SYSTEMS WITH INCREASED UTILIZATION FACTOR OF LUMINOUS FLUX

Fig.21 shows an optical system comprising the following elements: 1 – specular parabolic of revolution, 2 –spherical specular surface, 3 – conical specular surface that links elements 1 and 2, 4 – end of a light guide with diameter D. The system enables to increase the acceptance angle, i.e. to capture more luminous flux from a light source. The surface 2 catches the flux that spreads outside the acceptance zone of reflector 1, and returns it back to the focal point coinciding with a light source [4]. These light rays then fall on the parabolic mirror 3, which focal point coincides with the focal point of the

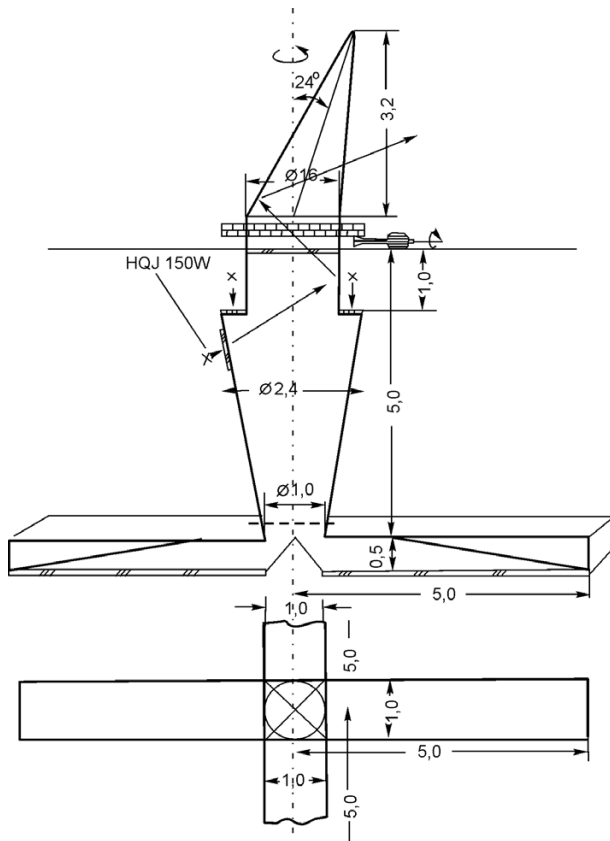


Fig.25. Heliostat system with rotation about vertical axis

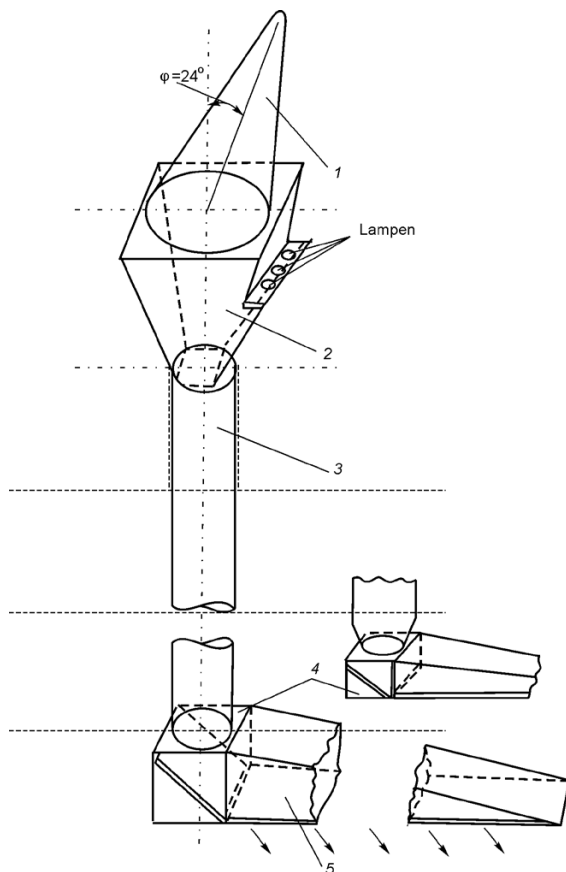


Fig.26. Heliostat system with horizontal flat HLG

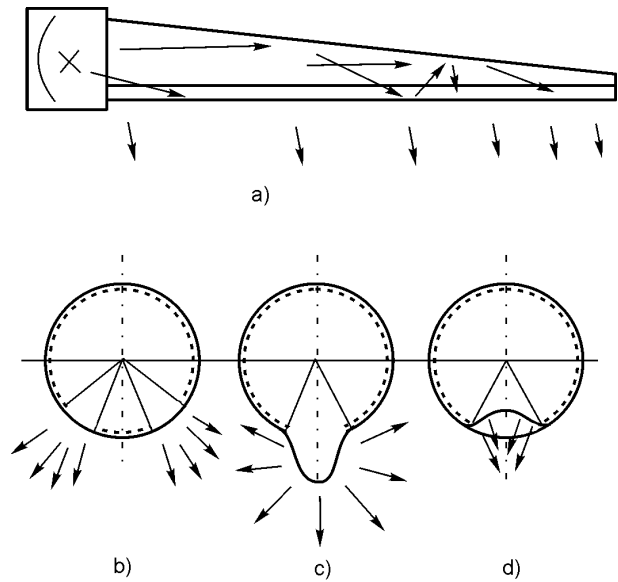


Fig.27. Decorative light guides

spherical surface. After second reflection from parabolic reflector, the total luminous flux is directed to the entrance of a light guide.

Fig.22 shows the similar scheme, where in order to decrease the dimensions, the spherical surface is replaced by the set of articulated spherical zones.

Fig.23 shows the optical scheme consisting of three specular reflectors: deep 2 and shallow 4 parabolic reflectors, and ellipsoid of revolution 5. The system, particularly with non spherical light sources, enables to increase

13. LIGHTING SYSTEM WITH HELIOSTAT AND FLAT WEDGE SHAPE HLG

Figs.24–26 show several options of lighting system with heliostats (both fixed or rotating about vertical axis) and flat wedge shape light guides.

The luminous surface of a light guide may have a shape of disk (Fig.24) or rectangle (Fig.25). The light from a heliostat passes through the end lighting light guide 3 with SOLF prismatic film and external reflector (Fig. 26). The system is designed to illuminate closed (or underground) spaces.

14. DECORATIVE LIGHT GUIDE

The exit opening of a flat light guide (a) may have different shapes and perform a decorative effect. It may differ by colour as well. Fig. 27 shows a flat wedge shape light guide with decorative slit:

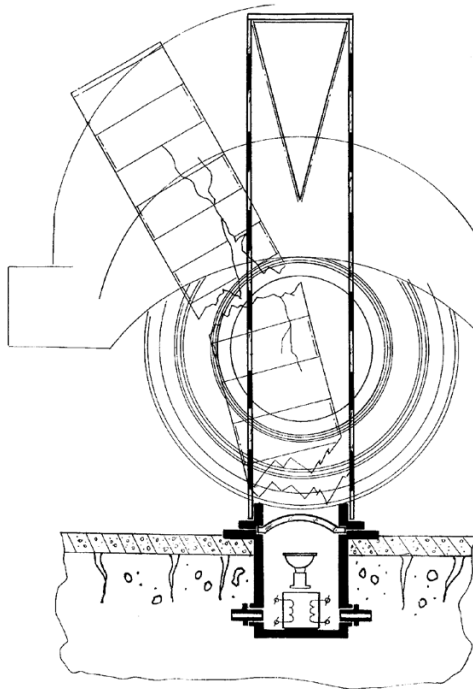


Fig.28. Optical scheme of luminous column

with two slits (b), with a nose like slit (c), and with a dent like slit (d).

15. ROAD COLUMN WITH “ZEBRA”

There are patents of luminous hollow cylindrical columns with “zebra”, which can be installed at pedestrian crossing (e.g. patent No. 3200599, BRD.). The main disadvantage of these systems is low vandal resistance, since it is easy to get access to the lamp. Besides, in case of emergency, a driver tries to avoid an accident and swings off the road and knocks down the column. In that case, the light source is broken down. The situation may be improved if we use hollow light guide (Fig.28).

REFERENCES

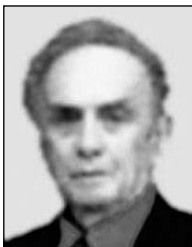
1. Aizenberg J.B., Bukhman G.B., Pyatigorskiy V.M., Solomatina N.M. Lighting installation for premises with pneumatic protecting constructions. US Patent 4.120.024, 1978
2. Aizenberg J.B. Integral lighting systems for rooms with insufficient daylighting. Light & Engineering, 2003, v. 11, № 3.
3. Patent USSR737693.
4. Patent USSR943474.



Julian B. Aizenberg,
Dr. of Tech. Sc., Prof.,
Academician of Energy
Academy of Science of RF,
Chief-Editor of Light &
Engineering (Svetotekhnika)
Journal at present



Aleksei A. Korobko,
Ph.D., graduated from MEPI
in 1971, leader scientist and
head of group of special soft
management in BL GROUP
Holding, member of editorial
board of Light & Engineering
Journal



Gennadiy B. Bukhman,
Ph.D., President
of “EKHOTECHSVET” in
Kiev, Ukraine



Vladimir M. Paytigorskiy,
Ph.D., graduate of MEPI, at
present, he is a chief designer
at VNISI of S.I. Vavilov,
Winner of the State Award

TOPICAL LIGHT DESIGN FOR CLASSICAL ARCHITECTURE

Nicolai I. Shchepetkov

MarkhI (SA), Moscow
E-mail: n_shchepetkov@inbox.ru

ABSTRACT

Modern light design of classical architecture in many cities in Russia and around the world invites the question: how far does the image created by artificial light at night time correspond to the daytime image of the monument? This article considers key methods of interpreting the image of classical, and other types of architectural objects using artificial illumination.

Keywords: classical architecture, light design, light image, authentic illumination, architectural tectonics, urbanistic context

Against the backdrop of tremendous and dazzling firework shows, which are so loved by the media and impressive video mappings projects in Russian cities, which often mark important occasions but also often “burn up” budgets tangible to local economies in the space of just a few minutes, a conversation about illumination of classical architecture can seem rather dull. After all, these architectural elements are always given more attention than, for example, constructivist or modernist architecture. But classical architecture has had the greatest weight in European culture since antiquity, by which all subsequent variations of classicism are guided. And this is essentially important. These monuments were conceived and created before a method of lighting them up at night was even invented. Their authors had no way of planning for an illumination interpretation of the building, which is now accomplished using electric light by very different people under very different circumstances. Therefore, finding a method to do this au-

thentically – or alternatively – is an important and current problem with theoretical, methodological, social and practical aspects.

Illuminating an architectural landmark of any style, scale or tectonics, follows one of two opposing principles: associative similarity to the daytime image or an alternative “counter image” (Fig. 1)¹. Numerous compromises between the two [1] are also possible. The first method, which dominated in Soviet light design and elsewhere until the 1980s with façade floodlighting, to a certain degree provided an imaginative association with solar illumination; in modern practice it is more and more seldom seen for various reasons. Most light designers use the second method, consciously or spontaneously, more or less successfully, and especially in light shows. With this method, there is no need to have knowledge of or analyse the tectonic and stylistic features of architectural landmarks. The designer can be freer and creative, less self-conscious, much closer to visual art. This is an attractive approach because taken on its own; the expressive potential of artificial light and colour is immense. The architecture serves simply as a screen, a canvas, though not ideal, on the surface of which a light artist implements his or her fantasies, and achieves an image, which is sometimes quite original but has nothing to do with the daytime traditional basic archetype.

If a compromise is attempted, certain key features of the landmark are highlighted, but as a whole, its light image is usually much fractured, spotty, and disproportionate in terms of its luminance and the hierarchy of its composite elements

¹ Figs. 1; 3 a; 4 a; 4 are pictures of the author.

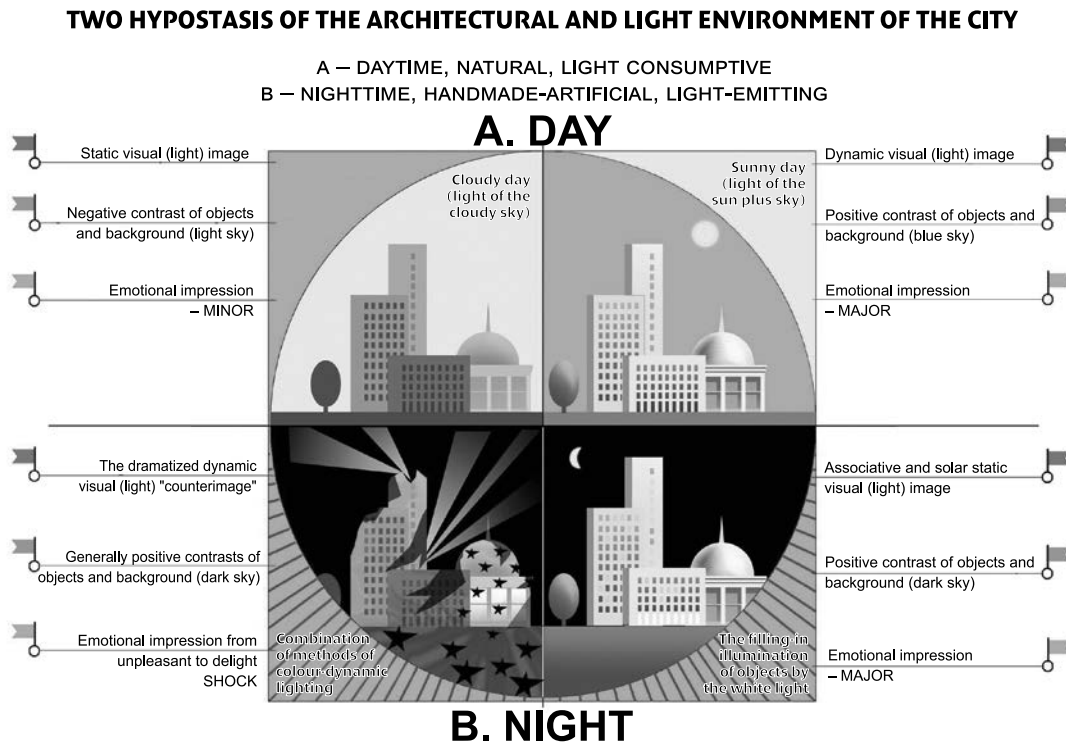


Fig. 1. Main archetypes of an architectural light image of landmarks in the daytime and their completely different interpretation under artificial illumination (an associative image and alternative “counter image”)

and features of the façade. The illuminated image usually does not match the building’s tectonic system, and can rarely be described as a work of art. Unfortunately, this approach prevails in today’s practice.

The above is only the first set of creative questions. The second is well described by Ludwig Mies Van der Rohe’s, one of the twentieth century’s greatest architects, famous aphorism – “God is in details”. Article [2] in particular talks about this, using examples of architecture of the Italian Renaissance. Light designers M. Selmo and F. de Rossi, who proved themselves as very creative professionals in the illumination of the ensemble of the Piazza dei Signori in Vicenza; they initially formulated a clear concept, which was later implemented. Their solution can be called a romantic interpretation of the first principle: an associative likening not to the solar, and to the moonlight image of the ensemble. This image was familiar during the time of Andrea Palladio, but formed under very different circumstances of a viewer’s visual adaptation to a city in darkness. Moonlight is similar to sunlight by its geometry and dynamics, but it completely different by its illumination intensity, spectrum and contrast. The lack of luminance contrasts typical for moonlight on the plastically

complex Basilica facades in Vicenza raises doubts about the cogency of the *Moonlight* conceptual version. With the implemented illumination, the facades have become visually flattened and “powdered”. Nevertheless, this example shows that like a theatrical stage, in a local fragment of a city environment, illumination can trigger certain emotions. This concept is one example to emulate, even though it can be criticized and alternative solutions proposed. That is an essence of any art form. It is a shame that the innovative and provocative practice from a century ago of issuing artistic manifestos full of creative ideas, has almost disappeared. There are not many formulated and disseminated ideologies in modern light design. An exception is perhaps R. Narboni – a thinker, writer and very fruitful designer. As a result, the implementation of illumination projects of classical architecture is rather patchy (Fig. 2); they require careful and committed comparative analysis to draw out trends, preferences and fashions.

The first consideration is the urban landscape context, without the analysis of which no architectural or light design solution can be made. A single lit landmark in a dark city can appear to be an eyesore, until it is joined by neighbouring illuminated buildings, forming a sort of light ensemble. To get



Fig. 2. Light architectonics of order architecture:

Negative (*a* – Stock exchange building in St Petersburg) and positive (*b* – Church of St. Magdalene in Paris) contrasts of the colonnade and a second tier wall. Entablature of the Stock exchange's periphery is visually ruined by the light strip on the frieze and cornice; Illumination of facades (*c* – Parthenon in Athenes, *d* – Victor Immanuel's Palace in Rome). The luminance contrast of the colonnade and a wall fails to provide an expressive spatially-tectonic effect

to this stage, a plan needs to be in place, defining a hierarchy of landmarks to illuminate, expressed by means of light characteristics. In developing such a plan, a competent light designer will determine a hierarchy not by scale and dimensions but by the respective historical and cultural value of landmarks. In this way, a small piece of classical architecture, hardly noticeable during the daytime, surrounded by larger, more visually dominant modern buildings, can become a local highlight in the night light ensemble due to a raised luminance, a special chromaticity, a contrast or dynamics of its illumination. In Moscow of the 1990s there were many examples of this practice. The small, two storeys classical house of the merchant Lobkov, an architecture landmark on the Sofiyskaya embankment, was illuminated in 1998, looked defiant until other illuminated facades appeared nearby. Today it can only be picked out from the riverside ensemble if you look for it specifically. Examples when such a highlight virtually disappears in a pointlessly glowing commercial environment are frequent. No subtly illuminated details of or porticos lit "positively" or "negatively" can help in this situation. The art of creating light ensembles is still in an embryonic state. Incidentally, the daytime situation of architectural ensembles also leaves much to be desired.

Leningrad, Paris and Washington had high-quality authentic illumination of classical landmarks during different periods of the twentieth century (Fig. 3). In the USA capital, neoclassical buildings, such as the White House, Lincoln and Jefferson memorials and the Capitol are filled with a solar-like white light. This light is traditionally and defiantly bright. It gives the buildings a flattened, stand out image, concealing important tectonic and plastic details [3]. Perhaps this solution is used based on urbanistic reasons: the landmarks are very visible in the night and contribute to views from a big distance. The Hôtel National des Invalides in Paris is intensively and cohesively "gilded" with the light of sodium lamps, which goes against the philosophy of Parisian experts from the 1990s, which aimed to illuminate architecture without distorting the "true" colours of its facades. According to these specialists, incandescent lamps were best for this purpose. The light view of University embankment in St Petersburg with its classical buildings, today and fifty years ago looks like cardboard stage scenery, due to the high positive contrast with the night environment. But still, it does look like a coherent single strip, as it does in the daytime, with an overall unifying effect sunlight, but with lesser contrasts. Under development is other unifying solution for

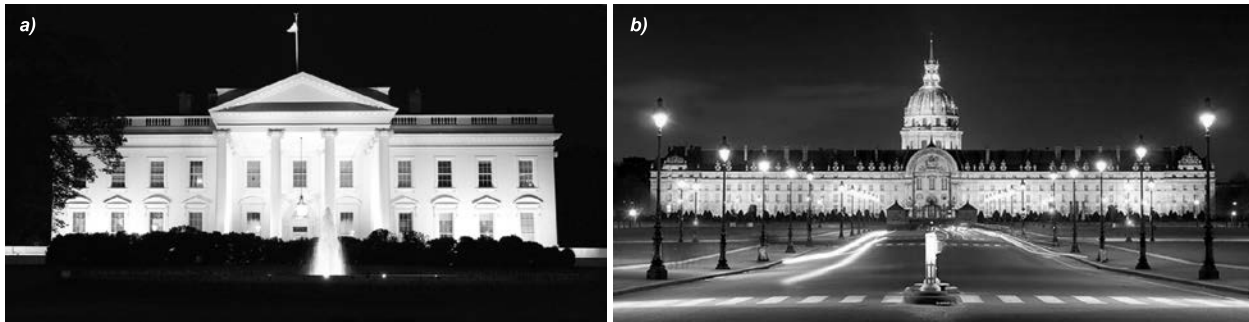


Fig. 3. A bathing architectural illumination effect using white light (*a* – the White House in Washington DC) and using colour light (*b* – Hôtel des Invalides in Paris)

the light view of the Dvortsovaya embankment. For now it remains visually fragmented and patchy because of the uncoordinated illumination of different building facades and landscape elements, as well as due to the flattening effect of bright light, for example on the comparatively over illuminated Senate and Synod buildings.

Selecting light methods, facilities and characteristics for classical landmarks based on the key architectural characteristic of tectonics, one is often forced to select a single tectonic system of a building over others, when several systems are working together. For example, the main facade of the Bolshoi theatre in Moscow combines two systems: order and wall. Today, the priority is given to second tier wall of the stage building with its bright crowning pediment: its average luminance in any light composition is higher than the foreground order portico (Fig. 4). Objectively, the hierarchy of architectonic systems in this building is inverted: the powerful eight-columned portico in the daytime, come rain or shine, plays a more important composition and image role than the background walls on each side and above it. And the portico order here is structurally truthful, unlike the decorative pilasters on the wall, though in other cases, a false order also can be illusory presented by light (as well as by colour, texture and plasticity in daytime illumination) like the real one, if the light designer so wishes. The insufficient luminance contrasts of the foreground columns and of the background wall of the theatre also reduces the visual activity of the portico, and the excessively illuminated pediment violates the integrity of the foreground. It is pleasing that, unlike the previous “light-strip” illumination, the entablature is kept monolithic. This situation of counterintuitive luminance composition could be easily avoided, if the illumination authors clearly understood the artistic problem when

calculating, designing and subsequently adjusting the light devices. A.G. Batova in her dissertation, has simulated a more convincing, tectonically hierarchical light image of the main facade of the Bolshoi [4] using Photoshop, in which the order visually dominates over the wall. In all fairness, one should say that as a whole the Bolshoi building is nevertheless one of the most successfully illuminated classical buildings in Moscow and is a good example for analysis of light compositions.

Discussing variations in illumination intensity visually estimated on luminance and contrast levels, on architectural element luminance distribution (uniform, spotty, gradient), as well as on nature of light and shade effects with white light, we have not touched upon other qualitative characteristics: illumination kinetics and chromaticity. For now, they remain beyond the scope of this discussion as they would strongly complicate it. However, in practice in Italy, as well as other countries, the operating principles of architectural illumination systems are varied in form and determined by municipal authorities or by landlords. And illumination chromaticity is perhaps the newest, least experienced, risky and unpredictable, but also the most effective parameter to consider. Its relationship with classical architecture is rather problematic, though there are examples of steady colour illumination of architectural landmarks. The closest and most provocative example in Moscow is the colour illumination of building facades using light emitting diodes on street Tverskaya in 2012. This project included many neo-classical facades from the Soviet period with wall and order tectonics. The result was a complete fiasco [5] and the system was abandoned. Active polychrome light, unharmonised and unconnected characteristically and dynamically, is an excessively blunt emotional instrument, which cannot be visually com-



Fig. 4. Different versions of the architectural illumination of the main facade of the Bolshoi theatre in Moscow: *a* – previous, *b* – existing, *c* – computer generated (A.G. Batova)

portable in a living and rhythmic environment. It can be very impressive in festive light shows, but that is a different setting. As a thunder storm with lightning is differs from a sunny and, even more so from an overcast day. It is difficult to imagine normal life in a constant flashing thunder-storm. In the long term there may be a place for an interactive light and colour environment in daily life, probably including classical landmarks; examples of this are growing due to advances in light emitting diodes and computer control systems. But these systems will assume a gentle, rather than narcotic exposure on the viewer's perceptive systems. This is a vast and unexplored area of scientific interest, which is very relevant but which is, unfortunately, under research yet.

Tendencies in modern light design in the West, according to a speech by R. Narboni at the "ARCHMoscow" event in May 2015, are evolving towards a decreasing light quantity in city spaces, with improved aesthetics of light design solutions. There are serious steps taken towards reducing light pollution of the night sky. In the European Union, standards of external illumination are being reconsidered with a view to reduce light intensity and of other parameters. Authorities of some cities, Prague as an example, have taking restrictive measures long ago. There are attempts to unite the aesthetics of light with the aesthetics of darkness. This will provide the contrasts necessary for light design art (although darkness is too often abundant in city environments). It is necessary to find a balance which will not detrimentally affect the life and functioning of the city at night. This is another challenge for research.

Classical architectural creating had managed to survive many paradigm shifts in history, theory and practice of architecture in daylight. Now is the time for the theory and practice of light design, wherein the main role in the interpretation of the

imaginative essence must be played by artificial electric light, which has almost limitless abilities. One can only hope that light designers with any basic education will have an understanding and an appreciation of the soul of classical architecture and will treat it with a piety. And that the labours of the newly born light design will rejuvenate ideas of the traditional architectural and urban theory.

The research is performed due to a grant of the Russian scientific fund "Past and Future of Classical Architecture" (project # 14–18–01601) in the MARKI(SA).

REFERENCES

1. *Shchepetkov N.I.* Light design of a city. – Moscow: Architectura-C, 2006, pp. 246–252.
2. *Revzina Yu.E., Shvidkovsky D.O.* Illumination of memorials of classical architecture. Authenticity searches// Svetotekhnika, 2015, # 6 pp. 12–16.
3. *Shchepetkov N.I.* Travel notes on light design in cities of the USA//Svetotekhnika, 2013, # 3, pp. 57–64.
4. *Batova A.G.* Principles of designing external illumination of architectural objects. Dissertation author's abstract of MARKI PhD, 2012.
5. A discussion on the subject "About a concept of creation of uniform light-and-colour environment of Moscow city"//Svetotekhnika, 2012, # 6, pp. 49–60.



Nikolai I. Shchepetkov,
Dr. of architecture,
Professor. Graduated from
the Moscow Architect
Institute in 1965. The Head
of the Chair "Architectural
physics" of the Moscow
Architect Institute. A winner

of the State prize of the Russian Federation for architectural illumination of Moscow. Member of the "Light and Engineering" Journal Editorial Board

FROM LIGHT URBANISM TO NOCTURNAL URBANISM

Roger Narboni

ITMO University, Lighting Design CONCEPTO
roger.narboni@concepto.fr

ABSTRACT

The field known as “light urbanism” began in France during the late 1980s, but the idea of thinking about urban lighting prior to the technical project and in correlation with urban planning studies had already been in practice during the establishment of five new towns outside of Paris planned by the Ile-de-France region’s Master plan in 1964–1965. Light urbanism is now naturally incorporated into urban planning strategies on all scales (megalopolis, cities’ network, conurbations, towns, villages and urban development zones), although a large number of cities in the world still have not yet perceived the necessity and utility of systematically associating it with conventional urban planning or daytime urbanism.

Key words: light urbanism, urban lighting, nocturnal urbanism, lighting master plan

1. THE ORIGINS OF LIGHT URBANISM

The field known as “light urbanism” began in France during the late 1980s, but the idea of thinking about urban lighting prior to the technical project and in correlation with urban planning studies had already been in practice during the establishment of five new towns outside of Paris planned by the Ile-de-France region’s Master plan in 1964–1965.

These first lighting studies, which we might call nowadays «Lighting Master Plans», at that time were supposed to prioritize and differentiate the systems and types of lightings according to the types of roads, and in particular, to fulfil

the separation between automobile and pedestrian networks sought after by urban planners in some of these cities.

During the early weeks of 1988, the lighting design studio CONCEPTO started and conducted the first holistic study for a Lighting Master Plan (LMP or SDAL in French), called “City lights”, at the request of Philips Lighting Company for the entire city of Montpellier, which is located in southern France.

This innovative and informative study was the first of its kind.

Light urbanism strategy was launched, but this study was not supported by everyone. Many, including elected officials, architects and city planners, were unwilling to back it. Nevertheless, the LMP for Montpellier study was quickly followed by additional ones: the LMPs for the French cities of Evry (Essonne), Beziers and Brides-les-Bains (a small town located in the Alps where part of the 1992 Winter Olympic Games was held).

The first approach to light urbanism was relatively chaotic, hindered by a stuttering methodology. Moreover, they had been deliberately stalled by the lighting designer regarding urban development vocabulary, in particular by the Master Plans for development and urbanization (or SDAU in French), which established the strategic direction of a territory and coordinated local urbanization programs with the region’s development policy. At that time, the LMP was also supposed to fix the lighting strategy so that it could be implemented gradually throughout an urban area.

Back then, the idea was to make a dramatic distinction regarding the technical vision of a city at

night, which was partial, biased and focused on either functional lighting or the illumination of architectural heritage and instead to imagine the contrary, holistic studies which would offer the capacity to simultaneously address the nocturnal landscape, the urban lighting of pathways and public spaces, the luminous ambiances for pedestrians and the enhancement of historical, modern or contemporary architectures.

Rapidly, during the early months of 1989, the first lighting master plans dedicated to City marketing followed these first lighting strategies: those of Lyon, perhaps the most famous of them, had been initiated by the city's elected officials and technical services in collaboration with Alain Guilhot, Lyon's lighting designer. The same year, the LMP for the city of Edinburgh in Scotland came out, created by the British lighting design studio Lighting Design Partnership.

The lighting master plan for the French city of Caen, created in 1990 by the French lighting designer Pierre Bideau, made another critical step for light urbanism with the political decision to illuminate 44 city monuments within less than three years.

Later in 1990, for the first time in France, CONCEPTO formed a lighting master plan for a social housing district called Clou Bouchet in the town of Niort as part of the city and district social development policy. It was an opportunity to apply this approach of light urbanism to everyday spaces that were considered disadvantaged and neglected so as to bring them, after remodelling, some dream at night.

With the lighting master plan for the French city of Nantes, designed in 1992 by CONCEPTO at the request of elected officials and services to support the new urban nightscape created by the ongoing redevelopment of Nantes' 50 hostages avenue and the realization of the second tramway line, light urbanism was at the service of the city's urban projects and new travel policy. At the time, this exemplary study emphasized the potential night time role that urban lighting could play in creating nocturnal ambiances beyond the restricted role of beautifying heritage buildings.

That year, the French lighting designer Louis Clair won the first international consultation for the development of the lighting master plan of Singapore. This was the beginning of the successful export of French lighting designers' know-how.

Light urbanism, conducted initially by French and English lighting designers, naturally spread to all European countries (first in Belgium, Germany, Switzerland, Italy, then Sweden, the Netherlands, and more recently Spain), then reached Asian countries (Japan, China, Thailand), North American cities (Detroit, Montreal, Quebec, Chicago, Philadelphia), central America cities (Mexico, Puebla), a few African cities (Casablanca, Algiers, Bamako) and Middle Eastern cities (Jerusalem, Beirut, Abu Dhabi).

Not long ago, it has been extended to major South American cities (LMP of Sao Paulo, Brazil in 2012 by CONCEPTO and LMP of Medellin, Colombia in 2014 as part of an international workshop during the EILD2014 congress of lighting designers).

2. LIGHT URBANISM NOWADAYS

Light urbanism today allows us to think about the nightscape and the night silhouette of a city or conurbation, gradually creating one of more identities, characteristics, potentials and luminous ambiances. It also allows a mastered planning of the public lighting as its renovation.

This approach is based on pedagogy, methodology and an instrument for mastering urban lighting development (the lighting master plan – LMP) now widely recognized and used by a large number of French and foreign cities.

Light urbanism is now naturally incorporated into urban planning strategies on all scales (megalopolis, cities' network, conurbations, towns, villages, and urban development zones), although a large number of cities in the world still have not yet perceived the necessity and utility of systematically associating it with conventional urban planning or daytime urbanism.

Recall that a LMP study takes place over a period of 4 months to over a year, depending on the size of the city concerned.

It meets several objectives:

- Sharing tools and vocabulary of a culture of light;
- Educating elected representatives and technical services while raising awareness of the visual and psychological impacts generated by urban lighting;
- Allowing a cross connection between various municipal services;

- Uniting public and private initiatives aimed at the same overall night time strategy.

This LMP study consists of:

- Analyzing in depth the existing technical state of the city at night (public lighting, luminous ambiances and both public and private illuminations);
- Developing a master plan that takes into account the city's history, geography, topography, landscape, morphology, architectures, personality, characteristics and future;
- Imagining and controlling the future night time image of the city;
- Identifying possible intervention sites as well as potentially interesting ones;
- Prioritizing;
- Conceptualizing the city skyline at night and its visual impact, near and far, and the various lightings actions programmed.

All documentation and cartographies produced validated and approved by the study's steering committee are gathered to form the city's LMP. These studies are searchable on demand, and they provide a basis for routine actions carried out by technical lighting services, development programs prior to any consultation, development work outsourced to private contractors, lighting major actions (enhancement of public spaces, notable architectures, infrastructures, historical places, natural sites and thematic urban routes) and drafting of specifications intended for future operators (public or private clients, project managers, and developers).

To date, the LMP is not a regulatory document enforceable on third parties. It is a set of recommendations and an invaluable tool for cities and developers, both public and private. It should be reviewed and updated regularly in order to reflect new urban strategies including the increasingly rapid evolution of lighting technology.

3. EVOLUTIONS

Light urbanism approaches have evolved in recent years alongside changes and developments within city nightlife.

We have moved from the monumental urban focus to instead taking into account the concept of neighbourhood, from concentrating on a city-wide scale, which had been proving more difficult to control, to a more manageable urban pro-

ject scale, from beautifying architectural heritage to prefiguring urban transformations, from over-illuminating city centres to creating genuine nocturnal atmospheres for disadvantaged and neglected suburbs.

Night time proximity dimension is better understood. Sidewalks near home, public spaces located in front of equipment and services and access routes to schools are considered essential by a growing number of residents.

Although citizens are very attentive to their urban environment and the role that lighting plays in its valuation, they are also deeply attached to lighting projects that take into account everyday city uses.

For an increasing number of residents, the dramatization of a city at night and the enhancement of its remarkable heritage too often come at the expense of nearby luminous atmospheres considered important in their daily perception and therefore in their assessment of the quality of life in their town or neighbourhood.

The transformation of industrial wastelands, the creation of large equipment and the renovation of a site have led to a slow and gradual change in the urban landscape. Neighbourhood revival issues are difficult to perceive by the locals. Infrastructure development is often seen as a nuisance by users. Landscape projects and parks are not rapidly adopted by the local residents due to the amount of time necessary for plant growth. Furthermore, large-scale or long-term development projects are often misunderstood by citizens.

How then can local project ownership be enabled?

How can residents be better assisted in visualizing spatial and temporal objectives?

How can the night time potential of an area be identified and experienced?

Through its power of attraction, its symbolic dimension and its ability to indicate intentions, there is a role, ephemeral or perennial, which urban lighting could play in the future to envisioning a place's transformation, exposing an urban issue or rediscovering a neglected territory. It is also, through its poetic dimension, a powerful tool for revealing the unseen, affirming lines of force, transforming a site, illustrating the evolution of a landscape, staging a construction site and positively affecting the nightly view supported by each person on its current and future environments.

Finally, the control of light pollution, the protection of the environment and the necessary reduction of energy consumption related to public lighting have now become the major objectives of any lighting strategy. Hence the current study of black infrastructures that complement the lighting master plans to rethink the role of darkness in the city, so as to identify, preserve and safeguard dark areas through managing and considering their connections and night crossings, to take into consideration their links, to protect nocturnal biodiversity and to allow, at night, a better relationship between nocturnal urban uses and the natural environment.

Like daytime urbanism, the continuous evolution and innovation of light urbanism has provided elected officials the ability to develop multiple and delicate images of their city at night. Over time, these images and nightscapes will be enhanced by the vision held by different lighting designers called upon to work on a site.

Consultation and participation of the local inhabitants along with the will to initiate a participatory democracy must now be systematically incorporated into the methodology of light urbanism. It is necessary for local residents to be able to express their opinion regarding the nocturnal feeling of their city, their wishes and desires at night, and participate in the development of the LMP, by way of night time exploratory courses and workshops dedicated to this.

The nocturnal journeys with local residents are an opportunity to exchange views with technical services, elected representatives and lighting designers. It also enables participating residents to acquire an understanding about the culture of urban lighting in addition to a common language that facilitates dialogue for the subsequent stages of proposals and recommendations for developing the LMP. And finally, residents will be given the opportunity to share in person the needs or shortages of lighting experiences, and to discuss issues of energy reduction, darkness and light pollution along with the resulting choices, contradictions and necessary trade-offs.

4. NEW LIGHTING STRATEGIES

Several complementary objectives are now responsible for the development of a city-wide lighting strategy:

- Giving a nocturnal identity or identities to the city and its neighbourhoods;
- Prequalifying public lighting (radical or incremental changes, implementation of delegated private management);
- Continuing or undermining the valuation of architectural and natural heritage;
- Creating attractive nocturnal atmospheres during a neighbourhood's urban renovation;
- Improving the connections between the city centre and its suburbs;
- Weaving a nocturnal social link;
- Coordinating the lightings of a multiplicity of urban actions;
- Supporting an infrastructure (metro, tramway and motorway);
- Highlighting a historical axe, major or symbolic;
- Inventing a large night time landscape;
- Developing nocturnal tourism;
- Establishing a night time image associated with an urban project;
- Imagining beforehand a major urban transformation;
- Celebrating a major sports or historical event with light;
- Initiating a sustainable development policy;
- Decreasing consumption and energy costs;
- Controlling and reducing light pollution;
- Studying black infrastructure and implementing plans to safeguard darkness;
- Respecting and protecting nocturnal biodiversity.

In France, given the age and obsolescence of public lighting facilities in a large number of towns and villages, one of the current major challenges of any new lighting strategy is the revision of policies for public lighting in order to implement, revive, or abandon illuminations realized over the past twenty years.

The French city of Valenciennes, for example, started its former lighting master plan in 1997. From 2011 to 2013, the Municipality decided to completely renovate it because of partial or total visual degradation observed across 90 initial illuminated sites. With this new LMP, 30 illuminated sites were abandoned entirely, 60 illuminations were completely renovated and 15 new illuminations were created.

Other French cities (Lorient, Lyon, Pau, Rennes, etc.) are also in the process of conducting this type of reflective assessment.

5. TOMORROW: THE LAUNCH OF NOCTURNAL URBANISM?

Light urbanism is now a mature discipline that is permanently fixed into the global perspective of the city.

Lighting Master Plans have become essential tools for multidisciplinary teams who need to think and study urban development and possible mutations of the city 24 hours a day.

They can help local governments make cities more attractive and welcoming at night in order to meet the expectations of the citizens of tomorrow.

It will thus be necessary, gradually and systematically, for lighting designers to devise consulting missions to help each city to actualize these new urban lighting design strategies. In 2014, the city of Rennes was the first city in France to establish a four-year mission for a lighting designer advisor, to support and complement architect and landscape architect advisors, accompany elected officials and services in realizing the LMP, monitor its implementation and advise developers and project managers working in the city.

Consultation and participation of the inhabitants in the construction of their night environment should also be developed and encouraged.

Light urbanism enriches the range available to urban planners, and this new situation is reinforced by the invasion of the night by multipurpose uses, which has reduced the distinction between day and night.

We must accompany the city's developments to its night territories as well.

It will also require in the future the establishment of a more systematic interdisciplinary approach to urban planning which takes into account 24-hour round-the-clock life in cities.

Light urbanism, as we have known it for nearly three decades, still focuses too much on the illumination of the city, but this fixation will disappear gradually and evolve into a nocturnal urbanism. It will not be derived from the incorporation of the night issue into the city as a simple extension of an ubiquitous daytime urban planning, but it will rather become a new discipline devoted to night time

periods, of which the content, approaches and methods have yet to be determined.

Consequently, what might this nocturnal urbanism resemble?

It will first become interested in drawing urban forms primarily dedicated to nocturnal practices of the city, by studying and relying on existing nocturnal uses of its inhabitants or those uses likely to be generated by this new morphology.

The city of tomorrow could just as well be initially thought in terms of the urban night instead of its sole daytime occupation.

Diverse sectors, the city's layers, would then be differently imagined according to the predominance of the periods of night time uses.

Housing property development programs could also be designed based on their night time ownership. Thus architecture designed to function mostly or solely at night (for example, "Learning Centres") would imply a different solar orientation and ground plan, an unusual relationship between full and empty facades, a more intimate and fusion relationship with artificial lighting.

The floor and facade materials will evolve to provide new opportunities to build volumes and luminous architectures that will illuminate intermediate public areas and façade bottoms, thus offering new perceptions of public space at night, finally released from the traditional lighting poles that will soon become useless day and night. It is the whole physiognomy of cities and streets that we have always known would be completely and definitively changed.

Public spaces, public access, the areas surroundings property development programs designed to be used primarily at night will be studied and designed by taking into account first the characteristics of the users' night vision (mesopic and scotopic vision).

It is with all these conditions that nocturnal urbanism will continue to evolve and develop well into the future. To our descendants, of course, it will appear as though this discipline has always existed.

REFERENCES

1. *Deleuil, Jean Michel*. Eclairer la ville autrement, innovation et expérimentations en éclairage public [Illuminating the city differently: innovation and experimentation in public lighting]. Editions Presses pol-

otechniques et universitaires romandes. Lausanne: 2009.

2. *Isensstadt, S., Petty M.M., & Neumann D.* Cities of light, two centuries of urban illumination. Editions Routledge. Australia: 2015.

3. *Montse, B. & Narboni, R.* By Night, Lumiere et architecture [By Night, Lighting and architecture]. Loft Publications. Barcelona: 2009.

4. *Narboni, Roger.* La lumière et le paysage, créer des paysages nocturnes [Lighting and the landscape, creating nightscapes]. Edition du Moniteur. Paris: 2003.

5. *Narboni, Roger.* Lumière et ambiances, concevoir des éclairages pour l'architecture et la ville [Lighting and atmosphere, lighting design for city architecture]. Edition du Moniteur. Paris: 2006.

6. *Narboni, Roger.* La nuit disparue [The Vanished Night]. Edition fondation Targetti. Florence: 2009.

7. *Narboni, Roger.* Les éclairages des villes, vers un urbanisme nocturne [The cities' lights: Moving towards nocturnal urban lighting design]. Collection Archigraphy. Edition Infolio. Bale: 2012.



Roger Narboni,

the world-renowned French lighting designer, visual artist and electrical engineer, director of CONCEPTO, founded in 1988, and has realized more than 200 landscape, urban, heritage and architectural lightings.

He launched in 1987 a new discipline called Light Urbanism and has realised since then more than 120 lighting master plans in France and abroad

VIDEO MAPPING FROM PRESENTATION TO ARCHITECTURE

Elena V. Barchugova and Nataliya A. Rohegova

MarkhI (State Academy), Moscow
E-mail: na.rohegova@markhi.ru

ABSTRACT

Modern society is subjected to constant global changes in information processing. As computer technologies penetrate into all spheres and vital functions, a new world outlook needs to be formed. Disciplinary boundaries are extended, and new connections are established; there is a need for interdisciplinary research. Architecture interacts with different fields in the sciences and humanities, as well as with new types of arts, in particular with the audiovisual art: video mapping (3D-mapping). The practice of video mapping in the city medium is growing. The development and integration of this art demands is analysing carefully to identify new ways of improving the city medium.

Keywords: video mapping, visualisation, availability, mass character, synthetic activity, city medium

Architectural video mapping (VM) arose from a specific type of audiovisual art directly connected with the development of computer technologies. Exterior, interior and landscape video projections and light installations are not just spectacular but also have information value (Fig. 1). At present, VM application cover clubs, museums, theatres, exhibitions and training centres, as well as to festive shows, which have already have become common. The nature and ways of mutual integration of architecture and audiovisual art forms require understanding and analysis.

The VM phenomenon has been a feature of city events for several decades. Specifically, VM refers to audio-video projections upon material objects,

including architecture. This method has developed out of presentations and advertisements promoting goods or services. At the beginning, when the prices for these technologies were high, VM was only used by large-scale businesses or municipal authorities.

The largest and most expensive examples of VM have been festivals of light, which take place in many big cities around the world. The scope of the action can be imagined from the statistics of the Moscow "Light Circle" festival in 2011, the creator of which was David Etkins, who had previously designed opening ceremonies for the Vancouver (2010) and Sydney (2000) Olympic Games. The area of the general projection was 25,500 m². There were forty light devices "Big Light", the rays of which extended in total for more than 40 km, eighty-one projectors, twelve acoustics lines with sound power of one MW and 2,184 m³ of metal structures. More than 1,000 people took part in preparation and implementation of the show.

In Moscow, the Light Festival becomes increasingly popular each year: in 2011 it covered three sites, in 2014 – seven sites, and in 2015 the "Light Circle" was developed on nine sites of the city and was declared by the United Nations and UNESCO as the gold standard partner of the International Year of Light and Light Technologies.

Besides the large-scale shows, many methods of VM have been introduced into various spheres of city dwellers' lives over the last decades.

The annual conference "CG EVENT", devoted to developments in the field of computer graphics, confirms that use of static and dynamic projections is beginning to be used en masse in different fields. Dynamic methods of information supply are deve-

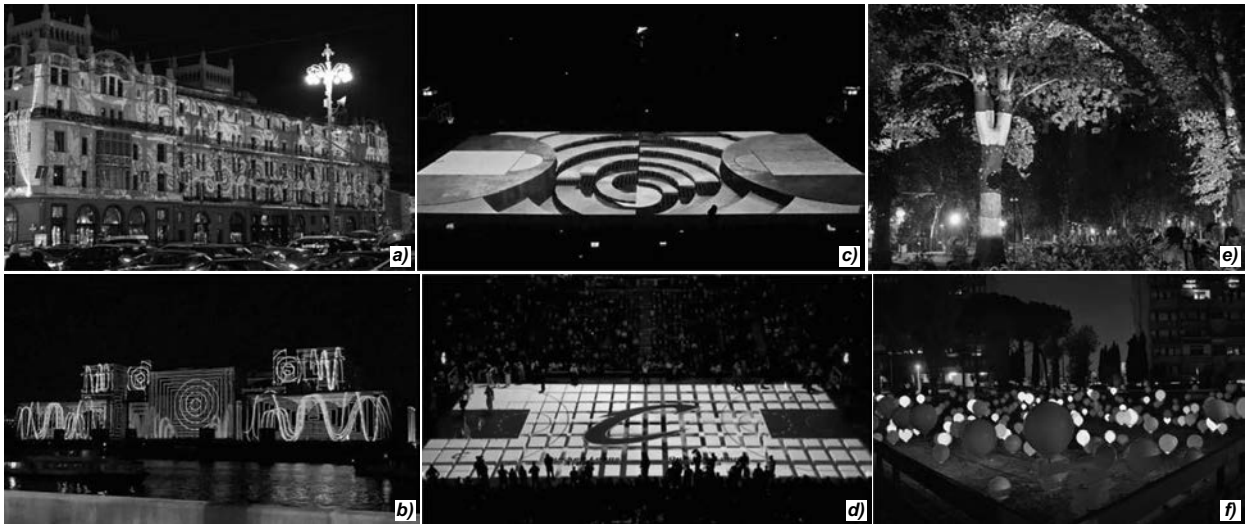


Fig. 1. Video mapping, exterior, interior and landscape examples: a) Metropol hotel building, Moscow, Winter fairytale show, 2013; b) Light Festival, Moscow, 2015, building of the Ministry of Defence of Russia; c, d – Birth of a new basketball team “ZENITH” festive sports show, St.-Petersburg, 2014, the Author: *Illuminarium3000* company; e) a composition by Italian *Apparati Effimeri* company, f) Roman Festival of Light, 2015

loping rapidly; they are now considered as expressive artistic facilities for a new media art.

Three kinds of interaction between architecture and audiovisual art can be distinguished by their degree of integration:

1. Synthesis of arts based on architecture. An audiovisual component is included into the architectural concept and used as one of the graphic means to form an architectural image. VM action always develops based on a single scenario (Fig. 2 and 3).

2. Synthetic activity on equal terms to create an art medium. An architectural construction (or just its interior) is designed to provide optimum conditions for implementation of many scenarios (Fig. 4–6). Each time a temporary art integrity is formed.

3. Audiovisual action is performed ignoring the specific character of the architectural component. The mapping is carried out upon any background surface suiting the size, including an architectural surface. The characteristics of the architecture are

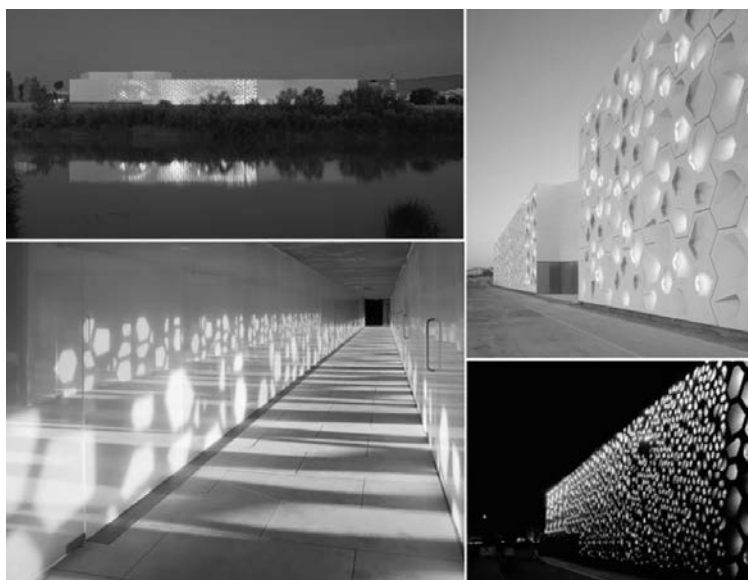


Fig. 2. Synthesis of arts based on architecture. Modern art centre in Cordoba, Spain, 2013, *Nieto Sobejano Arquitectos* architectural bureau

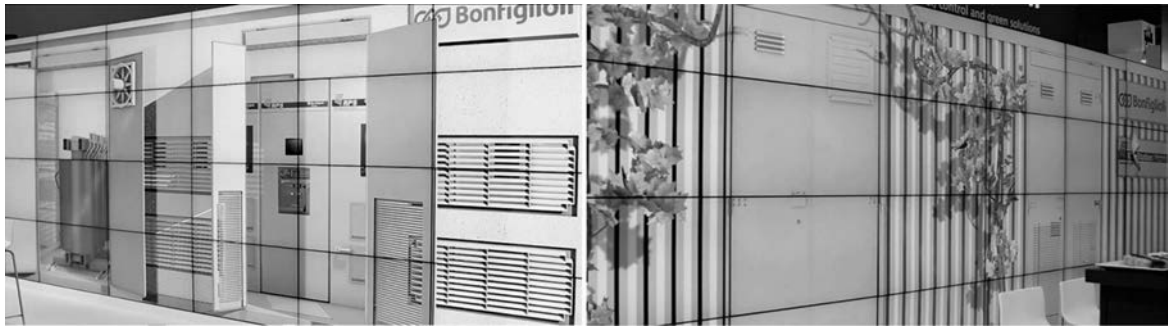


Fig. 3. Interior video mapping. Synthesis of arts based on architecture. Decoration of office walls by means of video mapping. A composition by *Apparati Effimeri* Company

not taken into consideration. Moreover, they are often completely ruined or deliberately deformed (Fig. 7).

If during the designing process, an architect has formed a creative concept, where the initial concept already included VM as a special graphic facility, then a new synthesis of arts can be described (Figs. 2 and 3). VM facilities in this case are not beyond one of the components of artistic architecture image. Sometimes visual effects are localised on transparent faces or interior surfaces of buildings occupying them partly or completely.

Exterior VM, which means image change and transformation of existing architectural objects with capture of surrounding space, is an altogether different phenomenon. The accent of the artistic process is transferred to an audiovisual action (Fig. 5). Imaginative unity in this case is reached by means of mapping art facilities. And the architecture plays a more modest role of an in-

tegral background surface, not only including the specific construction but also the all space of the surrounding natural or urbanised medium. This type of media show is usually expensive and has a short duration.

Interior VMs have two versions of interaction. If light installation is carried out in a room, which has not been specifically prepared for it, the likely outcome is a partial or full neglect of the architectural component. Art actions are transferred to the sphere of audiovisual illusions. As a rule, this is the case at festive and presentation events.

In the second case, when interior space and its surfaces are intended and designed for light installations and performance, synthetic activity takes place on a parity basis forming a temporary art integrity (Fig. 4). Such interior spaces are multipurpose, they permit use of many methods, and each time they involve the architecture into an alliance with the new scenic concept.



Fig. 4. Interior theatrical video mapping. *Anarchy Dance* theatre of dance (established in 2010) Taipei, Taiwan. Temporary art integrity. A combination of architectural and video components on a parity basis

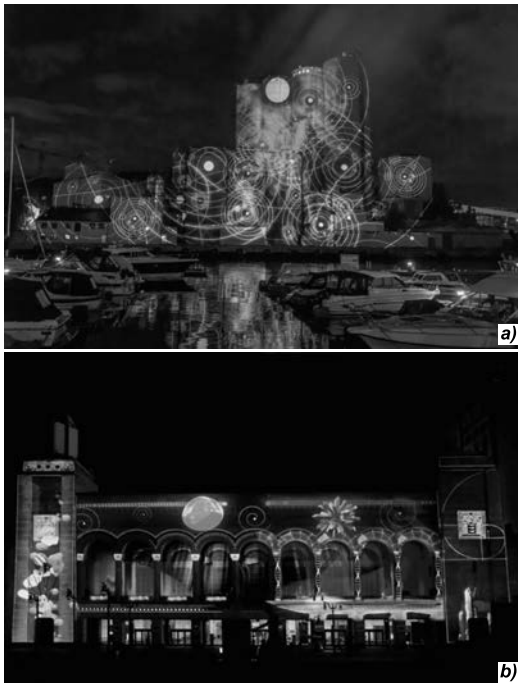


Fig. 5. Examples of neglect of the architectural component in presentation actions: *a* – Norwegian Festival, *Slemmestad*, 2014, the author: *Factory Light* company; *b* – *Moment Factory* company, decoration of the *Boardwalk Holl* building in Atlantic City, New Jersey state, the USA, 2012

Particularly dynamic and bright integrative interaction of architecture and VM occurs when temporary or mobile architectural constructions are used; where the dynamics of visual imagery are combined with physical transformations, which have been accommodated in the architectural object.

In addition to these listed forms of architecture and VM art integration, it is important to analyse some theoretical aspects, which have a direct relation to the subject at hand.

THE VISUAL AS A PRIMARY COMMUNICATION PROCESSES

In the modern information society, new methods of enhancing the role of evident communications appear constantly; visual facilities and methods emerge, which interact with or supplement each other. For most people, visual perception is the main channel of message transmission. The absence of a language barrier in the visual space and an increase in information transmission speeds are the qualities, which make visual information ubiquitous not only in mass media but also in art.

A rapid development of computer technologies plays an important role. In virtual space, new and impressive tools, dynamic expressive methods are being invented. They are used both in public art, and in highbrow art. To see this, one only needs to look at advertisements of art exhibitions on display at Moscow museums.

Other creative components are dependent on the visual component. Multisensory artworks cause various sensory responses in spectator, and can be described as a synaesthesia phenomenon. Examples of synaesthesia are sensations of colour hearing sense, visual images caused by tactile sensations and vice versa. Synaesthesia works as co-representation and co-feeling, which make the process of perception universal and memorable [1]. However, it should be stated that in action visual shows, the attention to comprehensive perception sensations sometimes outweighs the purpose of developing the viewer's cognitive abilities. The possibility of maximum comprehensive exposure of a spectator is the main goal, regardless of consequences which this exposure causes. Visual arts based on computer technologies manifest aiming for modelling and easy variability of the virtual realities, which do not have direct relation to reflection or study of physical realities.

MASS CHARACTER

One more characteristic feature of synthetic methods, which include the junction of architecture with the media arts, is their mass character.



Fig 6. *Glow festival* in Italian *Ostuni*. A combination architectural and video component on a parity basis

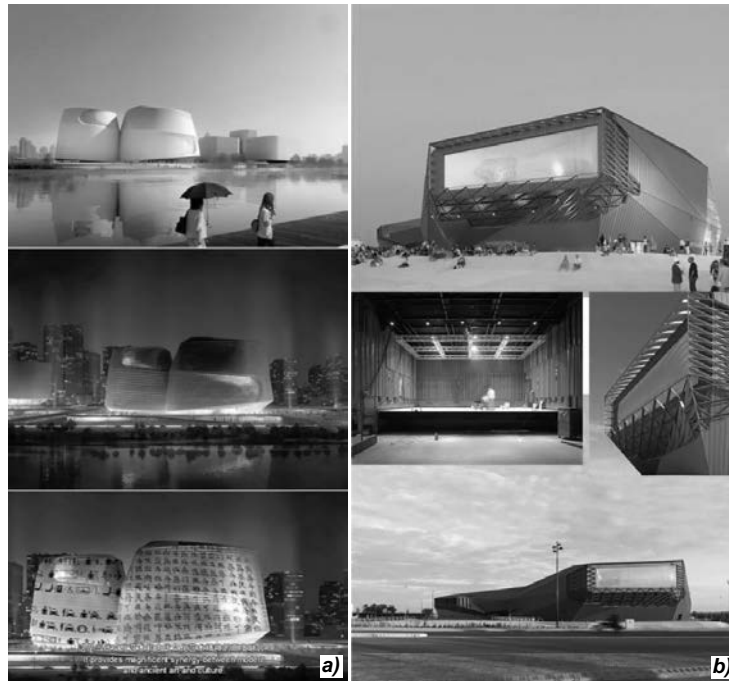


Fig. 7. Examples of harmonious combination of architecture and video art, temporary art integrity, and video mapping as a facilities of forming architectural image: a) a competitive project (the National Art Museum, Beijing, People's Republic of China, 2010, *UNStudio* architectural bureau; b) the *PALOMA*, Center of modern music, Nimes, France, *Tétrarc Architects* architectural Studio

Many authors have the opinion that in modern art ideas of the avant-garde from the early twentieth century a universal propagation of art and erasing the boundaries between art and utilitarian life are prevailing. Under closer examination, the difference between attitudes from the early twentieth and the early twenty-first century are significant.

The obvious difference is that the demand for early twentieth century avant-garde art was connected with its mass character. The Russian avant-garde was always supported by mass trends, by mass ideology and psychology, by mass perception. Therefore, it was successful in gaining popularity and trust. This occurred despite an obvious dissonance between the elitism of creative concepts on the one side, and the mass character of culture and expectations on the other. The understanding of the most prominent representatives of the Russian avant-garde was that the mass character was based not on an understanding of artworks or their creative concept but on the atmosphere around the artworks and their novelty [2]. For many people this position coincided with position of the young Russian state, which had declared the creation of a new fair social system, different to the overwhelming number of other world states.

At present, the mass character of art activity is also based on an acute understanding of the rearrangement of life, the change in its configuration, and of an ordinary and unique process speed. However, there is no direct message about social change or upheaval, which was there in the past. The expected changes are more likely concern the appearance of life and activity of people.

The expansion of art spaces and their involvement in new synthetic genres which appeal to synaesthetic perceptions [1] becomes a result of an interaction of the arts during an era of postmodernism. Architects, artists and animators make a point of reassessing the relationship between art and the ordinary, and involve it in an overall picture of art perception. This leads to a common artistic and cognitive approach.

The mass appeal and character of artistic projects today stems from a concept of availability. A certain level of computer graphic possessing facilities appears which can be easily mastered. The features of different artistic methods are rendered within computer programs, and users only need to combine them in the correct order.

One more important quality of synthetic art and architecture projects, is how interactive they are. Exterior and interior VMs easily connect with

spectators, promote them to exercise motive and think as parts of a creative act.

Interactivity is a form of elite art gravitating toward conceptualism. One of the popular forms of art today is performance. The development of art media is aligned with the dematerialization, which is an important idea in performance. The attention of the artist and spectator shifts towards a search of sense in the presentation of the artwork [3]. A spectator himself decides whether he/she is ready to take part in the action.

As part of a general move to create and to consume the visual, questions constantly arise about the future of modern spectators. An alarming trend is the propagation of so-called “clip thinking”. This develops because of a necessity to react to information supplied at a high-speed; this is based on visual images loosely coupled. Distinctive features of the clip thinking are intermittence of the information and simplicity of judgements contained within each sense fragment. A continuous information flow demands clearing memory space for perception of the next portion of information.

The emergence of audiovisual art forms and their interaction with architecture are not temporary phenomena. They will grow, which moves questions of psycho-ethics to the forefront. Erudition and education of people play an important role, as spectators are capable of independently tracking any information field, regardless of whether hypertext links forced on them or of whether hyperspace is.

In conclusion, it should be noted that in modern information society, which is based on a combined use of real and virtual spaces, all kinds of changes are taking place. In particular, architecture is integrating into absolutely new audiovisual expressive facilities.

Studying the degree of their interaction degree, from the synthesis of arts based on architecture to synaesthetic activity with support on its different components, becomes for contemporary architectural discourse. The persistent nature of integration of the visual arts with architecture and the aggressiveness of new forms of art activity sets problems for scientists and teachers on creation of modern educational technologies correspondent to the required level of the information society.

REFERENCES

1. *Zaitseva M.L.* Synaesthesia phenomenon in post-modernism art. URL: http://e-notabene.ru/psp/article_13379.html (Addressing date: 01.2016).
2. *Inshakova E. Yu.* On the edge of elite and mass cultures (concerning understanding of game space of Russian advance-guard) // Social sciences and modern age, 2001, # 1, pp. 162–174.
3. *Fadeyeva A.* World of art and world of performance. URL: http://uchit.net/catalog/Kultura_i_iskusstvo/101364 (Addressing date: 01.2016).



Elena V. Barchugova,

Ph.D., senior lecturer. Graduated from the Moscow Architectural Institute (MARkHI) in 1978. Professor of the MARkHI (State Academy), senior fellow of the Laboratory of Architectural Form Shaping of the Russian Academy of Architecture and Construction Sciences NIITIAG and of the Laboratory of Computer Technologies of the MARkHI. A member of the Union of Architects



Nataliya A. Rochegova,

Ph.D, senior lecturer. Graduated from the Moscow Architectural Institute (MARkHI) in 1970. Professor of the MARkHI (State Academy), senior fellow of the Laboratory of Architectural Form Shaping of the Russian Academy of Architecture and Construction Sciences NIITIAG and of the Laboratory of Computer Technologies of the MARkHI. A member of the Union of Architects

MODELS OF VISUAL DISCOMFORT FROM SOURCES OF GLARE

Vladimir P. Budak and Tatyana V. Meshkova

Moscow Power Institute National Research University, Moscow
E-mail: BudakVP@mpei.ru

ABSTRACT

The article analyses up-to-date models of glare discomfort from small and large artificial light sources, as well as the imitations to their application. Focus is given to the determination of discomfort glare from sources with a non-uniform luminance distribution, based on the physical sense of the phenomenon, and to the scale of discomfort glare criteria.

Keywords: indicator of discomfort glare, non-uniform luminance distribution, light emitting diodes, glare source

INTRODUCTION

All formulas for the quantitative evaluation of discomfort glare (DG) assume that a glare light source (GLS) and background have a uniform luminance distribution. However, in complex settings with glares from reflecting surfaces, it is not always clear what the GLS is, and what the background is.

In this case normalised illuminance values do not always provide comfort in the light medium, and in the event of a non-uniform luminance distribution in the observer field of vision, an additional characteristic is needed, for example, spatially-angular luminance distribution. All lighting programs are based on the principle of securing quantity indicators of illumination. With due regard for the new characteristic, it will be possible to simulate a preset illumination quality of a lighting installation (LI), which is more important from the point of view of comfort.

Currently, there are more than ten DG models all over the world, and each estimates glare in a different way. This makes an objective comparison of the models impossible. As a result, we receive relations between the factors, which can be reasons of DG emergence but not the real criterion of how well different models correspond to actual sensations.

PHYSICAL SENSE OF THE DISCOMFORT GLARE PHENOMENON

Glare can be described as noise for sight in bright illumination. *J. Veitch* and *J. Newsham* [1] describe it as follows: “Glare for light is the same as noise for sound. Just as noise is undesirable acoustic energy, glare is undesirable light energy”. The Illuminating Engineering Society of North America (*IESNA*) defines DG (discomfort glare) as “a sensations from luminance within field of vision, which is much more than luminance, for which an eye can adapt...” [2]. International commission on illumination (*CIE*) makes distinctions between the limited glare (*Disability Glare*) defined as “a glare, which worsens conditions of object visibility, not obligatory causing DG”, and DG (*Discomfort Glare*) specifically, which is defined as “a glare, which not necessarily worsens visibility of objects” [2].

In the domestic practice in Russia, the DG concept is considered together with the concept of the eye’s adaptation to the environment and with visual induction. According to the “Reference book on light engineering” (2006), a decrease of sight function in the presence of a bright GLS

in the visual field is defined as glare, which in turn is an example of a negative induction. In other words, it is a decrease of sight function in circumstances of non-uniform luminance distribution, as well as in case of a bright GLS in the field of vision. DG is also an example of negative inductive action. But in this case decrease of visual function is not necessary; only the comfort conditions sight are affected. And this fact is mostly revealed in course of time.

A decrease of visual functions with a raised luminance at the periphery of the field of vision in comparison with the luminance at its centre can usually be explained using an obscuring veil.

The difference between blinding and DG is perfectly described in the mentioned Reference book but in practice, in the European community glare and DG concepts are practically the same. And all known descriptions of DG sensation literally express glare sensations. In Europe these two concepts are not distinguished (except *UGR* concept, which will be considered below), and a threshold value of the glare is not established.

Therefore, based on the obscuring veil physical phenomenon, we consider that the physical sense of glare from GLSs causing a discomfort, most closely corresponds to *Newsham's* definition: DG from GLSs in the observer's field of vision is noise, the blinding effect of which is not sufficiently high to cause reduced sight function.

Similarly to the definition of noise, DG from GLSs is chaotic oscillations of different physical natures, which are differed by complexity of time structure of various intensity and frequency. Therefore, this is an unfavourably perceived light. As well as noise of the sound interval, DG from bright GLSs in an observer field of vision slows down a person's reactions when recognising the object, which reduces their attention and increases the number of errors when performing work tasks.

Let us assume that according to normal distribution of probability density p of random variable x , DG sensation can be described as follows:

$$p(x) = \frac{1}{\sigma\sqrt{2\pi}} e^{-\frac{(x-\mu)^2}{2\sigma^2}}, \quad (1)$$

Where μ is the mathematical expectation (average distribution), median and mode of the distri-

bution, σ is mean-square deviation (σ^2 is dispersion) of the distribution.

Then DG from the GLS will be similar to the *SNR* relation (*Signal to Noise Ratio*):

$$SNR = \frac{P_{\text{signal}}}{P_{\text{noise}}} = \frac{L_{\text{signal}}}{\sigma_{\text{noise}}},$$

where P_{signal} is average signal power, P_{noise} is average noise power, L_{signal} is average signal luminance (GLS luminance), σ_{noise} is mean-square deviation of noise distribution. Both the signal and the noise are measured in the system pass-band.

Let us assume that the background has a Poisson distribution, for which dispersion σ^2 is equal to the mathematical expectation. Then:

$$SNR = \frac{L_{\text{signal}}}{\sqrt{L_{\text{noise}}}}, \quad (2)$$

where L_{noise} is background luminance.

A REVIEW OF DISCOMFORT GLARE MODELS

Main general parameters of DG models are GLS luminous intensity, which is determined using the source luminance, size and location, and also the adaptation state of the observer's eye. Instability of sensations of an observer is taken into consideration in two models: *VCP* (*Visual Comfort Probability* is probability of visual comfort) and *DGP* (*Discomfort Glare Probability* is DG probability). They express blinding degree (as a percentage ratio) of the observers who consider blinding degree at a preset reference level or above it. The other models consider DG as an average or an average on the observer scale. And none of the models take into consideration any cultural differences between the observers.

It is worth considering briefly the history of *VCP* model development. *M. Luckiesh* and *L. Holladay* were the first to apply psychophysical evaluation to the glare. They developed a scale of comfort-discomfort glare, or a gradation of sensations from scarcely noticeable to intolerable and painful. Their research was a precondition of the comprehensive measurement of DG sensations, which was the beginning of *VCP* model development

[3]. In *M. Luckiesh* and *S. Guth's* research from 1949, dependences of DG sensation as a boundary luminance value between the comfort glare and DG within luminance interval 1080–5488cd/m², on the GLS size, background luminance or luminance field were studied. Reference experiments were performed with the GLS size of 0.0011sr, reference research of background luminance or luminance field were performed at 34cd/m². The GLS location in the visual field was also taken into consideration. And in this case reference research was made at the line of sight level [4].

Experimental installations in these studies consisted of an expanded visual field of uniform luminance created by two thirds of a 2-metre integrating sphere with a lamp located near to its centre, which provided a uniform illuminance field. Light sources were placed behind round openings in the sphere surface designated for bright light sources. The observers were located in the sphere centre so that the head of each observer was precisely in the centre.

The experimental technique included an evaluation of glare sensation during a short GLS emergence within the observer's visual field providing uniform background luminance distribution. At short GLS exposures, adaptation luminance was taken to be equal to the background luminance. The research cycle included three one second "turn on" periods divided into one second "turn off" periods with a five second pause. The observers were permitted to perform as much cycles as was necessary for the evaluation. For evaluation of *BCD* (*Brightness in the Visual Field at Borderline Between Comfort and Discomfort*), fifty observers adjusted initial luminance to determine their own *BCD* criterion.

In subsequent experiments, background luminance values amounted to 3.4; 34 and 340cd/m², GLS size values were equal to (0.0001–0.126) sr, and GLS positions relative to the vision line vertically, horizontally and diagonally were (0–100) grad. Ten observers took part in these experiments. In the research process, only preliminary conclusions on the considered linear GLSs were obtained, and a need for further research was confirmed.

M. Luckiesh and *S. Guth* informally confirmed that GLS exposure duration did not strongly influence DG evaluations, and *VCP* model did not include exposure duration as a dependent parameter [4].

These studies generated much discussion. Some questions were raised about the experiment with ten observers and the criteria for their selection from the initial fifty. A need for further research with continuous and short exposures as well as for additional research concerning the difference of laboratory and real measurement results was also revealed.

In spite of the fact that *IESNA* officially recommends the use of the *VCP* model, there are some limitations, because this model was only tested and confirmed for LIs with secondary optics fluorescent lamp luminaires [2]. The *VCP* model should not be used with very small GLSs, such as incandescent lamps and HP discharge lamps, and with very big GLSs, such as ceiling and built in luminaires, as well as with non-uniform GLSs, such as parabolic reflectors. Taking into consideration these limitations, it can be said that DG evaluation in accordance with *IESNA* is actually only correct for a very small part of lighting facilities (for GLS of directional light).

IESNA recommends the following formula to determine visual comfort probability:

$$VCP = \frac{100}{\sqrt{2\pi}} \int_{-\infty}^G e^{-t^2/2} dt,$$

where $G = 6.374 - 1.3227 \ln(DGR)$; *DGR* (*Discomfort Glare Rating*) is DG degree determined as

$$DRG = \left[\sum_{i=1}^N \frac{0.5L_i Q_i}{p_i L_a^{0.44}} \right]^{N^{0.0914}},$$

$Q = 20.4\omega + 1.52\omega^{0.2} - 0.075$, L_i is dimensional luminance of the lighting part of the i^{th} luminaire in the observer's eyes direction, cd/m²; ω_i is solid angle of the lighting part of the i^{th} luminaire from the observation point, sr; p_i is GLS position index relative to the sight line of the observer according to Guth; L_a is background luminance, cd/m² calculated as $E_{ind} \cdot \pi^{-1}$, which is a reflected component of the vertical illuminance at eye level of a standard observer (it is considered at the height of sight line of the standard observer to be equal to the reflected vertical illuminance on the walls at this height); N is the number of luminaires in the lighting installation.

It should be noted that the results of *M. Luckiesh* and *S. Guth* from 1949 on finding DG boundary level were similar to Gaussian noise distribution, and this confirms our assumption concerning sensation physical sense. In appearance, formula (2) corresponds to a normal Gaussian distribution (1) with $\mu = 0$ and $\sigma = 1$.

Next, we will consider British DG indicator (*British Glare Index*). The joint research of *S. Guth* (USA) and *R. Hopkinson* (Great Britain) started a big effort on DG work at the end of the 1940s, which created a basis for the British Glare Index. To determine DG sensation level, Hopkinson used four points on a semantic scale: “simply intolerable”, “simply inconvenient”, “simply acceptable” and “insensible”. His experimental installation included a model in the shape of black-and-white pictures of a class room. The GLSs were formed as holes in the pictures with back illumination. Adaptation luminance was created using illumination from the front. When changing GLS luminance, the observers were asked to adjust luminance adaptation so that the GLS correspond to one of the semantic scale points.

The basic formula of the DG British indicator (sensation) from a single GLS is *Glare Sensation* (g):

$$g = \frac{0.9L_s^{1.6}\omega_s^{0.8}}{L_b p^{1.6}}, \quad (3)$$

where L_s is GLS luminance, cd/m^2 ; ω_s is solid angle constricted by the lighting part of the i^{th} luminaire from the observation point, sr ; L_b is average luminance of the vision field of the observer, including the glare GLS, cd/m^2 ; p is GLS position index in relation to the sight line according to *M. Luckiesh* and *S. Guth* (determined using the Table of values based on the room’s geometry, which includes GLS located at an interval up to 62° higher than the sight line) [5].

DG general indicator, *Glare Index* (GI) is a result of a summation by all GLSs in the lighting installation:

$$GI = 10 \cdot \lg(0.5 \sum g),$$

where g is determined according to formula (3).

There also exists a model known as the “DG limitation system”. *J. De Boer* (Germany), has considered that the sum of “contributions” of separate

GLSs used in *VCP* and *GI* indicators was not correct, and proposed another approach to the calculation of total GLS action. But his colleagues *Andt*, *Bodman* and *Mak* in their work from 1959 analysed different formulas with such a summation and found that any of them were not suited for cases where several GLS were observed. *J. De Boer* was convinced that a reliable system of DG determination should be based on subjective values of a lighting installation as a whole, instead of summing up “contributions” of separate GLSs [5].

The “limitation glare system” does not contain an equation to determine sensations and parameters influencing blinding degree, but simply sets luminance limits. Hence this approach is limited in its DG evaluation possibility from a specific lighting installation by correspondent luminance boundary conditions.

In an attempt to unite the best features of the main systems of discomfort glare evaluation, including *VCP*, British indicator of discomfort glare and glare limitation system, the Technical CIE committee TC3–4 developed the DG indicator *CGI* (*CIE Glare Index*) (Publication CIE # 55, 1983). The basic formula for *CGI* calculation is as follows:

$$CGI = 10 \cdot \lg \left[0.1 \frac{1 + E_d/500}{E_d + E_i} \sum_{i=1}^N \frac{L_i^2 \cdot \omega_i}{p_i^2} \right],$$

where E_d and E_i are direct (from all GLSs) and reflected (from surrounding surfaces) illuminances accordingly on the pupil of an observer’s eye.

The $(1 + E_d/500)/(E_d + E_i)$ relation provides covariance in the numerator and adaptation in the denominator. Covariance means that glare changes directly as well as E_d in comparison with counter dispersion, which means that glare decreases with E_d growth [6]. Adaptation provides a reality for very dark rooms, where E_i is very weak, and so the *CGI* value does not decrease to infinity (thus glare does not occur in a cave lit with a candle, where E_i is almost zero) [7]. At the CIE session of 1989, at the suggestion of CIE TC3–13 technical committee, this relation in the final formula was replaced with $1/L_b$ for *CGI* for the following reasons:

1. Calculation of E_d requires great time and effort. And as the exclusion of this parameter does not lead to significant loss in accuracy, it was decided to exclude it.

2. Covariance and adaptation are factors, which demand additional exploration before they can be introduced into calculation practice [8]. When replacing $(1 + E_d/500)/(E_d + E_i)$ relation with $1/L_b$, *CGI* obviously does not provide covariance for the direct adaptation component.

Further, by replacing constants 10 and 0.1 with 8 and 0.25 accordingly in the *CGI* final formula, CIE introduced a united discomfort indicator *UGR* (*Unified Glare Rating*) as a DG criterion:

$$UGR = 8lg \left[\frac{0,25}{L_b} \sum_{i=1}^N \frac{L_i^2 \omega_i}{p_i^2} \right]. \quad (4)$$

L_b is determined here as a uniform luminance in the field of vision, which provides vertical illuminance on the observer's pupil identical to the illuminance in field of vision without GLSs.

CIE also introduced some expansions to main expression (4) for small GLSs, big lighting surfaces and for "reflected non-uniform light" but without references to any research. So, it is not clear, how these expansions were obtained.

In the domestic practice in Russia, for regulation of raised luminance areas creating DG sensations, DG indicator M has been used until recently:

$$M = \left[\sum_{i=1}^N \frac{L_i^2 \omega_i}{p_i^2 L_a} \right]^{0.5},$$

where L_i is average luminance of the i^{th} spot of a raised luminance in direction of the observer eyes, cd/m^2 ; ω_i is the solid angle, which constricts the i^{th} spot relative to the observer eyes, sr; L_a is average luminance of the observer field of adaptation, cd/m^2 ; p_i is the position index of the i^{th} spot relative to the observer sight line according to *Guth*; N is number of spots in the observer's field of vision. And to determine GLS p_i the following dependence [9] is used:

$$p_i = \exp \left[\left((35.2 - 0.31889\alpha_i - 1.22e^{2\alpha_i/9}) 10^{-3} \theta_i + (21 + 0.26667\alpha_i - 0.002963\alpha_i^2) 10^{-5} \theta_i^2 \right) \right],$$

where α_i is the angle between the vertical and the plane passing through the line of sight of the observer and of the i^{th} GLS, grade; θ_i is the angle be-

tween the observer's line of sight and the direction to the i^{th} GLS, grade.

Of all the quantitative methods of DG determination, a method developed at the Moscow Power Institute under the direction of *M.M. Epaneshnikov* is worthy of attention. Its quantitative characteristic is M_d , indicator of DG, which causing DG for one spot is expressed as

$$M_d = \frac{L_{sp}}{\varphi(\theta)} \sqrt{\frac{\omega}{L_a}},$$

where L_{sp} is luminance of the spot causing DG; ω is the solid angle constricting this spot relative to the observer's eyes, sr; L_a is luminance of adaptation; $\varphi(\theta)$ is the position index determined using a special nomogram [10].

$M_d = 25$ value corresponds to the conditions, at which half of the observers do not notice DG.

One more quantitative evaluation is down to determination of such L_{sp} value, which lies on the comfort – discomfort boundary. We name it L_b . According to *Benneth* [11]:

$$L_b = \frac{95L_a^{0.3} \exp(0.05 \cdot \theta)}{\omega}.$$

At present in Russia, the *UGR* indicator (4) recommended by CIE for DG evaluation is used. It allows transferring from the quality evaluation of discomfort glare luminance to a calculation indicator. However, formula (4) is only correct for GLSs of a small angular size: $0.003 \leq \omega \leq 0.1$.

To determine the DG indicator, GOST P54943–2012 standard is used: "Buildings and constructions. Methods of determination of discomfort glare indicator with artificial illumination indoors".

All of the approaches to DG sensation determination considered above are united by the assumption of GLS equi-luminosity. However, there is a method of *URG* calculation based on the luminance cards for non-uniform GLSs.

To evaluate DG, CIE proposed to use luminance distribution (CIE205:2013). Due to a high definition of the luminance cards, a single luminaire can be divided into several parts. On the luminance card, different combinations of pixels are selected, which are considered to be a single luminaire for *URG* calculation. But as *URG* depends

on the division number and on the classification algorithm, such a calculation cannot be correct. For the calculation, formula (4) for small size GLSs is used based on luminous intensity. Therefore, this method is not suited for DG calculation from GLSs of non-uniform luminance, because it is based on the *URG* indicator formulation, which was obtained when researching small size GLSs of a uniform luminance.

DISCOMFORT GLARE. EXPERIMENTAL PROBLEMS

There are very few basic mechanisms leading to DG. Frei at al. studied relation of DG sensation influences on pupil size change and on the eye iris. They found out that DG form changes of the pupil size. *S. Berman* and others investigated electric activity connected with facial muscles, and its relation to DG. The results of this research showed that although a considerable correlation exists between motions of facial muscles and DG subject evaluation, the motions of face muscles probably is not a reason of DG but its consequence. And so a reason for DG still hasn't been revealed. It is also supposed that an objective DG measure evaluation exists, which is not based on subjective data [12].

Subjective research of DG revealed some big disagreements. The studies showed a rather weak correlation between the predicted values and answers of the observers. *Manabe* estimated 42 lighting installations with 63 observers. A correlation was estimated between each model and DG evaluation conditions. The correlation for the *VPC* model amounted to 0.63, therefore a considerable number of deviations were found to be unexplainable. Nevertheless, when in later research, formula (4) was used for the calculation, the correlation was higher, and this confirmed that *URG* is the best of the calculation models.

Weak correlation factors can be numerous. There are for example, problems of measuring luminance of modern luminaires, there are procedures and psychological factors, as well as demographic differences between the observers. (Luminance levels are calculated using measurement of average illuminance from the luminaires under test but it is only correct for uniform luminance GLSs.)

The correlation is also influenced by the quality of DG determination technique training: in-

correct instructions lead to considerable differences and deviations in the results. According to *Lool* and *Bennett's* research (1981), observers' responses also depend on the range of stimulus presented in the research. And in the later studies of *S. Guth* (1951) the role of the stimulus exposure duration was studied, and no essential importance of it was revealed.

Some psychological factors, such as mood, stress and anxiety can influence the correlation evaluation results [12]. And in this case, a big GLS exposure duration (for hours) can be perceived differently than a short one.

Bennett (in 1972 – 1977) revealed an influence of demographic differences on DG sensations. He also found a slight correlation between DG sensation and eye colour. He revealed a dependence of this sensation on the position of the observer inside or out of a room.

CONCLUSION

None of the formulas considered above for indoor DG models are suitable for determining DG from GLSs of an uncertain configuration with non-uniform luminance distribution as in most situations GLS size exceeds 0.1sr, and in all experiments, only GLS with a uniform luminance distribution were considered.

When using different models for small and large GLSs, it is obvious that their direct comparison is impossible, because the dependent variable (DG level) is a subjective parameter (measured differently) in each calculation model.

The main cause of the difference in DG formulation is the absence of an accepted objective approach to studying DG sensations. An experiment's success depends on competent DG determination technique training, and all researchers used different scales of glare sensation and subjectively interpreted each scale division when obtaining subjective estimations. For instance, *M. Luckiesh*. and *S. Guth* [3] determined that GLS discomfort glare luminance in the field of vision amounted to (1030–3570) cd/m².

Summarising all of the above, one can come to a conclusion that a DG model for GLSs with a non-uniform luminance distribution in the observer's field of vision, is not available at present, and existing formulas and methods do not ensure results corresponding to the facts.

The formula for the determination of visual comfort probability recommended by *IESNA* (3), approximately resembles a normal distribution (1), and this confirms physical sense of the DG phenomenon according to *Newsham*. Therefore, we assume that the DG model from GLSs of an uncertain configuration with a non-uniform luminance distribution should not be a set of multifunctions but should follow the normal distribution law.

Besides, based on the obscuring veil concept, one can define the boundary “comfort glare–DG” as the state of an observer, when his/her eyes have not yet adapted to a higher luminance, and GLS luminance in the field of vision interfered with the accomplishment of visual tasks.

DG sensation is analytically indeterminable; so, there are currently no reliable data providing a reason for this phenomenon, and consequently in order to simulate DG from GLSs of uncertain configuration with a non-uniform luminance distribution, suitable experiments are needed. To perform them correctly, the technique of *M. Luckiesh* and *S. Guth S* [4] should be considered, as according to this analysis, the *VCP* model is best matched to the physical reason of the phenomenon.

REFERENCES

1. *Veitch J.A., Newsham G.R.* Determinants of lighting quality I: State of the Science // *Illum. Eng. Soc.* 1998, Vol. 27, No. 1, pp. 92–106.
2. *The IESNA Lighting Handbook: Reference and Application, Ninth Edition / Ed. Rea, Mark S.* – New York: IESNA, 2000.
3. *Luckiesh M., Holladay L.L.* Glare and Visibility // *Transactions of the IES*, 1925. V.20. P. 221.
4. *Luckiesh M., Guth S.K.* Brightness in the visual field at borderline between comfort and discomfort // *Illuminating Engineering*, 1949. V.44, No. 11. P. 650.
5. *DeBoer J.B.* StraßenLeuchtdichte und BlendungsFreiheit // *Lichttechnik*. 1958. P. 359.
6. *Einhorn H.D.* Discomfort glare: a formula to bridge differences // *Lighting Research and Technology*. 1979, Vol. 11, No. 2. P. 90.
7. *Poulton K.* Discomfort Glare / *Proc. CIE*, 19th Sess., Kyoto, Japan, 1979.
8. *Pai T.R., Gulati V.C.* Unified Glare Rating System: Practical Approach for Evaluating Discomfort Glare / *Proc. CIE*, 23rd Sess., New Delhi, India, 1995.
9. *Reference Book on Light Engineering / Under editorship of Yu.B. Aizenberg.* Third revised edition. Moscow: Znakh, 2006. 972 P.
10. *Meshkov V.V., Epaneshnikov M.M.* Illumination installations. Moscow: Energiya, 1972.
11. *Luzov A.V.* Eye and light. – Moscow: Energoatomizdat, 1983. 144 p.
12. *Clear R.D.* Discomfort glare: what do we actually know? // *Lighting Research and Technology*. 2013, Vol. 45, pp. 141–158.



Tatyana V. Meshkova,

an engineer. Graduated from the Moscow Power Institute (TU) in 2010. Head of the Project Control Department of NTC Joint-Stock Company. A post-graduate student of the Chair “Lights and Engineering” of the Moscow Power Institute National Research University



Vladimir P. Budak,

Professor, Dr. of Tech. Sciences. He was graduated from the Moscow Power Institute in 1981. At present, he is the Professor of the Light & Engineering Chair of the Moscow Power Institute Scientific-and-Research Organization as well as Editorial board member of the *Svetotekhnika* Journal

Ignorance is better than false knowledge
Nicolas Boileau-Despréaux

ILLUMINATION DESIGN: PROBLEMS OF TRANSLATION AND CRITERIA OF EVALUATION

Egor E. Nilov and Vitaly N. Stepanov

E-mail: vitaly.stepanov@philips.com
PHILIPS Light solutions Eurasia Open Company, Moscow

ABSTRACT

Based on a short insight into the history of artificial illumination development, the authors show how two different approaches to design and implementation of artificial illumination were formed and a correspondent basic terminology appeared. The light design term was born as a result of inadequate transformation of an English word combination “*lighting design*”. But due to domination of the word “design”, the term obtained more complex, deep and obliging sense than the original.

Implementation of the sense, which is put attributed to the concept of light design requires creating a new school of designing artificial illumination, and this can lead to a qualitative improvement of the artificial light environment in which we live.

Keywords: illumination, designing, design, light design.

The discussion on creating “a school of the domestic light design” in Russia [1] is reminiscent of the bible story about the construction of the Tower of Babel. Everyone speaks the same language using the same words, but everyone puts their own sense into them, and as a result, a feeling of mutual misunderstanding takes place. *Socrates* said: “Wisdom begins from a definition of terms”. It has become necessary to clear up terminology used by people associated with design and implementation of artificial illumination solutions. In doing so, it is important to recognise that the theory and

practice of artificial electric illumination, and hence its terminology were mainly formed abroad, and appeared in Russian later. Therefore, it is logical to retrace the evolution of foreign terms, and then analyse how they were interpreted in our country.

In the first half of the twentieth century the drivers of development in all light engineering fields (light sources, light devices, rationing and designing of artificial illumination) were the USA, with a significant contribution from Germany and the Netherlands (with *Osram* and *Philips*, respectively). It was specifically in the USA that the main lighting terminology was formed. During the period, when creation of effective light sources and light devices was of paramount importance, such terms as “*illumination*” and “*engineering*” (designing, technological development) were used. These terms were reflected in the name of the first professional public organization: *Illuminating Engineering Society of the North America (IESNA)* established in 1906. Its main purpose was a wide expansion of lighting knowledge and experience. These terms were also used in the name of a specialist journal of that time “*Illuminating Engineer*”.

Use of the word *lighting* (illumination) became a result of the natural trend of American English for search of shorter and more capacious words, and also a reflection of the fact that architects who had used word the *daylighting* (natural illumination) for a long time became interested in artificial illumination. The term *illumination* gradually disappeared. In Russian it became used to talk

about to decorative (festive) illumination, and today is usually used in this sense. The word *design* came to English from Latin. As a noun it can mean conception, intention, project, plan, drawing, sketch, structure, as well as process of accomplishment of a technical description of a future object, i.e. designing and as a verb means to project, to design, to describe, etc.

The *lighting design* word combination is primarily understood as “illumination designing”. For example, the *Lighting by Design* book name [2] is translated into Russian as “Illumination according to a conception”.

After the Second World War, after restoration and then after a rapid growth of the world economy, the consumer society blossomed. People stopped limiting themselves in all things, a new value was assigned to living comfortably and beautifully. The *design* word obtained a new content. Apart from engineers, architects and interior designers began to engage with illumination. The *Lighting Design and Application* journal (use and design of illumination), a publication division of *IESNA*, which gives priority to the technological aspects of illumination, extensively promotes a cooperation of light engineers and architects to give illumination aesthetic qualities.

It was precisely architects, starting with Americans *R. Kelly* and *W. Lam* [2], who began to form a new school of illumination designing. Unlike the so-called “*quantitative lighting design*” (designing in order to obtain preset quantity indicators of illumination) [3], illumination designing was developed, which was focused on perception (*perception-oriented lighting design*). Its target was formation of such a visually perceived light medium (*visual environment*), in which tasks of visibility and orientation provision would be simultaneously solved, and an “atmosphere” with certain aesthetic properties would be created. In the cited literature, such an approach was first named “*qualitative lighting design*” (designing to obtain preset illumination qualities), then the term was gradually transformed into “*architectural lighting design*” (illumination designing consistent with architecture).

Origin of the term *architectural lighting design* dates back to 1927, when the founder of the Lighting Institute of the Higher technical school of Karlsruhe *Joachim Teichmüller* introduced the *Lichtarchitektur* (light architecture) term. It means “an architecture, in which light is understood as

a building material and is consciously used in architectural designing” [3].

The new approach to illumination design appeared to be fruitful and attracted many supporters. In 2007, at the *Professional Lighting Design Convention (PLDC)* congress in London, work in the field of *architectural lighting design* obtained international acknowledgment and a correspondent profession was established.

The design term appeared in Russian in 1920. From the very beginning it had an aesthetic component and was defined as “art design” of subjects that is things, which people use. Theoretical aspects of design were studied within such scientific-applied profession as “technical aesthetic”.

In the 1970s in the USSR one more attempt was made to introduce into practice the light architecture term [4] in order to use interiors, buildings and cities in architectural designing. Many people, especially architects, realised that illumination (both natural and artificial) along with its utilitarian functions, can perform information and aesthetic functions. But up to the end of the twentieth century, illumination and design in Russia were not connected with each other. Where it was necessary, terms like “floodlight”, “architectural illumination”, or “art illumination” were used, and if a case related to illumination of building facades, sculpture memorials and other objects, the term “local lighting” was used.

Using the term “design” in Russian in relation to illumination was introduced by *N.I. Shchepetkov* in his book [5]. To suggest that light design is a simple word combination is ambiguous. The fact of the matter is that when directly translating a foreign word into Russian its polysemy is also transferred. What does the word design mean: design as a process, design as a conception, or design as a result? With reference to a city, other terms are usually used: “shape” (image), “plan of development”, “architectural designing”, “town development”, “city environment” and others. By reading Shchepetkov’s book [5], one can understand that it is not a question of a designing a city but of architectural illumination (of separate objects, ensembles and of a city as a whole). That is “design” does not refer to the city but to its illumination. The book name clarified two inconsistent transformations into Russian: “illumination” in spoken language was reduced to “light”, and the word



Fig. 1. Three versions of Mao Zedong's portrait

combination “*lighting design*” instead of “illumination designing” changed to “light design”.

But the fact remains: the word combination light design was taken up, multiplied, widespread and eventually turned into a common term.

Naturally, the question arises: what type of illumination can be referred to as a product of light design and what can't be? *N.I. Shchepetkov* treats the light design concept broadly, supposing that the first experience of external electric illumination in Petersburg of 1874 can be considered as the reference point in the development history of light design [1, p. 60]. This approach allows considering almost any illumination to be light design and supposes that all interested parties can take part in this activity, including those without special professional training. It is clear that such an interpretation wrong and unrealistic.

It is logical to consider that criteria used for the evaluation of industrial, graphic and any other design type results, are applicable to illumination design, in particular principles, which were formulated by the German designer *Dieter Rams* [6]: 1) innovation (use of latest achievements in technology); 2) usefulness (the design highlights the profitability of a product and disguises anything that can interfere with such an evaluation); 3) aesthetics (beauty); 4) intuitive clarity; 5) unobtrusiveness (products of design are not decorative objects or art subjects; design should be neutral and undemonstrative); 6) honesty (design should not present a product as more innovative, powerful or valuable than it really is; it should not manipulate consumers' expectations and make unrealistic promises); 7) timelessness, or modernity (design does not tend to be fashionable and consequently it will never become outdated); 8) scrupulous reasoning (no details are overlooked; attention to detail means respect to the consumers); 9) a considerate

attitude to the environment (design promotes natural resource conservation and minimizes physical and visual pollution of the environment across the product's life cycle); 10) minimalism and simplicity (“less is more”, concentration on the essential, freedom from the superfluous, maximum simplification).

As far as external city illumination is concerned, each of the criteria listed above could be expanded further. But as they are beyond the scope of this article, we will only give an example interpretation of one criterion: usefulness.

The usefulness criterion can be defined as meeting several sets of requirements [7]:

A. Main universal requirements: safe pedestrian traffic; fast and seamless visual orientation; a sensation of personal safety related to the ability to recognise people's faces from a distance no less than three metres; visual comfort (as low as practicable level of glare, even better – total absence); “pleasantness” of illumination, which is dependent on the primary direction of light incidence, on a “simulating” action of illumination, on colour rendition characteristics of light source radiation, as well as on the luminance ratio and distribution in the vision field.

B. Main social (public) requirements: safe traffic and safe interaction of pedestrians and transport; illumination energy efficiency; reliability of illumination; convenience of maintenance for the illumination systems; environmental safety of illumination systems (minimum light pollution).

C. Main aesthetic personal and public requirements: harmony and balance of the light environment; originality and individuality of a city image (which is determined, among other things, by the design of the luminaires and their supports); recognisable (iconography) characteristic townscapes.

D. Requirements of knowledge and development: interactivity, which is a possibility of interaction and of change with the light environment according to personal preferences; illumination adaptability (taking into account the time of day, pedestrian and transport traffic density, weather conditions, etc.); a possibility to carry out research and to obtain new knowledge.

In considering the above parameters when answering the question whether some illumination methods can be related to design, we add the following.

Illumination is a result of the interaction between light and objects in the environment, and this result is perceived by people's vision. In an ideal case, the object environment created and the illumination facilities should be united by a single vision or concept. This unity occurs in cinema, theatre, museums, and in the process of designing metro stations, when scenery is conceived and created, locations for shooting are sought for a long time, special structures are designed, illumination facilities with the necessary properties are created. Such an undertaking is too difficult for one person, and it is performed by groups of people and sometimes by groups of organisations or companies. People creating illumination systems in these spheres justifiably and proudly call themselves illumination designers.

Much more often, situations occur, when the object environment is entirely pre-set and is not subject to change, and illumination facilities have to be selected from a long, but nevertheless limited list of lighting products available on the market. In this case, psychological features of our perception: stability and integrity of visual perception, play a dominant role.

The examples given below explain some of this.

In 1972, one of pop art's founders, *Andy Warhol*, became prominent after showcasing some portraits of the Chairman Mao (Fig. 1). As the source sample he used a photo from the *Mao Zedong's* quotation collection published by the China Communist Party, and then painted elements of the background, face and clothes using different colours similar to how children do it colouring books. Using the same method, portraits of other famous people were made: Marilyn Monroe, Elizabeth Taylor, Mohammed Ali, Lenin, etc. The trick consisted of using easily recognisable images of very well-known people. In this case the viewer always got

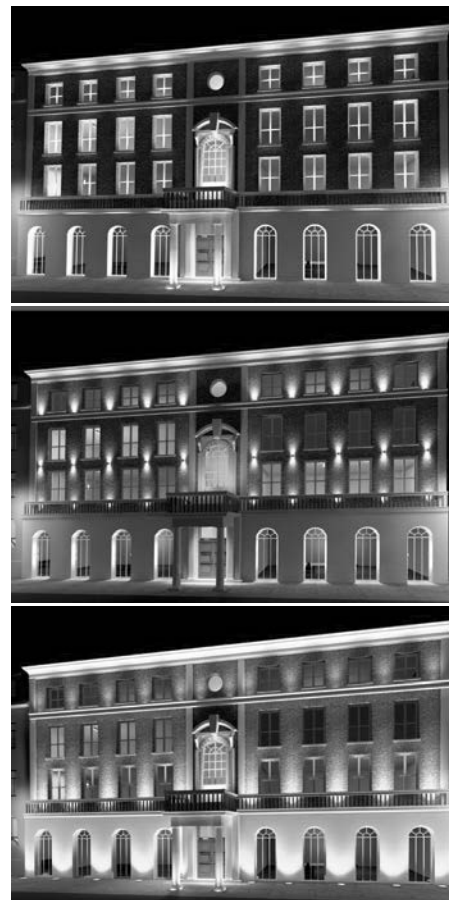


Fig. 2. Three versions of illumination of a building facade [8]

to the heart of the image first, i.e. the represented object, and details in this context, which were colours, almost didn't play any role in perception. Unnatural colour combinations claimed to be "eccentric". It was obvious that if objects known to nobody were used, the trick would not be so successful. The images would not be interesting to anybody.

Similarly, the perception of a building's illuminated facade, when its architecture is familiar to the observers, does not depend in practice on the illumination methods used. Most parts of buildings in Russian cities are illuminated using one of the methods presented in Fig.2. This type of lighting solutions cannot be called "design". "Illumination" is the most suitable term for these cases.

CONCLUSION

When the term "light design" was introduced into Russian language and practice, it raised the stakes and requirements for these activities to a much higher level than before. In international practice of artificial illumination, such "oblig-

ing" terms are not used. Instead, more specific and clear words are preferred, for example, “*architectural*” or “*city beautification*” (city decoration). But a blessing in disguise: light design is possible (there are many examples of this), it requires much knowledge and skill, and crucially, professionalism and responsibility from people who deal with it. Light design is impossible without a comprehensive approach to projects and demands to take into account many factors: social, environmental, economic, architectural features of the object and of the city as a whole. Light design cannot and should not be limited to forming visualisations occasionally supported with calculations: rather it should determine the content of all stages of the work (from conception to implementation) concerning an object of any scope. It should solve not only aesthetic illumination tasks but also really improve living conditions and generate positive results.

It follows from these conclusions that creating a school of the light design is a complex task, the solution of which demands knowledge integration across various fields of science and technology, critical analysis of the available domestic and international experience, development of correspondent programmes and training techniques.

REFERENCES

1. On the subject of the article of Bystryantseva N.V., Lekus E.Yu. and Matveeva N.V.. School of the

domestic light design: strategy and tactics// Svetotekhnika, 2015, # 4, pp. 65 – 66 (Karpenko V.E., Lebedkova S.M., Ovcharov A.T., Sanzharov V.B., Silkina M.A., Snetkov V.Yu, Hadzhin A.G., Shchepetkov N.I.) // Svetotekhnika. 2015, # 5, pp.60 – 68.

2. *Cuttle C.* Lighting by Design. 2nd ed. Architectural Press, 2008. 224 p. URL: eknigi.org (Addressing date: 09.2015).

3. *Ganslandt R., Hofmann H.* Handbook of Lighting Design.—Erco edition, 1992, 289 p. URL: <http://www.erco.com> (Addressing date: 09.2015).

4. *Gusev N.M., Makarevich V.G.* Light architecture. Stroiizdat, Moscow, 1973, 248 p.

5. *Shchepetkov N.I.* Light design of a city. Moscow: Architecture-C, 2006, 320 p.

6. *Rams D.*: ten principles for good design. URL: <https://www.vitsoe.com/eg/about/good-design>(Addressing date: 09.2015).

7. *Raynham P.J.* Public lighting in cities. In the book “City.People.Light. Future urban lighting concepts”. LUCI, 2007.

8. *Tulla A.* Three ways to light a building façade. URL: <http://luxreview.com/design-clinic/2014/11/three-ways-to-light-a-building-facade>.

FROM THE EDITORIAL TEAM:

The editors invite comments and responses to E. Nilov and V. Stepanov’s article. We will publish the most poignant commentary in a special discussion piece.



Egor E. Nilov,

an engineer. Graduated from the Moscow Power Institute (TU) in 2007 and the Moscow International Higher School of Business MIRBIS (Institute) in 2015.

The head of the Illumination Control Systems department of Philips light solutions Eurasia Open Company



Vitaly N. Stepanov,

Ph.D. Graduated from the Moscow Power Institute in 1976. A technical adviser of Philips light solutions Eurasia Open Company



Fig. 2. Light architectonics of order architecture:

Negative (*a* – Stock exchange building in St.-Petersburg) and positive (*b* – Church of St. Magdalene in Paris) contrasts of the colonnade and a second tier wall. Entablature of the Stock exchange’s periphery is visually ruined by the light strip on the frieze and cornice; Illumination of facades (*c* – Parthenon in Athenes, *d* – Victor Immanuel’s Palace in Rome). The luminance contrast of the colonnade and a wall fails to provide an expressive spatially-tectonic effect

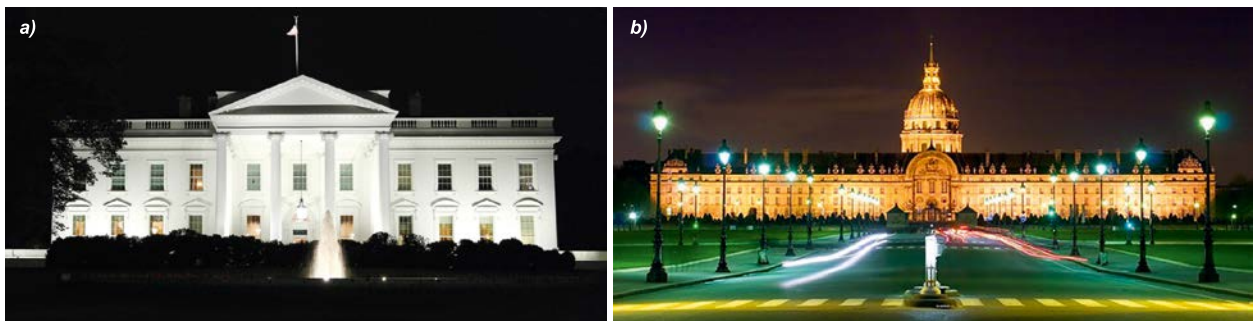


Fig. 3. A bathing architectural illumination effect using white light (*a* – the White House in Washington DC) and using colour light (*b* – Hôtel des Invalides in Paris)



Fig. 4. Different versions of the architectural illumination of the main facade of the Bolshoi Theatre in Moscow: *a* – previous, *b* – existing, *c* – computer generated (A.G. Batova)

Elena V. Barchugova and Nataliya A. Rohegova
Video Mapping from Presentation to Architecture



Fig. 1. Video mapping, exterior, interior and landscape examples: a) Metropol hotel building, Moscow, Winter fairytale show, 2013; b) Light Festival, Moscow, 2015, building of the Ministry of Defence of Russia; c, d – Birth of a new basketball team “ZENITH” festive sports show, St-Petersburg, 2014, the Author: *Illuminarium3000* company; e) a composition by Italian *Apparati Effimeri* company, f) Roman Festival of Light, 2015



Fig. 4. Interior theatrical video mapping. *Anarchy Dance* theatre of dance (established in 2010) Taipei, Taiwan. Temporary art integrity. A combination of architectural and video components on a parity basis

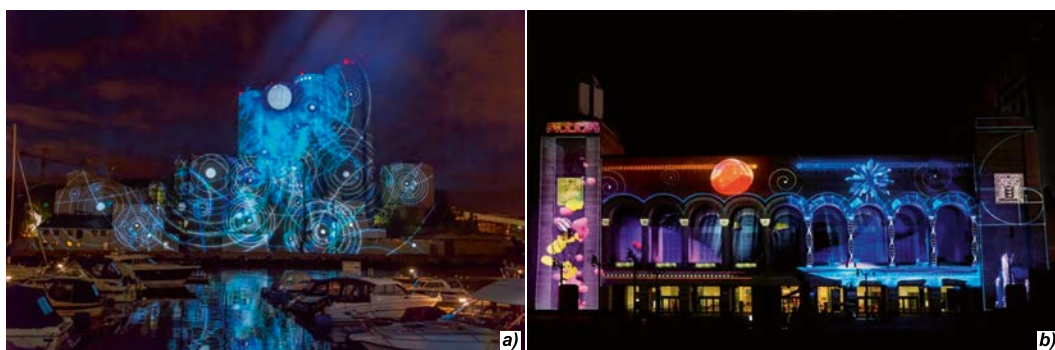


Fig. 5. Examples of neglect of the architectural component in presentation actions: a – Norwegian Festival, *Slemmestad*, 2014, the author: *Factory Light* company; b – *Moment Factory* company, decoration of the *Boardwalk Hall* building in Atlantic City, New Jersey state, the USA, 2012

Basic System for the Preliminary Experimental Photometric Characterization of a LED Based Luminaire

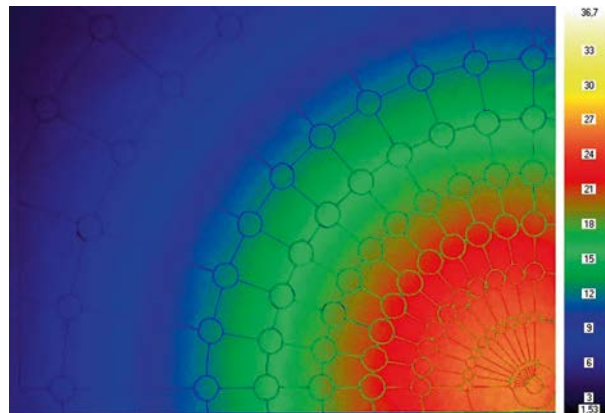


Fig. 4. Typical luminance colours distribution for targets surface #1 (in front of the light source)

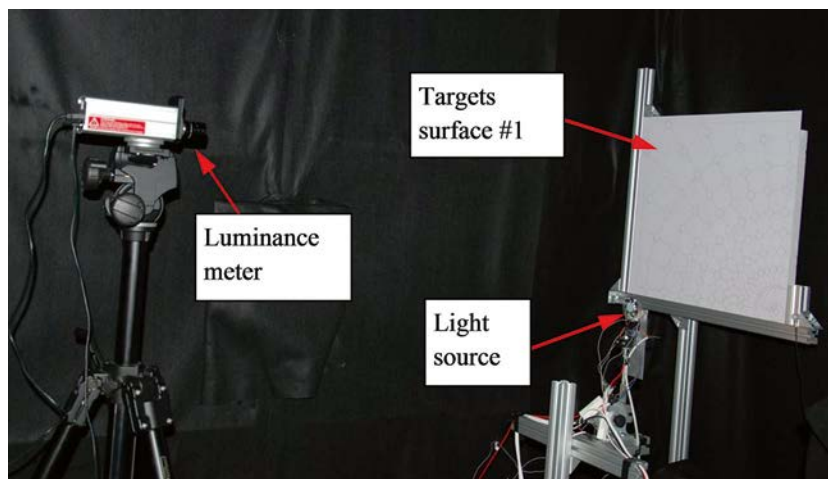


Fig. 5. Facility layout

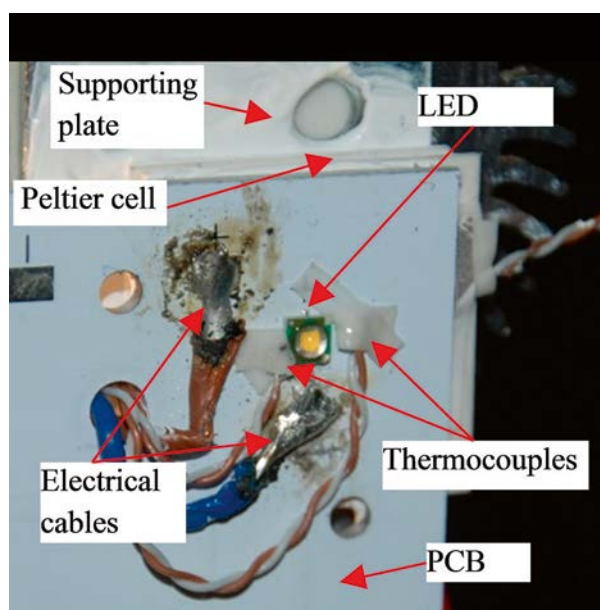


Fig. 6. Detail of the light source used for the calibration test

Investigation of Heat Transfer Types in an Automobile Fog Lamp with Computational Fluid Dynamic Analysis

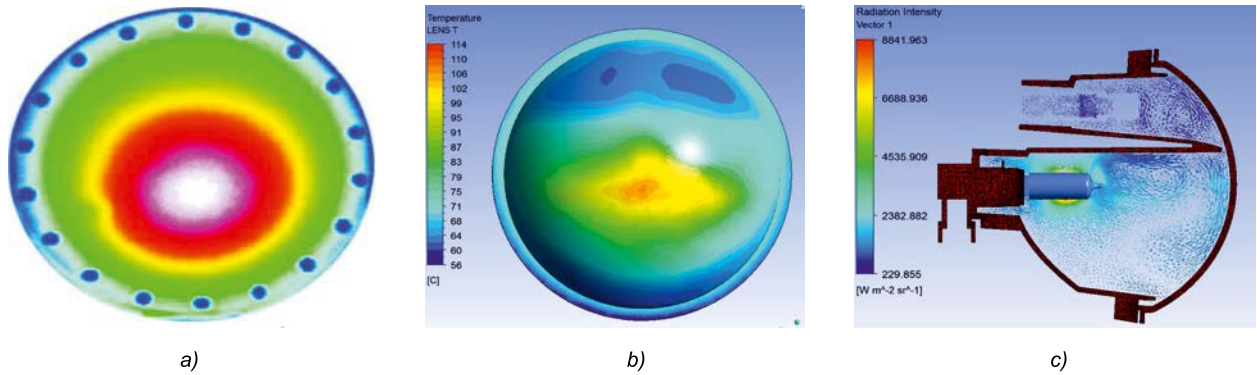


Fig. 8. a) Langebach et al. [34] $Ra = 2.101$; b) Temperature distribution on lens; c) Temperature distribution of internal air

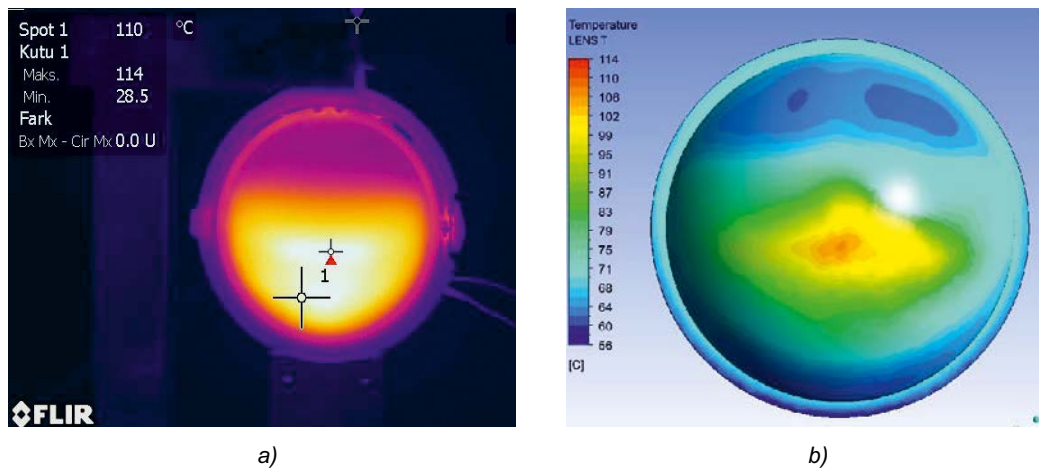


Fig. 9. a) Thermal camera picture during test; b) Temperature distribution on lens with Ansys CFX 12.1

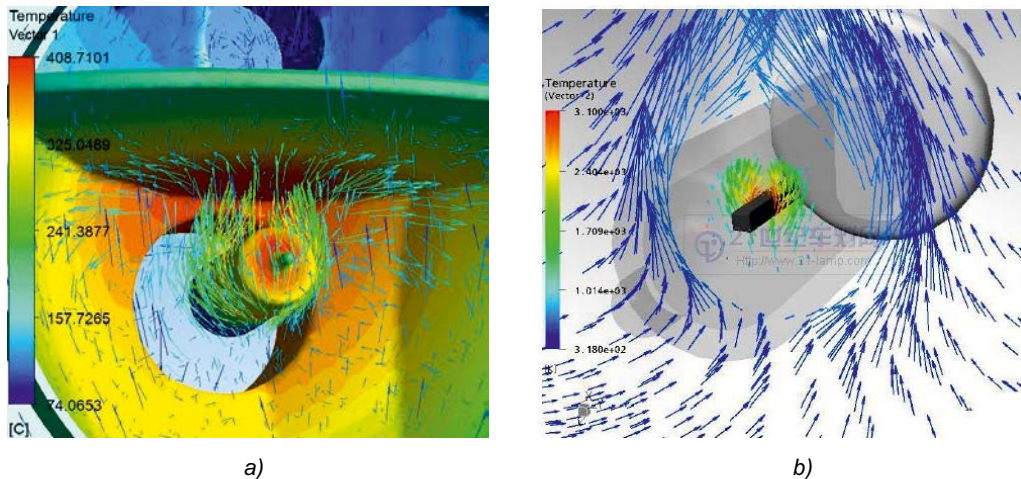


Fig. 11. Temperature distribution: a) around the H8 bulb in this study; b) in the Fischer study [8]

BASIC SYSTEM FOR THE PRELIMINARY EXPERIMENTAL PHOTOMETRIC CHARACTERIZATION OF A LED BASED LUMINAIRE

Giovanni Ciampi¹, Antonio Rosato¹, Michelangelo Scorpio², and Sergio Sibilio¹

¹*Second University of Naples, Department of Architecture and Industrial Design
"Luigi Vanvitelli", Built Environment Control Laboratory, Italy*

²*University of Sannio, Department of Engineering, Italy
E-mail: mscorpio@email.it*

ABSTRACT

This paper presents a simplified and low-cost system set-up for the photometric characterization of small Light Emitting Diodes based luminaires. The structure has a photometric bench within a dark room equipped with both a traditional luminance meter and an imaging luminance measurement device that acquires a luminance distribution of suitable targets upon which the luminous flux emitted by a light source strikes on. Starting from the acquired luminance distribution, the reflectance of the targets surface and considering the application of cosine square law, the luminous intensity distribution of the source considered can be easily obtained.

Information about the reliability and accuracy of the facility and the methodology have been deduced using a single light emitting diode as light source and comparing the experimental data with the manufacturer data.

Keywords: LED, imaging luminance measurement device, luminous intensity evaluation, luminous flux evaluation, luminance distribution acquisition

1. INTRODUCTION

With the growing use of solid state lighting (SSL) as light sources, it is more and more important to characterize the whole system of light source

and fixture, rather than the single source. Differently from luminaires using other types of light source, in the case of LED based luminaires the light source cannot be easily separated from the fixture. As consequence, they should be characterized by means of "absolute photometry" rather than the "relative photometry" [1]; this leads to a greater use of goniophotometers. Despite their advantage for the characterization of the LEDs, the goniophotometer use is affected by maintenance and purchase costs. In particular, the capital cost of a goniophotometer is more than 100,000 € and it increases at increasing of the size of the considered luminaire. In this perspective, it can be desirable to have a low cost system (compared with a goniophotometer) that allows the developing luminaire characterization from the photometric point of view and with appropriate accuracy.

Some authors have previously proposed a simplified approach for the photometric evaluation of artificial narrow-beam light sources [2].

In the present work, a simplified experimental apparatus set up is presented, which was developed at the Department of Architecture and Industrial Design "Luigi Vanvitelli" to evaluate the photometry of a LED source or a LED based small luminaire. The measurement methodology was described and the accuracy of the system was evaluated with the simplified application to a single LED source. The proposed apparatus is a system with purchasing and maintenance costs lower

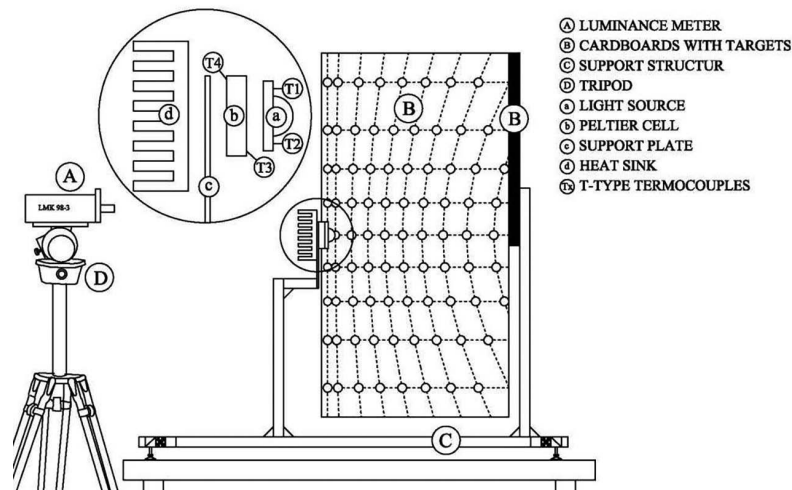


Fig. 1. Schematic view of the experimental set-up

than a goniophotometer system. It is able to give indicative results with an adequate accuracy and it can be used in every step of the design process of a new luminaire.

The apparatus developed allows evaluating the luminous intensity distribution into an entire half-space and can be applied not only to a light source with a narrow-beam photometry, but also to a source with any type of photometry distribution. In order to develop a low cost device, a simplified and cheaper material (cardboard) than Lambert's surface was considered for targets. The system is based on the use of an imaging luminance measurement device to acquire the luminance distribution produced by a light source on suitable targets and converting the luminance distribution into an illuminance distribution: the luminous intensity distribution of the light source analysed is deduced through the Lambert's law.

In order to evaluate the accuracy of the system, two different verifications were carried out. The first was made to control the measured luminance values, comparing the measurements performed with an imaging luminance measurement device and those carried out using a traditional luminance meter; the second evaluation was made to estimate the reliability and accuracy of the measurement methodology, comparing the experimental luminous intensity distribution of the analysed light source with that provided by the manufacturer.

2. EXPERIMENTAL SET-UP

At the Department of Architecture and Industrial Design "Luigi Vanvitelli", a dark room inside

a 3.0 m x 3.0 m (plan) x 3.0 m (height) opaque box was realized. According to Appendix A of the European Standard EN13032-1[3] and EN13032-4[4], the walls of the dark room were coated with a black textile attached to a rigid trestle with the aim of reducing the stray light as much as possible. By means of an air-conditioning system, the environmental temperature value of the room was controlled.

Fig. 1 shows a schematic view of the experimental apparatus designed and set-up. The system, placed in the dark room, consists of a supporting structure, a light source, a DC power supply, a Peltier cell, a heat sink, a data acquisition unit, an imaging luminance measurement device, and two targets surfaces.

The light source under consideration (a) was placed on and thermally connected to a Peltier cell (b) and fixed to a supporting plate (c) and a heat sink (d). Using the Peltier cell, it is possible to make the LED "junction temperature" stable with the generated heat dissipated by the heat sink. The supporting structure (C) is a modular structure realized using aluminium profiles and permits to rigidly assemble light source, target surfaces, instrumentations and all other items required by the measurements. The modular aluminium profiles allow to adjust the exact position of the light source. The luminous flux emitted by the light source falls on two targets surfaces (B) providing a luminance distribution that is captured by the luminance meter (A).

In the set-up presented, the target surfaces (B) were arranged to form an imaginary cube with an edge size of 1.000 m where the light source was placed in the centre; rotating the light source

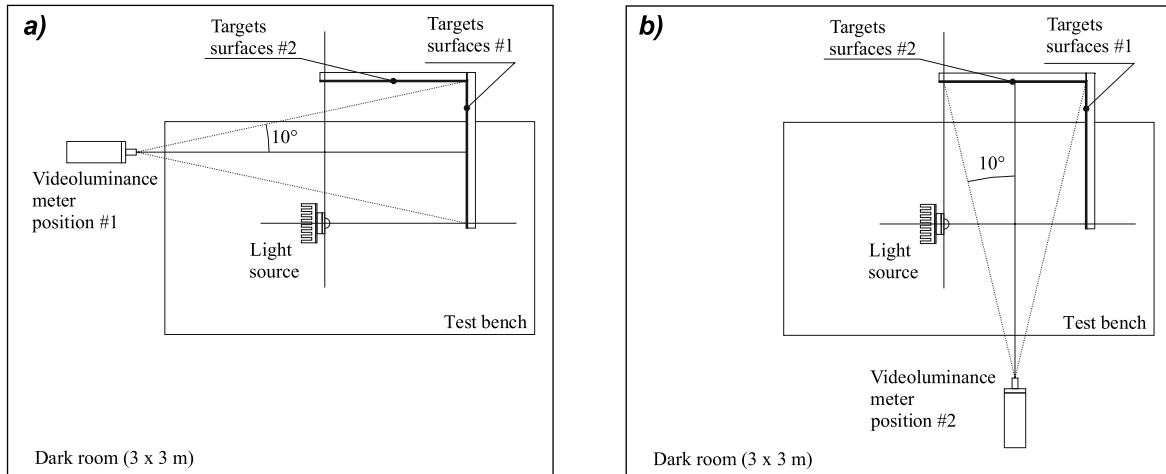


Fig. 2. Darkroom's layout with imaging luminance measurement device position #1 (a) and position #2 (b)

with step of 90° around $\gamma = 0^\circ$ axis, it is possible to examine the entire half-space. The targets surface #1 was placed on a vertical position in front of the light source at a distance of 0.500 m and targets surface #2 (also in a vertical position) was placed on the side of the light source, at a distance of 0.500 m from the source and on an orthogonal position to targets surface #1. Figs 2a and 2b show the layout of the dark room with the identification of the light source position, the two targets surfaces position and the two positions, in which the imaging luminance measurement device was placed to capture the luminance distribution on targets surfaces #1 (Fig. 2a) and the luminance distribution on targets surfaces #2 (Fig. 2b).

The $C-\gamma$ reference system [3,5] was chosen for the presentation of the luminous intensity distribution and consequently to identify the position of the targets. For the aim of this work, the luminous intensity evaluation was carried out considering angular steps of 5° for γ angles and 10° for C angles. The luminance meter (a traditional luminance meter or an imaging luminance measurement device) was placed on a professional photographic tripod equipped with a head that permits a precise movement in 3 directions. Finally, the current and voltage supply of LED and Peltier cell and temperature values were acquired and stored using a multi-meter FLUKE NetDAQ 2640A [6].

Thermocouples T-type (accuracy $\pm 1^\circ\text{C}$) were used to measure the temperature values in five different points of the systems: thermocouples (T1 and T2) were placed on the surface of the Printed Circuit Board (PCB) as close as possible to the LED source, thermocouple (T3) was placed on the

surface of Peltier cell, PCB side, thermocouple (T4) was placed on the other surface of Peltier cell and the last one (T5) was placed in proximity of the light source to control the environmental temperature.

The distance between emitting and targets area was chosen according to the photometric distance low. In this way, it is possible consider the light source as a point source and use the Lambert law for calculating the luminous intensity value with a negligible error lower than 0.5 % [7]. Defined the position of the light source, the Lambert law allows to calculate the value of the luminous intensity I_γ emitted by light source in a direction g , knowing the illuminance value E on a target in the direction γ , the distance d between light source and point considered, and the angle α between the normal to the surface of the considered target and the direction of the incident light, by the relation:

$$I_\gamma = \frac{E \cdot d^2}{\cos \alpha} \tag{1}$$

Considering the target's surface as a Lambertian surface, it is possible to use the relation:

$$E = \frac{\pi L_\gamma}{\rho} \tag{2}$$

where L_γ is the luminance value measured on the surface of the target in the direction γ and ρ is the reflectance value of the target's surface. Combining the eq. (1) and eq. (2), the relation used in this work to calculate the luminous intensity value in the direction γ is obtained:

$$I_{\gamma} = \frac{\pi \cdot L_{\gamma} \cdot d^2}{\rho \cdot \cos \alpha} \quad (3)$$

3. PHOTOMETRIC CHARACTERIZATION OF THE TARGETS

This study starts with the selection of an appropriate material for the target surfaces. In order to characterize the cardboard surface from the photometric point of view, for the different positions of the light source and luminance meter, the reflectance values and the deviation from a Lambertian diffuser were measured.

The reflectance values of the surface of the two cardboards have been measured with a spectrophotometer Konica Minolta 2600d (size of integrating sphere: $\varnothing 52$ mm, wavelength range: from 360 nm to 740 nm and spectral reflectance: standard deviation within 0.1 %); for every cardboard, three survey measurement points were considered. On each measuring point, the reflectance values were acquired for three different illuminants (A, D₅₀ and D₆₅) and, for every illuminant, they were acquired considering the Secular Component Included (SCI) and the Specular Component Excluded (SCE). The reflectance values acquired for different measurement points and for different illuminants, highlight that the percentage difference between the values obtained with and without the specular component ranges from 0.28 % to 0.33 %; this very small difference among the reflectance va-

lues acquired allows considering an overall mean reflectance value of 72.19 % for all the targets.

Fig. 3a shows the system arranged to evaluate the spatial variation of luminance values on the same point of a surface, evaluated by moving both the light source and the luminance meter according to a circular path; for each position of the luminance meter and light source, three acquisitions of the luminance value were performed.

In order to acquire the luminance values, a traditional luminance meter (LS110) [8] (acceptance angle = $1/3^\circ$, accuracy = $\pm 2\%$, ± 1 digit of measured value) was used. As reported in Figs. 2a and 2b considering the relative spatial position of the light source, the targets and luminance meter during the luminance distribution acquisition, the light emitted strikes on the targets with an angle that ranges from 0° to 55° . For this reason, the cardboard surface was characterized placing the light source at 0° , 30° and 55° with respect to the normal direction to the surface under investigation, whereas the luminance values were acquired for five directions -20° , -10° , 0° , 10° and 20° with respect to the normal direction to the surface. Assuming as a reference value the luminance L_0 evaluated at 0° , the relative percentage variation ΔL is calculated as:

$$\Delta L = \frac{L_{\theta} - L_0}{L_0} \times 100 [\%], \quad (4)$$

where L_{θ} is the luminance value measured in the direction θ .

Fig. 3b shows, for each light position, the percentage variations $\Delta L\%$ as a function of the diffe-

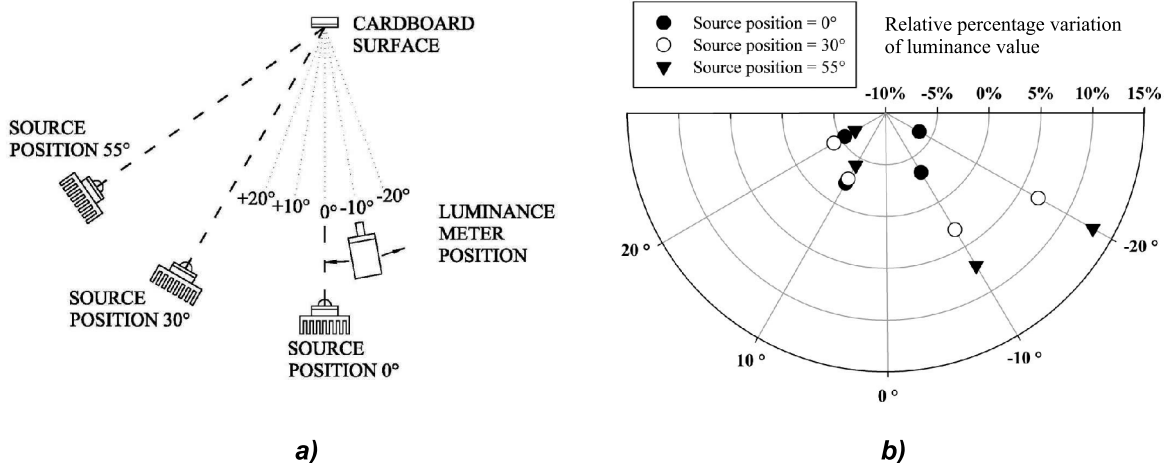


Fig. 3. System arranged to characterize the spatial variation of the luminance value for a surface (a) and the relative spatial percentage variation of luminance (b)

rent directions in which the luminance values were measured. From the diagram, it can be inferred that the percentage variation is always less than 10 %, except in the case in which the light source is at an angle of 55° and the luminance meter at an angle of -20° . Viewing the difference values plotted in Fig. 3b, the influence of the surface specula component can be identified; it can be seen, for the light source ranging at 30° and 55° , that the variation of the luminous distribution increases when the luminance meter moves to the direction of the specula reflection corresponding to -10° and to -20° .

For the purpose of this work and taking into account the experimental results, the cardboards surface (and then targets surface) has been approximated to a Lambert's surface. As a consequence of this hypothesis, the reflectance can be considered constant in all directions and thereby the luminance value acquired on a target is the same regardless the viewing angle.

4. METHODOLOGY

In order to consider the light source as a point source with a negligible error, the diffusely reflective surface was positioned in the far field.

The luminous intensity distribution of the light source is calculated, using eq. (3), starting from the acquisition of luminance distribution of the targets.

The measurements have been performed using a luminance and colour measuring camera LMK 98-3 Colour [9] manufactured by *TECHNO TEAM* [10] equipped with a CCD *Sony ICX 285 AL* with a resolution of 1380×1032 pixels and a pixel size of $6.45\mu\text{m} \times 6.45\mu\text{m}$. During tests, it was used a TT25 lens with a focal length of 25 mm and a measuring field angle of 19.9° (width) \times 15.1° (height); the instrument has a relative spectral response with correction factor f'_1 equal to 2.7 % and accuracy equal to $\pm 4.7\%$. The measured luminance data are stored as a colours distribution, where different colours correspond to different luminance values, or in table form where each pixel of picture is coupled with a luminance value; the luminance values are expressed for both colours distribution and table form in cd/m^2 .

Fig. 4 shows a typical acquired luminance distribution related to the white card board targets. As reported in Fig. 4, the cardboard surface has been formerly marked with concentric rings and circles

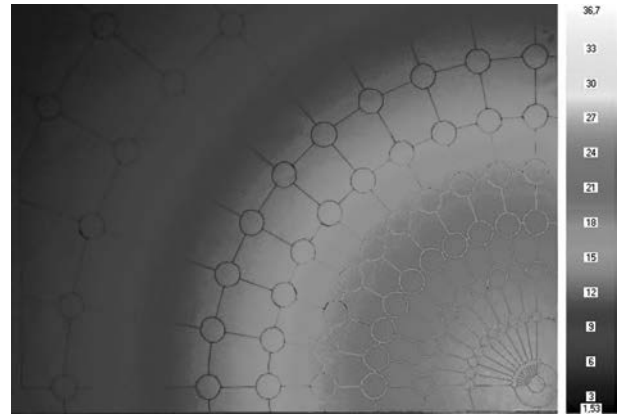


Fig. 4. Typical luminance colours distribution for targets surface #1 (in front of the light source)

corresponding to selected measurement points; the luminance is acquired for a circle with a diameter of $7.7 \text{ E-}03 \text{ m}$ with an area corresponding to 333 pixels of the CCD matrix. The luminance value attributed to this circle, used to derive the luminous intensity value in that direction, has been averaged from the 333 luminance values.

The acquisition has been developed in three steps:

- #1, were placed inside the dark room all the parts of the bench-test and thus were verified relative position and alignment;
- #2, were acquired the luminance values of all the targets marked upon the surface of the two white cardboards by the LMK imaging luminance measurement device equipped with the TT25 lens. Data acquisition started only when the electrical and thermal stabilization of the light source was achieved [4,11]. The acquired luminance distributions were processed using the LMK management software to obtain the luminance mean value for each target;
- #3, the results obtained from the luminance distribution were utilized in eq. (3) to derive the luminous intensity distribution.

Fig. 5 shows the layout of the experimental facility with the relative position of the luminance meter, the targets surface #1 and the light source.

Finally, in order to have a supplementary check for the luminance values acquired by the imaging luminance measurement device, some measurements were jointly carried out using also a traditional luminance meter [8] (model LS110 with an acceptance angle = $1/3^\circ$, accuracy = $\pm 2\%$, ± 1 digit of measured value). The luminance values on the targets were acquired placing, one at a time, the

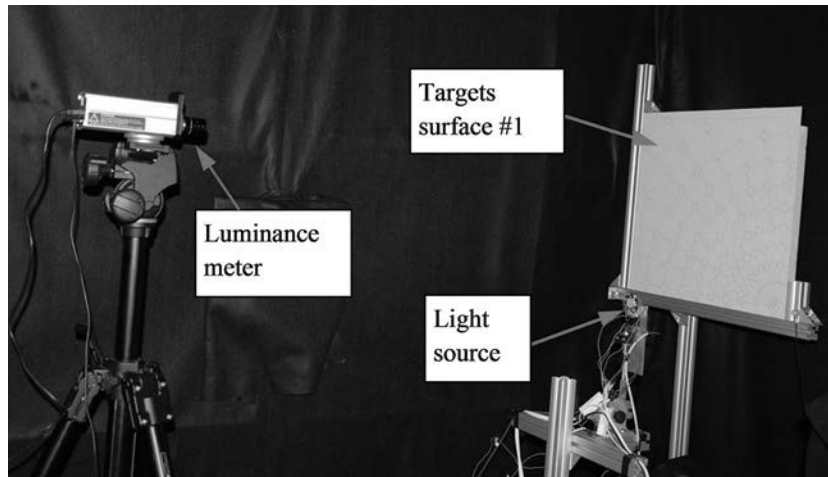


Fig. 5. Facility layout

two luminance meters in the same position and calculating the relative percentage error $e_{r,L}$, defined [12] as:

$$e_{r,L} = \frac{L_V - L_T}{L_T} \times 100 [\%], \quad (5)$$

where L_V is the luminance value acquired with the imaging luminance measurement device and L_T is the luminance value acquired with the traditional luminance meter assumed as a reference value.

The results show that $e_{r,L}$ is always lower than 6 %: it ranges from -5.71 % to 5.35 % and generally assumes negative values inferring that the luminance values acquired with the imaging luminance measurement device are generally lower than those acquired with the traditional luminance meter. In particular, on targets surface #1, the maximum percentage error was calculated for C40- γ 42.5 (LMK: 7.44 cd/m² – LS110: 7.76 cd/m² with a percentage error of -4.16 %) and on targets surface #2 for C70- γ 47.5 (LMK: 5.66 cd/m² – LS110: 6.00 cd/m² with a percentage error of -5.71 %).

5. RESULTS AND DISCUSSION

A Cree LED X-Lamp XP-E [13] with a declared value of the luminous flux of 35.409 lm, with an input wattage of 0.30 W was used as a light source to calibrate the facility and assess the methodology in terms of luminous intensity distribution and total luminous flux.

In order to achieve experimental results comparable with the manufacturer data, during the calibration test, the light source was supplied with

an input wattage of 0.30 W and a forward current of 105 mA. The junction temperature of the LED was kept constant for the duration of the test at a value of 25 °C, while the room temperature was kept at 21 °C; all the electrical and thermal parameters were controlled and stored throughout the entire test.

Fig. 6 shows a detailed description of the analysed light source equipped with PCB, the placement of the thermocouples T1 and T2 (Fig. 1), the electric cables, the Peltier cell and the supporting plate. Thermal conductive sticky tape was used to reduce the thermal resistance between the PCB surface and thermocouples.

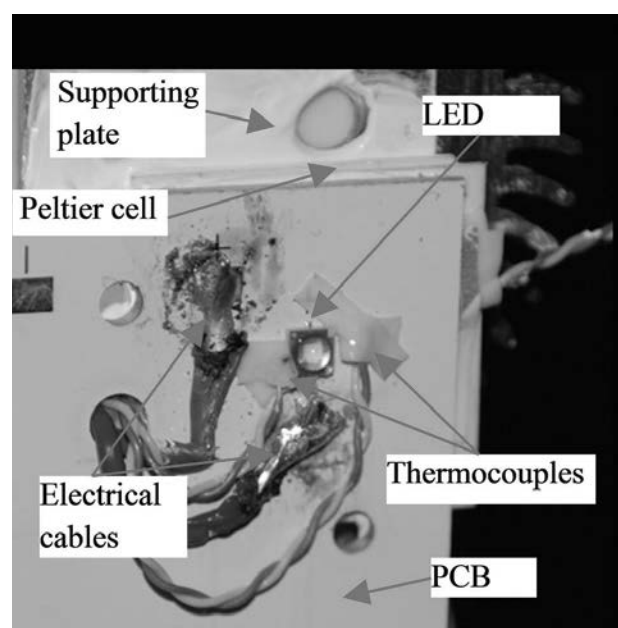


Fig. 6. Detail of the light source used for the calibration test

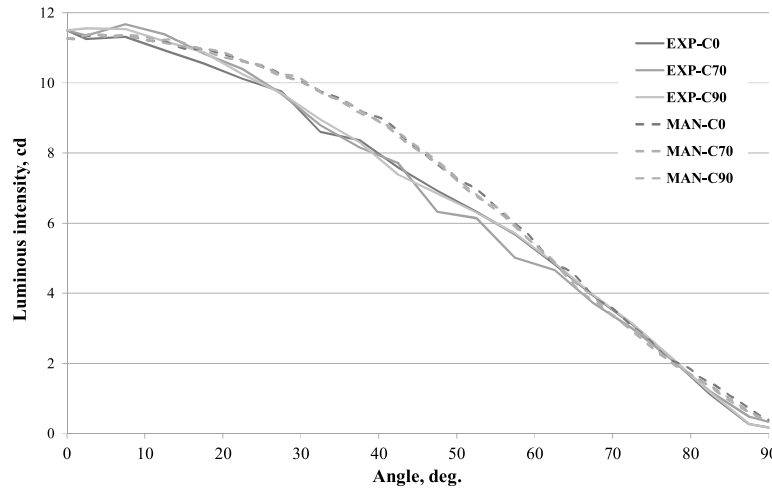


Fig. 7. Comparison between experimental and manufacturer luminous intensity distribution for C0, C90 and C70 (C-angle of maximum value of luminous intensity) and different γ -angles

In Fig. 7, the absolute luminous intensity distribution lines with reference to experimental (continuous line) and manufacturer (dashed line) data are plotted for three C-angle (C0, C70 and C90) and different γ -angle; C70 represent the C-angle, on which the maximum experimental value of the luminous intensity was detected.

The relative percentage error $e_{r, I}$ is calculated assuming the manufacturer data as reference values and it is defined [12] as:

$$e_{r, I} = \frac{I_{EXP} - I_{MAN}}{I_{MAN}} \times 100 [\%], \quad (6)$$

where I_{EXP} is the luminous intensity value calculated experimentally and I_{MAN} is the luminous intensity value from the manufacturer.

Fig. 7 shows a good agreement between the experimental and manufacturer data. In particular, it can be highlighted that while manufacturer data exhibit almost similar values of luminous intensity for the different γ -angle and C-angle, the experimental data are slightly affected by the specific direction. Analysing the experimental data, it is possible to identify four different ranges for the γ -angle, for which different values of the relative percentage error were observed:

- γ -angles between 0° and 30° , where the percentage errors are positive and negative and range from 2.77 % to -5.50 %;
- γ -angles between 30° and 60° , where the percentage errors are only negative and range from -4.16 % to -18.52 %;

- γ -angles between 60° and 80° , where the percentage errors are positive and negative and range from 7.61 % to -4.79 %;
- γ -angles between 80° and 90° , where the percentage errors are only negative. In this range of γ -angles, it is possible to see that the values of the percentage error are very variable. For the directions C70- $\gamma 82.5$, C70- $\gamma 90$ and C90- $\gamma 82.5$ the percentage errors are lower than 20 %, for the directions C0- $\gamma 82.5$ and C70- $\gamma 87.5$ the percentage errors are respectively equal to -22.42 % and -23.63 %, while for all other directions the percentage errors are greater than 40 %.

Considering eq. (6), the negative values of the percentage error involve that the experimental data are lower than manufacturer data. The large difference between experimental and manufacturer data was observed for γ -angles between 82.5° and 90° and can be charged to the electrical cables and thermocouples that spread the light emitted in these directions.

By means of the experimental data on the luminous intensity distribution of the analysed source, the total luminous flux was calculated.

The total luminous flux will be obtained as the sum of the single luminous flux calculated for all the directions. In this study, it was assumed that all the light emitted by the light source falls on an imaginary single half-sphere (where the source is located at the origin) and it was chosen to divide the half-sphere into 648 zones enclosed by the lines $\Delta C=10^\circ$ and $\Delta \gamma=5^\circ$, from which the solid angle was derived.

The value of total luminous flux derived by experimental measurements is equal to 31.49 lm, while

the value given by the manufacturer is of 35.409 lm. Comparing the experimental and manufacturer values of the total luminous flux and assuming the manufacturer value as a reference, it can be derived a relative percentage error [12] equal to -11 %. The experimental results confirm the potential utilization and improvement of the proposed system as it leads to comparable results presented in similar work [2].

6. CONCLUSIONS

In this paper, a simplified facility for small LED light source characterization, developed and set-up at the Built Environment Control Lab of the Department of Architecture and Industrial Design of Second University of Naples, has been presented and fully described. They have been listed the assumptions taken and the methodology followed as well as the results about the reliability and accuracy of the experimental results have been deduced. The aim of this work is to define an experimental device, by which it is possible to determine the luminous intensity distribution and the total luminous flux of a small LED based luminaire. The facility is intended to develop a system with purchasing and maintenance costs much lower than a goniophotometer system to obtain indicative results and which can be used in every step of the design process of a new luminaire.

The reliability and accuracy of the proposed facility and the methodology has been tested using a single LED as a light source and by comparing the experimental data with those available by the manufacturer. Differences have been observed in terms of both distribution and absolute values of the luminous intensity.

The results highlighted that the measurements are affected by the spatial distribution of the target surfaces reflectance and the relative positioning of the source and luminancemeter. Excluding the luminous intensity calculated in directions in which shading effects occur due to the electrical cables and the thermocouple, a maximum relative percentage error of -18.52 % was found. Final-

ly, a relative percentage error of -11 % between the experimental and manufacturer value of the total luminous flux was observed.

REFERENCES

1. IES LM-79-08, New York: Illuminating Engineering Society, 2008.
2. Bellia L, Spada G. Photometric characterization of small sources with high dynamic range illuminance mapping. *Lighting Research and Technology*, 2014, 46, pp. 329-340.
3. EN13032-1 Measurement and presentation of photometric data of lamps and luminaires. Part 1: Measurement and file format.
4. EN13032-4: Measurement and presentation of photometric data of lamps and luminaires. Part 4: LED lamps, modules and luminaires.
5. Commission Internationale de l'Eclairage, The photometry and goniophotometry of luminaires, CIE Publication 121, 1996.
6. http://us.flukecal.com/products/data-acquisition-and-test-equipment/data-acquisition/netdaq-networked-data-acquisition-unit?quick-tabs_product_details=2.
7. Commission Internationale de l'Eclairage, The measurement of absolute luminous intensity distribution, CIE Publication 70, 1987.
8. Konica Minolta, Luminance Meter LS110.
9. Techno Team, Luminance and color measuring camera LMK 98-3 Color.
10. TechnoTeam. Retrieved 24 November 2014, from http://www.technoteam.de/product_overview/rigo801/products/index_eng.html.
11. Commission Internationale de l'Eclairage, Test Method for LED Lamps, LED Luminaires and LED Modules, CIE International Standard S025/E:2015.
12. UNI CEI ENV 13005:2000 Guide to the Expression of Uncertainty in Measurement.
13. Cree. Retrieved 24 November 2014, from <http://www.cree.com/LED-Components-and-Modules/Products/XLamp/Discrete-Directional/XLamp-XPE>.

**Giovanni Ciampi,**

graduated in Energetic Engineering from University of Sannio (Italy) in 2012. At present, he is a Ph.D. Student in Scientific Disciplinary Sector ING-IND/11 at Second University of Naples, Department of Architecture and Industrial Design “Luigi Vanvitelli” (Aversa, Italy)

**Antonio Rosato,**

Ph.D. in Energetics, Associate Professor, graduated from University of Naples Federico II (Italy) in 2005, engineering faculty. At present, he is Associate Professor at the Department of Architecture and Industrial Design “Luigi Vanvitelli” of Second University of Naples

**Michelangelo Scorpio,**

Ph.D. in Environment and Structures Representation, Protection and Safety and Land Management, graduated from University of Naples Federico II (Italy) in 2008, engineering faculty. From August 2015, he is working as Research Assistant at the University of Sannio, Department of Engineering (Italy) on the “Characterization of smart windows for visual comfort and energy saving”

**Sergio Sibilio,**

Ph.D. in Applied Thermodynamics, Full Professor, graduated from University of Naples Federico II (Italy) in 1986, engineering faculty. At present, he is Full Professor at the Department of Architecture and Industrial Design “Luigi Vanvitelli” of Second University of Naples and scientific coordinator of Research Team E3 – Energy Efficiency & Environment

COMPARISON OF ROAD LIGHTING CALCULATIONS WITH MEASUREMENTS USING CONVENTIONAL AND CAMERA LUMINANCE METERS

Burcu Büyükkınacı¹, Sermin Onaygil², Önder Güler², and M. Berker Yurtseven²

¹*ISBAK Inc., Istanbul, Turkey*

²*Istanbul Technical University, Energy Institute, Istanbul, Turkey*

E-mail: bbuyukkinaci@isbak.com.tr

ABSTRACT

Istanbul Technical University (ITU) and Istanbul Transportation Communication and Security Technologies Inc. (ISBAK) with the support of Ministry of Science Industry and Technology (MOSIT) are carrying out a common project to develop a road lighting automation system with an ability of dimming luminous flux of the luminaires according to the traffic speed and flow. Before establishing such a system, where the road lighting levels change dynamically, we need to make visibility calculations under different road lighting scenarios. Visibility calculations are based on luminance measurements. The process of road lighting luminance measurements are time consuming if a conventional luminance meter is used since it can only perform point-by-point measurements. On the other hand, a camera luminance meter captures the luminance of the entire calculation field on the road scene which speeds up the measuring process. To find an easy way to make luminance measurements under many different road lighting scenarios, it is considered to use a camera luminance meter. In this study, a comparison of road lighting calculations with measurements using conventional and camera luminance meters are made and measurement results are given.

Keywords: camera luminance meter, luminance measurement, road lighting

1. INTRODUCTION

Before establishing any road lighting installation, calculations are made in order to determine the optimum lighting installation parameters for satisfying the desired road luminance levels. Computer software's are the most common tools for road lighting calculations today. These software's are capable of giving very similar results as the actual road lighting measurements as long as the design parameter data are entered properly.

European Standard EN13201-3 [1] and CIE140 Recommendations [2] describe how to carry out road lighting luminance measurements. It is required to measure the luminance of 60 separate measurement points on the calculation field, which is defined as the area between two lighting poles.

The measurements using conventional luminance meters are reliable but point by point measurement process is hard and very time consuming. The changing conditions, such as weather and traffic density makes it even harder to accomplish the overall road luminance measurements. There is also a danger for workers to conduct the measurement on road with active traffic flow. To solve these problems luminance measuring cameras are recently preferred for making the measurement process faster and easier. The camera luminance meter captures the luminance of the entire calculation field on the road scene which speeds up the measuring process. A luminance measuring cam-

era also allows multiple point measurements at the same instant.

This study is a comparison of conventional luminance meter, camera luminance meter and calculation software results for road lighting measurements under different road lighting classes.

The measurements are carried out on a test road, which is established in Istanbul Technical University (ITU) Ayazaga Campus in Istanbul, Turkey. The road is actually a test field for a common project of Istanbul Technical University and Istanbul Transportation Communication and Security Technologies Inc. (ISBAK), with the support of Ministry of Science Industry and Technology (MoSIT), titled as 0660.STZ.2014: "Developing Control Strategies for Road Lighting in the Context of Energy Efficiency and Creating Dimming Scenarios According to Visual Performance Requirements". This study is a confirmation of camera luminance meter results to decide to carry on with a camera luminance meter for future work.

2. LITERATURE REVIEW

It is possible to calibrate a camera for luminance measurements. To use a digital camera for measurement of luminance, one photographs a source of known luminance and thereby obtains the conversion factor that links luminance (in candela per square meter) to the value of a pixel in an image. Hiscocks, in his study, describes the calibration of the camera and the interpretation of the image data [3].

Wüller and Gabele suggested a method for the usage of digital still cameras as luminance meters independent of the exposure settings. A calibration of the camera is performed with the help of an OECF (optoelectronic conversion function) measurement and the luminance is calculated with the camera's digital RGB output values. They point out that, to use a digital camera as a luminance meter one has to consider that these cameras are not exact measuring instruments. Digital still cameras are constructed with a main focus on getting pleasant pictures out of the camera. However, for many applications the luminance results of a digital camera will be sufficient. There are measuring tasks, which do not need the absolute luminance value but, for example, the luminance distribution in the whole scene or luminance ratios [4].

Hongyi and Linjie introduced a new method that adopted recently developed high dynamic range (HDR) photogrammetry to measure the luminance and XYZ coordinates of millions of points across a road scene with the same device, a camera, and a MatLab code for data treatment and visualization. Eight HDR images of the roadway environments under different viewing conditions were generated using the HDR photogrammetric techniques and calibrated. From each HDR image, synchronous light and geometry data were extracted in Radiance and further analyzed to identify potential roadway environmental hazards using the MatLab code. The accuracy of luminance measurement was proven in the literature as averagely 1.5 % – 10.1 % [5].

Inanici researched the potential, limitations and applicability of the High Dynamic Range (HDR) photography technique as a luminance mapping tool. In his study, multiple exposure photographs of static scenes were taken with a commercially available digital camera to capture the wide luminance variation within the scenes. The camera response function was computationally derived by using Photosphere software, and was used to fuse the multiple photographs into an HDR image. The vignetting effects and point spread function of the camera and lens system were determined. Laboratory and field studies showed that the pixel values in the HDR photographs correspond to the physical quantity of luminance with reasonable precision and repeatability [6].

Manzano and Cabello evaluated the visibility levels for road lighting in Argentina by means of CCD image processing [7].

Under the sponsorship of the National Surface Transportation Safety Centre for Excellence (NSTSCE), an effort was undertaken to develop a system of image capture to analyze luminance data gathered in naturalistic driving research. The primary method used in this research was the calibration of smaller, more mobile luminance cameras through the use of an imaging photometer. In a controlled, static environment, images were captured simultaneously with both the luminance cameras as well as the imaging photometer. The luminance cameras enable adjustments to gain, shutter, and exposure variables and data were collected through varying combinations of such hardware configurations. Using known variables, such as gain and shutter and luminance camera re-

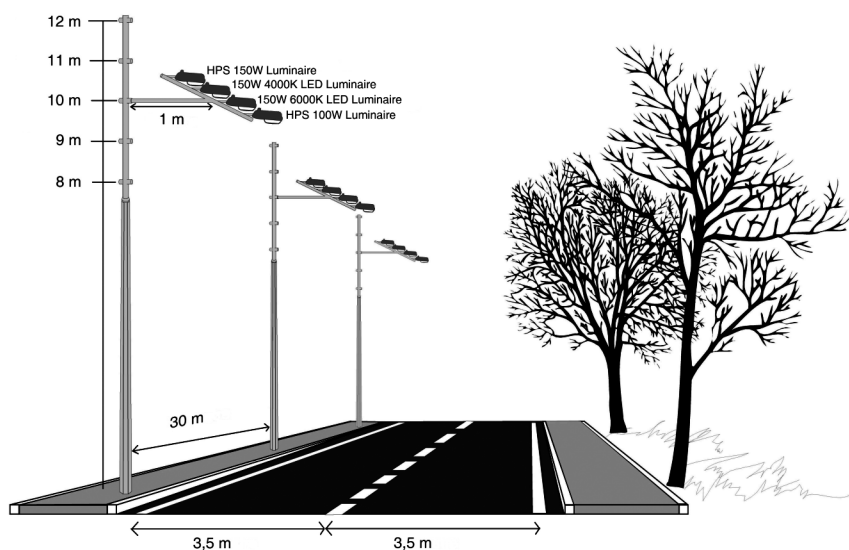


Fig. 1. ITU-ISBAK Test Road

turned gray values, the luminance was determined and compared to photometer-measured luminance. The accuracy of such comparisons was determined. Following this static calibration, luminance cameras were then installed in a vehicle and data were collected through a range of dynamic environments. Cameras were manually set to known gain and shutter values to capture a range of luminance values. The calibration of a luminance camera for recording luminance data was found to be successful with a relatively high level of accuracy, based on comparisons to known luminance values [8].

The Cerema and Ifsttar, two public institutes of the scientific network of the French Department of Transportation, are working to promote innovative camera-based solutions for assessing and improving highway visibility [9]. In this context, the Département Laboratoire et CECP d'Angers (DL-RCA) of Cerema has developed an innovative system for human visual signal capture, called CYCLOPE [10].

There are also already calibrated luminance measuring cameras and softwares available on the market [11]. These luminance measuring cameras capture images and calculate from the image data (gray values per pixel) the luminance in the respective points of the road. Thus, these luminance images contain information about the light and the geometry, thus permitting any measuring tasks to be solved in a very simple and time-efficient way. For

the photometric measurement of long stretches of roads, image series can be captured

Armas and Laugis used an LMK camera developed by the TechnoTeam Company for measuring roadway luminance [12, 13]. Ylinen et al. also used the LMK Mobile Advanced luminance measuring camera for evaluation of LED street lighting [14]. Ekrias et al. used LMK Mobile Advanced to make road lighting measurements for studying the impacts of vehicle headlights on luminance contrasts of targets located on the road [15].

In this study a LMK Mobile Advanced luminance measuring camera is used and the results are compared with a conventional point by point luminance meter.

3. GEOMETRY OF THE TEST ROAD

The test road is 250 meters long with two lanes. Each lane is 3.5 meters wide and the total width of the road is 7 meters. The road surface reflection property class is R4 with an average luminance coefficient of $0.08 \text{ cd/m}^2 \cdot \text{lx}$. Lighting arrangement is single sided from left. Eight lighting poles are installed with 30 meters spacing. The height of the lighting poles can be adjusted between eight to twelve meters and the overhang can be adjusted between 0.5 and 1.5 meters. Two luminaires with high pressure sodium lamp and two LED luminaires are placed on each pole. Luminous flux of the luminaires can be dimmed to desired level. Thus, different quality criteria can be ensured for

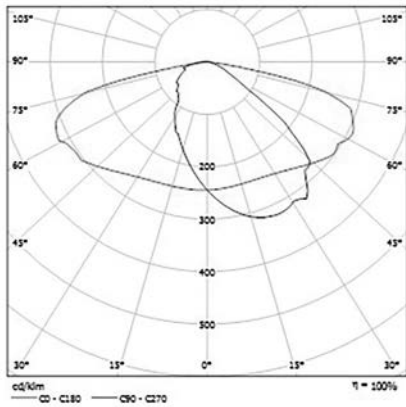


Fig. 2. ISBAK Lightra Power LXMLED150W luminance distribution

different lighting classes on the test road. The geometry of the test road and installation parameters is shown in Fig. 1.

The luminous intensity distribution is measured in ITU Energy Institute Energy Efficiency and

Lighting Technique Laboratories using Radiant Near Field Measurement System. Light Intensity Diagram is given in Fig. 2.

The luminous flux for corresponding dimming levels (1–10V control system) of ISBAK LightraPower LXMLED150W LED luminaire is measured in ITU Energy Institute Energy Efficiency and Lighting Technique Laboratories using Labsphere Ulbricht Sphere. The total luminous flux of the LED luminaire is measured as 19240 lm with a total power consumption of 152.2 W at nominal operation condition. The change in luminous flux for different dim levels as measured is given in Fig. 3.

4. CALCULATIONS AND FIELD MEASUREMENTS

Road lighting calculations of the test road, geometry of which is given in section 3, are carried out with Dialux 4.11 Software using different lu-

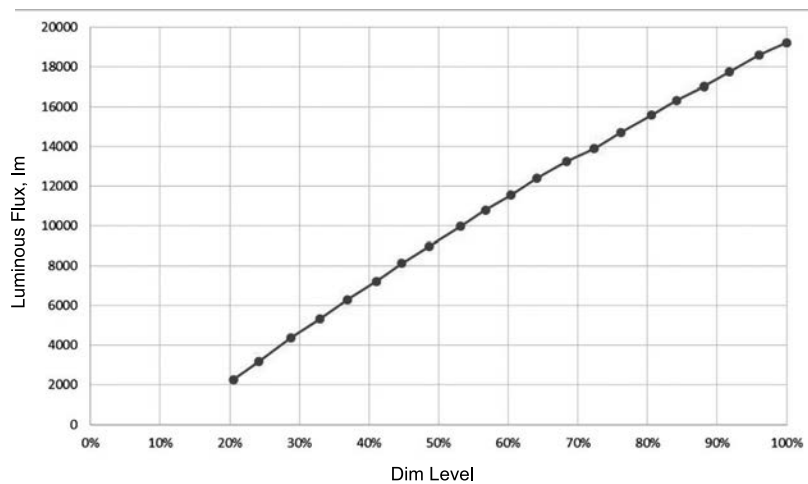


Fig. 3. Dim level vs luminous flux



Fig. 4. Test road luminance camera image

Table 1. Calculation results for different road lighting classes

M2			M3			M4			M5		
L_{avg} , cd/m ²	U_o	U_l	L_{avg} , cd/m ²	U_o	U_l	L_{avg} , cd/m ²	U_o	U_l	L_{avg} , cd/m ²	U_o	U_l
1.52	0.58	0.90	0.99	0.58	0.90	0.76	0.58	0.90	0.49	0.58	0.90

Table 2. Dimming levels, average luminance values and luminaire power consumptions for different scenarios

Road Lighting Class	Dimming Level, %	Luminous Flux, lm	Power Consumption, W
M2	56	10900	78.47
M3	36	7116	50.12
M4	27	5412	38.15
M5	17	3519	25.35

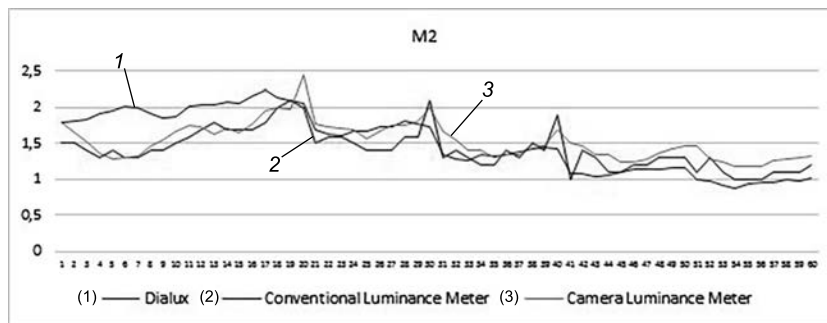


Fig. 5. Calculation and measurement results with conventional and camera luminance meters for all 60 points, for M2

luminous flux values given in Fig. 3, to ensure M2, M3, M4 and M5 road lighting classes. Since the installation is new, the lumen depreciation is not taken into account. In order to compare calculation and measurement results the maintenance factor is taken as 1.0. The calculation results are given in Table 1.

For field study, 6000 K LED luminaires, which are equipped with 1–10V control system, are dimmed to the required luminous flux values for each lighting class. Adjusted dimming levels, luminous flux and luminaire power consumptions for different road lighting classes are given in Table 2.

60 measurement points according to EN13201–3 [1] and CIE140 [2] are marked on the calculation area on the test road. LED luminaires are dimmed to different levels to ensure the desired luminance levels for M2, M3, M4 and M5 road lighting classes. Field measurements are carried out with both conventional and camera luminance meters under four scenarios, for fixed observer at 60 me-

ters as given in EN13201–3[1]. A sample photograph taken with luminance camera for measurement is shown in Fig. 4.

Calculation and measurement results with conventional and camera luminance meters for all 60 points, are given as graphics in Figs. 5–8 for M2, M3, M4 and M5 lighting classes, respectively.

Average road surface luminance calculations and measurement results for both conventional luminance meter and camera luminance meter are given together in Table 3.

Average and longitudinal luminance uniformities for different scenarios are given in Table 4.

5. RESULTS AND CONCLUSION

The point by point measurement process with a conventional luminance meter is hard and very time consuming. The changing conditions, such as weather and traffic density, make it even harder to accomplish the overall road luminance measu-

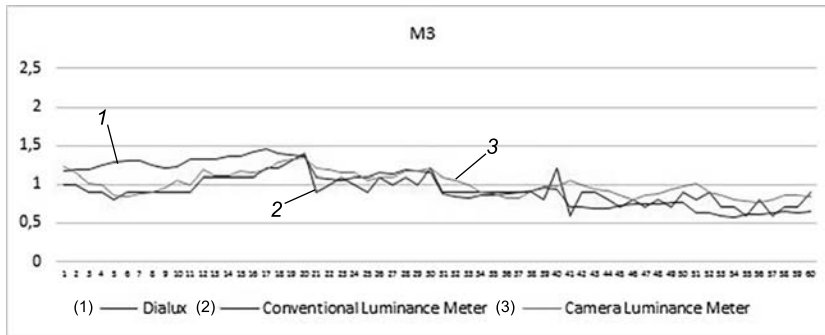


Fig. 6. Calculation and measurement results with conventional and camera luminance meters for all 60 points, for M3

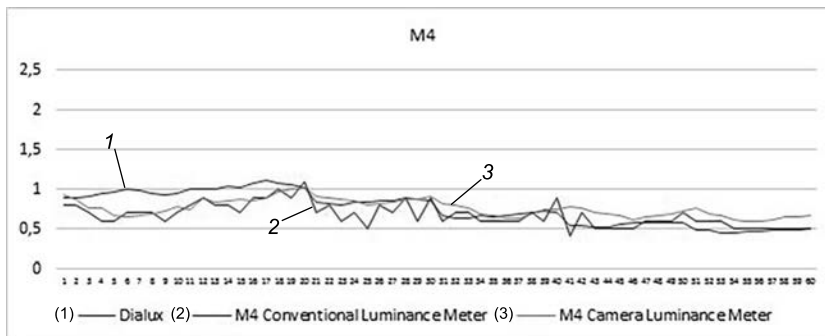


Fig. 7. Calculation and measurement results with conventional and camera luminance meters for all 60 points, for M4

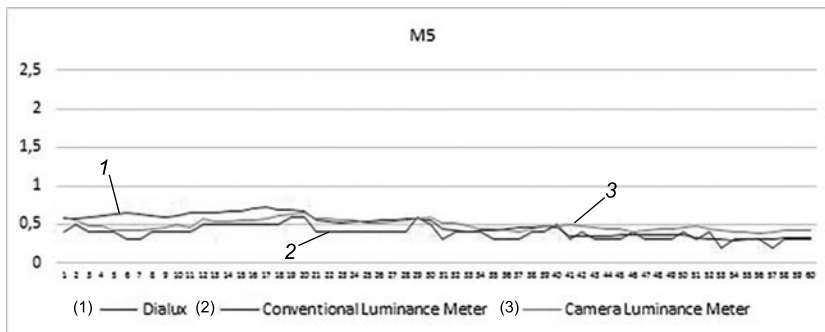


Fig. 8. Calculation and measurement results with conventional and camera luminance meters for all 60 points, for M5

rements. There is also a danger for workers to conduct the measurement on road with active traffic flow. Especially, when there is a need to make several measurements, work load increases more. To find an easy way to make luminance measurements camera luminance meters are used recently.

In order to validate the use of camera luminance meter for road lighting luminance measurements, four different lighting classes on the test road, road lighting calculations are carried out with Dialux 4.11 software and field measurements are carried out with both conventional and camera luminance meters under four scenarios, for fixed observer at 60 meters as given in EN13201–3. When all calculation and measurement results are compared, followings are found:

- Although the results of 60 points show differences which can be seen from Figs. 5–8, average road luminance values are found to be similar for calculation and camera luminance measurements. Conventional luminance meter results are lower than both calculation and camera luminance measurement results for average values.
- Average luminance uniformity and longitudinal uniformity measured with conventional luminance meter is closer to calculation results but camera luminance meter measurements are found to be higher for average luminance uniformity and lower for longitudinal uniformity, than both conventional luminance meter and calculation results. It is thought that, the reason may be the coordinate of the 60 points, defined in EN13201–3, do

Table 3. Average road surface luminance according to calculations, conventional luminance meter and camera luminance meter measurement results [cd/m²]

	Calculation	Camera Luminance Meter	Conventional Luminance Meter
M2	1.52	1.54	1.42
M3	0.99	1.01	0.92
M4	0.76	0.76	0.67
M5	0.49	0.49	0.39

Table 4. Average and longitudinal uniformities

	M2		M3		M4		M5	
	U _o	U _l	U _o	U _l	U _o	U _l	U _o	U _l
Calculation	0.58	0.90	0.58	0.90	0.58	0.90	0.58	0.90
Conventional Luminance Meter	0.71	0.93	0.65	1.00	0.59	0.86	0.52	1.00
Camera Luminance Meter	0.77	0.83	0.77	0.77	0.78	0.78	0.80	0.80

not collide with each other for measurements and calculations. For conventional luminance meter measurements, the 60 points are exactly marked on the road according to EN13201–3, while these points are determined by the software used for camera luminance meter.

It is shown by this study that, camera luminance meter results are acceptable for road lighting measurements, which provides advantages for saving time in road lighting research and applications.

ACKNOWLEDGEMENT

The authors would like to thank the MoSIT and ISBAK for funding the ITU within the scope of San-Tez 0660.STZ.2014 project.

REFERENCES

1. EN13201–3 Road lighting Part 3: Calculation of Performance. Publication 270–2003.
2. CIE140–2000 Road Lighting Calculations, International Commission on Illumination, 2000.
3. Peter D. Hiscocks, P. Eng, Measuring Luminance with a Digital Camera, 16 February 2014 (<http://www.ee.ryerson.ca/~phiscock/astronomy/light-pollution/luminance-notes-2.pdf>).
4. DietmarWüllera, HelkeGabeleb, The usage of digital cameras as luminance meters Proc. SPIE6502, Digital Photography III, 65020U (20 February 2007).

5. HongyiCai*, Linjie Li, Measuring Light and Geometry Data of Roadway Environments with a Camera, Journal of Transportation Technologies, 2014, 4, pp. 44–62.
6. MN Inanici, Evaluation of high dynamic range photography as a luminance data acquisition system, Lighting Res. Technol. 38,2 (2006) pp. 123–136.
7. Manzano E.R., Cabello A.J., Visibility Measurements with CCD in Road Lighting, IngineriaIluminatului (Lighting Engineering), issue 4 – March 2000
8. Jason E. Meyer, Ronald B. Gibbons, Christopher J. Edwards, Development and Validation of a Luminance Camera Final Report, Submitted: February 11, 2009.
9. Aubert, D., Boucher, V., Bremond, R., Charbonnier, P., Cord, A., Dumont, E., Foucher, P., Fournela, F., Greffier, F., Gruyer, D., Hautiere, N., Muzet, V., Nicolle, P. And Tarel, J. – P., Digital imaging for assessing and improving highway visibility, In Proc. of Transport Research Arena (TRA' 2014), Paris.
10. Boucher, V., Greffier, F. And Fournela F., High speed acquisition system of photo-colorimetric images to record and model the human visual signal, In Proc. SPIE7073, Applications of Digital Image Processing XXXI.,2008.
11. TechnoTeam, n.d., “LMK Mobile Advanced Specification,” 2012. (http://www.technoteam.de/products/lmk_luminance_measuring_camera/lmk_mobile_advanced/index_eng.html).

12. J. Armas, J. Laugis, "Road Safety by Improved Road Lighting: Road Lighting Measurements and Analysis," 2007. http://egdk.ttu.ee/files/kuressaare2007/Kuressaare2007_83Armas-Laugis.pdf.

13. J. Armas, J. Laugis, "Increase Pedestrian Safety by Critical Crossroads: Lighting Measurements and Analysis," The 12th European Conference on Power Electronics and Applications, Aalborg, 2–5 September 2007, pp. 1–10.

14. A. Ylinen, L. Tahkamo, M. Puolakka and L. Halonen, "Road Lighting Quality, Energy Efficiency,

and Mesopic Design-LED Street Lighting Case Study," LEUKOS, Vol. 8, No. 1, 2011, pp. 9–24.

15. A. Ekrias, M. Eloholma, L. Halonen, The Contribution of Vehicle Headlights to Visibility of Target in Road Lighting Environments, International Review of Electrical Engineering (I.R.E.E.), Vol. 3, N. 1, January – February 2008.



Burcu Büyükkınacı

received the Diploma in Electrical Engineering from Yıldız Technical University in 2002 and M. Sc. degree in Energy Science and Technology program from Istanbul Technical University in 2008. She is studying for a Ph.D. in Istanbul Technical University. Her field of study is road lighting and automation scenarios for road lighting systems. She is a R&D Engineer at Istanbul Metropolitan Municipality ISBAK Istanbul Transportation Communication and Security Technologies Inc.



Sermin Onaygil,

general illumination techniques as well as road and tunnel lighting, lighting automation and energy efficient measures in lighting can be listed within her basic working areas. She is the founder member of Turkish National Committee on Illumination and currently she is the Vice President of the Committee. She represents Turkey in Division 4 of International Commission on Illumination entitled *Lighting and Signaling for Transport* and actively takes part in various kinds of studies within this division. Sermin Onaygil works as an academic at the Energy

Institute in Istanbul Technical University and she is the chairman of Energy Planning and Management Division within this Institute. She actively takes part in the projects on energy efficient lighting solutions in cooperation with the Ministry of Energy and Natural Resources and she also directs master and Ph.D. thesis in these study field



Önder Güler

received the B.Sc., M.Sc. and Ph.D. degrees in Electrical Engineering Department from the Istanbul Technical University (ITU) in 1991, 1995 and 2001 respectively. He worked as a research and teaching assistant in Electrical Engineering Department between 1994 and 2003. He has been working as a Professor at Energy Institute of ITU since 2015. His research area are road lighting, energy saving, energy management in industry and building, wind energy, electrical energy quality. Dr. Güler is a member of Turkish National Illumination Committee and Chamber of Electrical Engineers



M. Berker Yurtseven

graduated from Istanbul University, Mechanical Engineering Department in 2003. He got the M.Sc. degree from Istanbul Technical University, Energy Institute in 2006. His research interests include photometric and radiometric measurements of LEDs, thermal management and statistical analyses

ARTIFICIAL NEURAL NETWORK MODELLING OF COLOUR TEMPERATURE VARIATIONS WITH DIFFERENT TYPES OF ARMATURES AND LIGHT SOURCES

Aysel ERSOY YILMAZ

*Istanbul University Engineering Faculty, Electrical-Electronics
Engineering Dept., Istanbul, Turkey
E-mail: aersoy@istanbul.edu.tr*

ABSTRACT

The continually growing demand for energy and the related resource problems have increased the importance of detailed consumption habits. A significant percentage – approximately 20 % at present – of the total electrical energy consumed is used in residential areas, in the work-place, and for street and road lighting. In the past, lighting was mainly used to improve visibility and safety, but efficiency and aesthetics are now playing a big role in the lighting sector, hence different types of lamps are now sold on the market. In this study incandescent, compact fluorescent and LED type lamps, which are widely used among the customers, were selected as different types of light sources. To represent the different armature types transparent glass prisms were prepared with different thickness and shapes. Initially the colour temperature of incandescent, compact fluorescent and LED type lamps was recorded under laboratory conditions. The aim of this study is to model an artificial neural network (ANN) for estimating colour temperature values from obtained input values. When obtained and estimated data are compared, it is observed that the estimation process and method is successful for this type of data.

Keywords: colour temperature (T_c), correlated colour temperature (CCT), artificial neural network, residential lighting, brightness, lamps

1. INTRODUCTION

Whilst lighting is a major need in many sectors, it is also one of the core needs of many people. Studies carried out in medicine and engineering have shown that lighting in an area affects people psychologically [1–4], hence by using this effect, people senses are frequently manipulated for trading purposes. Shops, which set up their lighting in a particular way around certain products, will attract the customer to buy that item [5]. In the same way, it is possible to manage people perceptions using a suitably lit stage or by applying special lighting to a scene. The colour of the lighting, and also the temperature of the light emitted, has a major effect here [4–10]. The simplest way to measure the colour of the light is to determine its colour temperature value. Colour temperature describes the appearance of light provided by a light source. The correlated colour temperature of a selective radiator is the temperature at which a black-body would produce the same colour as that of the selective radiator. It is measured in Kelvin (K), [10]. For incandescent lamps the term colour temperature (T_c) is applicable instead of correlated colour temperature (CCT), which is used for light sources with much differ spectrum. The colours in artificial light are divided mainly into three classes according to the colour temperature. This classification is hot colours with colour temperature values below 3300K, warm colours with colour tempera-

ture values between 3300K and 5500K, and cold colours with colour temperature values above 5300 K. In this classification the hot colours are towards the red end of the spectrum whilst the cold temperatures are towards the blue end [9–10]. To display the products in the best way and also in order to increase sales, the bakery aisle is lit with colour temperatures from 3000 K to 4000K, the drinks aisle from 4000K to 6000 K, the fruit and vegetable aisle from 3000 K to 4000K, the dairy aisle at approximately 4000 K and the meat aisle from 3000K to 4000 K [9].

A study in Turkey about the lighting sources used in shopping malls claimed that the use of low level lighting with high colour temperature made the area dull and oppressive whilst high level lighting with low colour temperature made the area feel artificial and remote [5]. In a similar study on residential areas, it is claimed that low colour temperature lighting is necessary in areas used for rest [8]. Sitting rooms, which people use for long periods, should be lit with low colour temperatures – not with white, light blue or other light colours having high CCT. As a common consensus, it is recommended that the activity and colour temperature should be chosen in a way to improve visual comfort [8–12].

Brightness (of a perceived aperture colour) is defined as the attribute by which an area of colour of finite size is perceived to emit, transmit, or reflect a greater or lesser amount of light. No judgment is made as to whether the light comes from a reflecting, transmitting or self-luminous object [10]. It is measured in cd/m^2 and gives an idea for the efficiency of the light source.

The aim of this study is to investigate and model the armature effect on the characteristics of the light source. For this purpose the most widely used light bulbs in residential lighting; incandescent wired, compact fluorescent and LED type lights were selected. Initially, the lights were tested in an experimental unit to measure light level, brightness and colour temperature.

While investigating the effect of prepared armatures (glass prisms) over the light source; the light source is radiated on a white paper cylinder and the reflected light over the paper cylinder to the prepared armatures were measured.

At the next stage the effect of glass housing with different shapes such as triangular, rectangular and pentagonal prisms and with different thicknesses

(2mm and 4mm) but equal properties were used to represent different type of armatures. By using the measured values, such as the brightness and colour temperatures, an artificial neural network (ANN) algorithm is trained finally these values are estimated successfully according to the thickness and shape of the prepared glass housing.

2. MATERIALS AND SYSTEM

Several types of lamps, which are widely used in residential lighting, were chosen for this study. Initially, an incandescent wire lamp, with a power of 28 W and a colour temperature of 2800 K, was selected. At the next stage, a white light compact fluorescent lamp with a power of 23 W and a colour temperature of 6500 K, was selected. Finally, a LED lamp, with a power of 4.8 W and CCT 4000 K, was selected. Before starting the experiment, all of the lamps were lit for min. 100 hours in order to enable proper ageing of the lamps and hence to simulate normal operating conditions. The measuring equipment is drawn in Fig. 1.a. For lighting measurements, day light entering from doors or windows in the area can affect the accuracy of the results, hence the measurements were made in a light-tight box with the dimensions of 100 x 100 x 100 cm and which is at least 10 times bigger than the light sources. To measure the colour temperature and brightness of the light source, reflection, absorption and transmission properties were taken into account by using a white paper cylinder with a diameter of 10 cm. Measurements were taken on the middle point of the perpendicular surface, Fig. 1.b. A Konica-Minolta CS-200 Chroma Meter was used during the measurements. The angle of the device was set to 0.1° aperture, which can focus on any specific item in the area the lamp illuminates and measure the light properties even of very small areas. Measurements are then transferred to a computer using a CS-S10w program to provide an analysis and sketch values in graphical form. Measurements are initially made only with paper; however, at the next stage; glass prisms manufactured in different ways were used to make the same measurements. Triangular, rectangular and pentagonal prisms, with the size of 30cm*30cm, were prepared by using glass sheets with two different thicknesses (2 mm and 4 mm). The laboratory conditions were kept stable for each measurement, which was repeated at least 5 times for each condition.

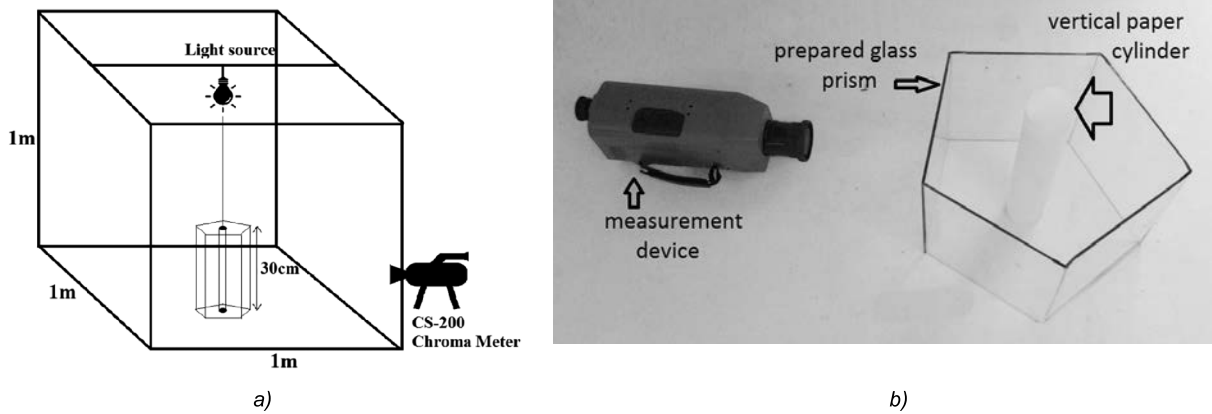


Fig.1 a) Experimental set up for brightness and colour temperature measurements;
 b) A photograph of inside installation of experimental set up

Artificial Neural Network

Artificial Neural Networks (ANN), created by modelling a human nerve cell neuron and, therefore, the learning and decision-making skills of the human brain, are methods used with the aim of transferring data to artificial systems. It is a method used as an alternative solution system when classic problem solving methods are insufficient or do not give satisfactory results. Artificial Neural Networks are used for prediction and optimization problems, using its nonlinearity and missing data completion capabilities [13–15]. Artificial Neural Networks are generally structured in three layers. The first layer reflects the input values of the problem, system or duration. So, the neuron (node) number equals the number of data entered. The final layer contains the same number of neurons as the results (output) that are expected to be obtained. The hidden layer between these two is the most important layer of the artificial neural network, and the number of neurons depends on the problem type, aim and usage method. No definite criteria are defined for how to determine the number of neurons in the hidden layer. Experience, trial and error, and good analysis of the problem structure enable the user to choose the correct number of neurons [15]. The ANN

structure is formed in three layers, called the input layer, hidden layer and output layer. It is depicted in Fig. 2.

In this study, feed forward neural network is used. Feed forward networks have one-way connections from the input to the output layers. They are most commonly used for the prediction, the recognition of the pattern, and the nonlinear function fitting. The training algorithm of this study is Levenberg-Marquardt (L–M) algorithm whose mathematical formulation is given below.

$$F(x) = \frac{1}{2} \sum_{i=1}^m [f_i(x)]^2 \tag{1}$$

3. RESULTS

In this study, initially, the brightness and colour temperatures of the lamps were measured. Values obtained from the measurements after the 100 hours aging of the lamps are given in Table 1. As a result of this measurement, the brightest lighting unit in this experiment was the LED, whilst the least bright was the incandescent lamp. When the lighting units in the experiment are compared by colour temperature, the compact fluorescent light has the highest colour temperature, whilst

Table 1. Brightness and colour temperature values of the analyzed lighting units

Light Source	Incandescent	LED	Compact Fluorescent Light
Brightness	1.82 cd/m ²	9.69 cd/m ²	7.82 cd/m ²
CCT	T _c = 2992 K	4375 K	6980 K

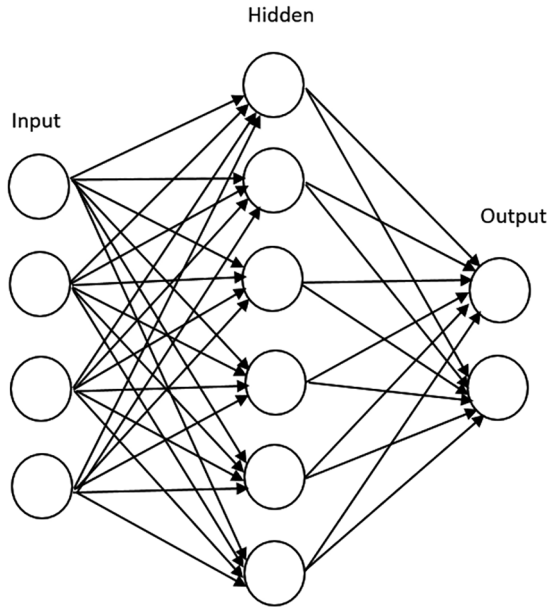


Fig. 2. ANN Structure

the incandescent wired lamp has the lowest colour temperature.

The white coloured cylinder, which has a diameter of 10cm, is placed inside the experimental unit and fitted with prisms of various thicknesses and shapes. Under these conditions, the brightness and colour temperature values measured from the cylinder for the incandescent wired lamp are given in Table 2. The highest brightness value at the end of this measurement was recorded with the 2 mm thick pentagonal prism, whilst the lowest brightness value was recorded with the experimental unit when no prism was used. When prism thickness is increasing from 2 mm to 4 mm brightness values is decreasing by 1.5 % in the triangular prism, 0.96 % in the rectangular prism, and 0.93 % in the pentagonal prism. Similarly, the highest colour temperature value was recorded with the 2 mm thick pen-

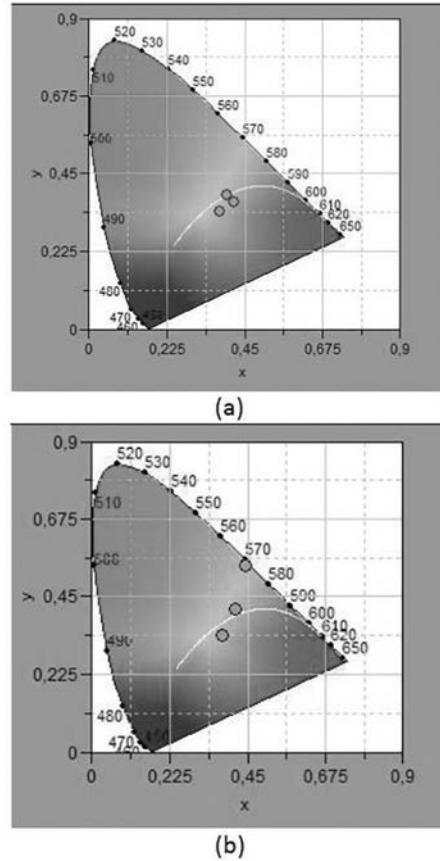


Fig. 3. Colour diagram of incandescent wired lamp; a) without a prism and with a 2 mm thick pentagonal prism; b) without a prism and with a 4 mm thick pentagonal prism

tagonal prism, whilst the lowest value was recorded from the experimental unit when no prism was used. When prism thickness was increased from 2 mm to 4 mm, colour temperature values decreased in triangular, rectangular and pentagonal prisms by 7.57 %, 0.40 % and 0.43 % respectively. Fig.3 shows the colour temperature diagram of the results from measurements taken with the white cylinder and lamp in cases where the incandescent

Table 2. Brightness and colour temperature values for the incandescent wired light in different situations

Glass thickness	Prism Type	Brightness, cd/m ²	T _c , K
-	NA	1.55	2425
2mm	Triangular Prism	2.01	3076
	Rectangular Prism	2.08	3225
	Pentagonal Prism	2.16	3730
4mm	Triangular Prism	1.98	2843
	Rectangular Prism	2.06	3212
	Pentagonal Prism	2.14	3714

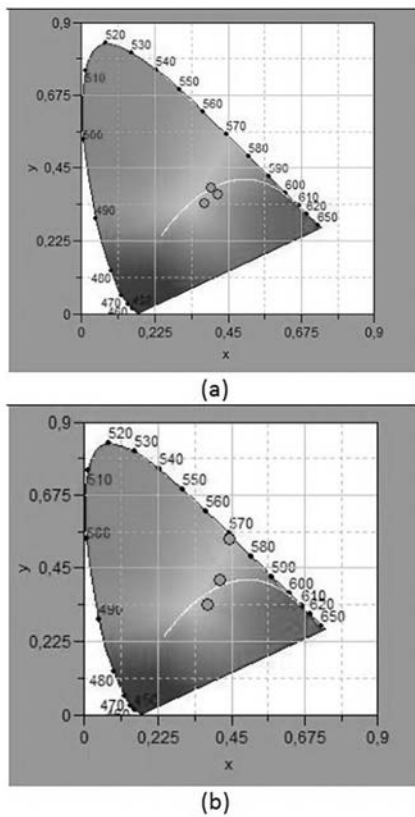


Fig.4. Colour diagram of LED lamp; a) without a prism and with a 2 mm thickness pentagonal prism; b) without a prism and with a 4 mm thick pentagonal prism

wired lighting element was used without a prism of either thicknesses or when the pentagonal prism was present. In Fig. 3.a colour diagram of incandescent wired lamp was given without a prism and with a 2 mm thickness pentagonal prism. In Fig. 3.b the same measurement was repeated for 4 mm thickness pentagonal prism. In both figures the third dot indicates the average value of the two measurements drawn in the same graph.

When the LED lamp was used in place of an incandescent wired lamp, the measured brightness and colour temperature values from the same experimental setup are given in Table 3. The measurements made with a white paper cylinder inside the prism, show that brightness and colour temperature values increased in every situation. The highest brightness level was recorded with a 2 mm thickness pentagonal prism, whilst the lowest brightness was recorded when no prism was used. Increasing prism thickness from 2 mm to 4 mm affected the brightness measurements in a negative way and resulted in decreases of between 2 to 6 %. Similarly, the highest colour temperature was recorded with the 2 mm thickness pentagonal prism, whilst the lowest colour temperature was recorded when no prism was used in the experimental setup. Increasing glass thickness from 2 mm to 4 mm resulted a reduction in colour temperature by 0.26 %, 0.35 % and 0.35 % for triangular, rectangular and pentagonal prisms respectively. Fig. 4 shows the colour temperature of results from measurements taken from the white cylinder and lamp in cases where the LED lamp was used without a prism and when a pentagonal prism of two different thicknesses was used. As it is given before, the third dot in the graphics reveals the average value of the two measurements.

Brightness and CCT values measured from the cylinder when using a compact fluorescent lamp are given in Table 4. In measurements under these conditions, as with the previous cases, the highest brightness and colour temperature values were obtained from the 2 mm thickness pentagonal prism, whilst the lowest values were recorded when no prism was used. When prism thickness was increased from 2 mm to 4 mm, the brightness values measured from the cylinder decreased by be-

Table 3. Brightness and CCT values for the LED lamp in different situations

Glass thickness	Prism Type	Brightness, cd/m ²	CCT, K
-	NA	6.99	3604
2mm	Triangular Prism	7.35 cd/m ²	4219
	Rectangular Prism	7.66 cd/m ²	4294
	Pentagonal Prism	7.73 cd/m ²	4316
4mm	Triangular Prism	7.05 cd/m ²	4208
	Rectangular Prism	7.17 cd/m ²	4279
	Pentagonal Prism	7.30 cd/m ²	4301

tween 3 to 9 %. When prism thickness was increased from 2 mm to 4 mm, colour temperature values decreased in triangular, rectangular and pentagonal prisms by 0.99 %, 0.38 % and 0.42 % respectively. Fig. 5 shows the correlated colour temperature diagram of results from measurements from the white cylinder and lamp in cases where the compact fluorescent lamp was used without a prism or when the pentagonal prism of either thickness was present.

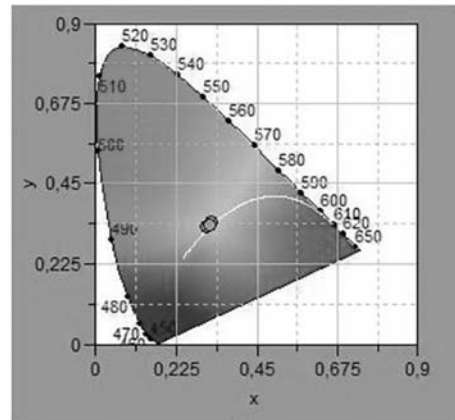
The conditions of the experimental setup when the incandescent wired lamp was used were modelled using the artificial neural networks. As a result of this modelling, the ANN aimed to predict the expected colour temperature values. The values predicted by ANN are given in Table 5. When these predicted results were compared to the actual results, the largest error was seen in the 2 mm thickness rectangular prism, with a difference of 11.85 %, however when using the 4 mm thick rectangular prism, ANN was able to predict the real colour temperature exactly (with a difference of less than 0.024 %).

The CCT values modelled by the ANN, using results from the experimental setup with a LED lamp, were given in Table 6. When the predicted results were compared to the actual results, the largest error was seen in the 2 mm thick triangular prism, with a difference of 6.66 %. In this case, ANN was able to predict the colour temperature exactly, when the prism is not used within the test setup.

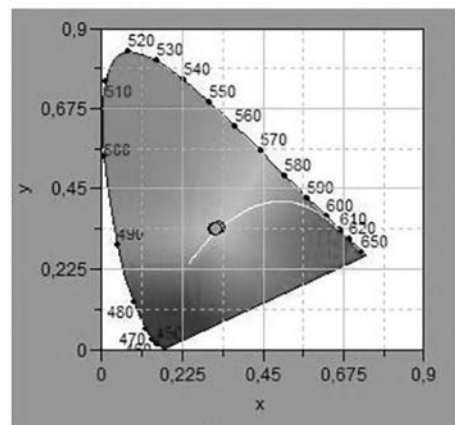
At the last stage, the CCT values of the compact fluorescent lamp were estimated by using ANN, Table 7. When these predicted results were compared to the actual results, the largest error was seen in the 4 mm thickness pentagonal prism with a difference of 3.92 %. The smallest error was seen when a 4 mm thickness triangular prism was used with a difference of 0.012 %.

Table 4. Brightness and CCT values for a compact fluorescent lamp in different conditions

Glass thickness	Prism Type	Brightness, cd/m ²	CCT, K
-	NA	8.1	6248
2mm	Triangular Prism	9.57	6368
	Rectangular Prism	10.38	6381
	Pentagonal Prism	10.83	6502
4mm	Triangular Prism	9.1	6305
	Rectangular Prism	9.43	6357
	Pentagonal Prism	10.43	6475



(a)



(b)

Fig. 5. Colour diagram of a compact fluorescent lamp; a) without a prism and with a 2 mm thickness pentagonal prism b) without a prism and with a 4 mm thickness pentagonal prism

4. CONCLUSION

Two different thicknesses and three different shapes of prisms were used with three types of lights with the aim of measuring the effect of glass shape and thickness on brightness and colour temperature of the lit area. As a result of these empirical ex-

Table 5. Colour temperature values predicted by the ANN for the incandescent lamp

Glass thickness	Prism Corner Number	Measured Colour Temperature, K	Estimated Colour Temperature value with ANN, K
0	0	2425	2427
2	3	3076	3413
2	4	3225	3670
2	5	3730	3718
4	3	2843	2844
4	4	3212	3212
4	5	3714	3706

Table 6. CCT values predicted by the ANN for the LED lamp

Glass thickness	Prism Corner Number	Measured CCT, K	Estimated with ANN CCT, K
0	0	3604	3604
2	3	4219	4500
2	4	4294	4341
2	5	4316	4311
4	3	4208	4203
4	4	4279	4271
4	5	4301	4293

Table 7. CCT values predicted by the ANN for the compact fluorescent lamp

Glass thickness	Prism Corner Number	Measured CCT, K	Estimated with ANN CCT, K
0	0	6248	6471
2	3	6368	6290
2	4	6381	6324
2	5	6502	6288
4	3	6305	6297
4	4	6357	6148
4	5	6475	6221

periments and completed modelling the following conclusions were made:

- The presence of a prism increased the brightness and colour temperature measured from the white cylinder in all type of lamps and also caused the colour temperature to cool progressively.
- For all lamp types the measured brightness and colour temperature is increased according to the number of corners of the prism. This is due to the diffracted light being more intensely directed to the centre.
- The thickness of glass affected the distribution of light, hence an increase in glass thick-

ness resulted a decrease in brightness and colour temperature.

- The predictions made with the ANN support the experimental results of the incandescent wired lamp and LED lamp, which show that the presence of a prism increases the colour temperature. This situation is not true for the compact fluorescent lamp.
- The predictions made with the ANN support the experimental results taken by using the incandescent wired lamp and LED lamp, which indicates that an increase in the number of corners of the prism increases the colour temperature, how-

ever, this situation is not true for the compact fluorescent lamp.

- The predictions made with the ANN support the experimental results for all lamp types, which show that an increase in the thickness of glass prism reduces the colour temperature.

When all these results are evaluated, it is possible to claim that thinner glass prisms, with an infinite number of corners, would be preferred to increase the brightness and colour temperature of the area. The protective glass used in the outer layer of present day retail products has an infinite number of corners. Thus, the aim and character of the area where the light is going to be used should be considered when choosing a lamp, in order to achieve the desired colour temperature and brightness. It was also seen that the ANN method is very successful in this study in predicting the colour temperature.

Acknowledgements: Author wishes to express her gratitude and appreciation to Prof. Dr. Mukden Ugur and Ömer Özgür Bozkurt for their valuable help to take the laboratory measurements of the study.

REFERENCES

1. *J. Entwistle*, *Hotels Designing with Light*, RotoVision, 160 pages, 2000.
2. *Z. Utlu, A. Hepbasli* "A study on the evaluation of energy utilization efficiency in the Turkish residential – commercial sector using energy and exergy analyses", *Energy and Buildings*, 2003, 35 (11), pp. 1145–1153.
3. *A. J. de Craen, P.J. Roos, A. Leonard de Vries, and J. Kleijnen*, "Effect of colour of drugs: systematic review of perceived effect of drugs and of their effectiveness", *BMJ (Clinical Research ed)*, 1996, 313(7072), pp. 1624–1626.
4. *B. Manav, Ö. Güler, S. Onaygil, M.Ş. Küçükdoğu*, "A Research on Office Workers' Colour Preferences: Five Colour Samples Under Six Lighting Alternatives". *Arkitekt*, 2009, Vol. 520–522, pp. 22–31.
5. *I. Sakarya*, (1997), *Teknik ve Estetik Yönden Aydınlatmanın, Alışveriş Merkezlerindeki Mekan Tasarımına Etkileri*, MSÜ Fen Bilimleri Enstitüsü, Graduate Thesis, 198 pages.
6. *Aykal D.F. Gümüş, B. Ünver R, Murat Ö.* "An Approach in Evaluation of Re-Functioned Historical

Buildings in view of Natural Lighting, A Case Study in Diyarbakir Turkey", *Light and Engineering*, 2011, Vol. 19–2, pp.64–76.

7. *Turner, J.*, *Retail Spaces: Lighting Solutions for Shops, Malls and Markets (Designing with Light)*, RotoVision, 160 pages, 1998.

8. *E. Erkin, S. Onaygil, Ö. Güler*, "Energy Saving by Compact Fluorescent Lamps in the Residences Considering User Satisfaction" *Light&Engineering (Svetotekhnika)*, 2008, Vol. 16, No. 1.

9. *Code for Lighting*, Butterworth-Heinemann, 130 pages, 2002.

10. *DiLaura, D., Houser, K., Mistrick, R., & Steffy, G.R.* *The IESNA lighting handbook*. Illuminating Engineering Society, 1087 pages, 2011.

11. *B. Öztürk, A. Ersoy Yılmaz, M. Ugur*, 'Aydınlatma Elemanlarının Parametrelerinin Yaşlanmaya Bağlı Değişimi', *3e Electrotech*, Vol.201, 2011, pp.190–200.

12. *Özbudak, B. Y., Gümüş, B., & Çetin, F. D.* (2003). 'İç Mekan Aydınlatmasında Renk ve Aydınlatma Sistemi İlişkisi', II. Ulusal Aydınlatma Sempozyumu Ve Sergisi Bildirileri, Diyarbakır. 2003.

13. *Çolak, S. Onaygil*, "Prediction of the Artificial Illuminance Using Neural Networks", *Lighting Research & Technology*, 1999, Vol. 31.2, pp. 63–66.

14. *Sevgen S., Şamli R., Sivri N., Kiremitçi V.Z.*, "Applying Artificial Neural Networks For The Estimation Of Chlorophyll-A Concentrations Along The Istanbul Coast", *Polish Journal Of Environmental Studies*, 2014, no.4, pp.1281–1287.

15. *S.V. Kartalapolous*, "Understanding Neural Networks and Fuzzy Logic: Basic Concepts and Applications", 232 pages, Wiley-IEEE Press, 1995.



Aysel ERSOY YILMAZ

received her M. Sc. and Ph.D. degrees in Electrical and Electronics Engineering from Istanbul University in 2003 and 2007, respectively. She has published more than 30 national and international

papers in journals and conferences. Since spring 2008, she has been working as an Assistant Professor at the Electrical and Electronics Engineering Department of Istanbul University

RESEARCH OF PROCESSES IN THE LEDS LUMINAIRE IN CASE OF THE VOLTAGE TEMPERATURE COEFFICIENT OF SEPARATE LEDS VARIATION

Nikolai N. Bespalov, Sergei S. Kapitonov, and Anastasiya V. Kapitonova

*The Mordovia University of N.P. Ogaryov, Federal State Budgetary Educational Institution
 of the Higher Vocational Training, Saransk
 E-mail: kapss88@mail.ru*

ABSTRACT

A model of a luminaire with light emitting diodes, developed in the *Multisim* environment, is described. A study of the processes in the luminaire with changing a voltage temperature coefficient of separate LEDs is documented. Conclusions are drawn concerning LED selection by values of voltage temperature coefficient for the construction LED based luminaires.

Keywords: light emitting diode, model, voltage-current characteristic, semiconductor structure, temperature, voltage temperature coefficient

The service life of modern luminaires with light emitting diodes (LED) is equal to the service life of the separate LEDs, according to their manufac-

turers. This can reach 70–100 thousand h. This information is completely incorrect as a luminaire, besides the LED light sources (for example LED modules), contains devices with a much shorter service life than the light emitting diodes themselves. For example, the control device (the driver) of the luminaire with LEDs has a service life of about 40–60 thousand hours. A service life of the LED light source is not the same as that of a separate LED, unless all LEDs in the luminaire have identical electric and thermal parameters. In this way, even LEDs selected together for some parameters, have a value spread for other parameters. Accordingly, the real reliability of luminaires with LEDs is significantly lower than the design and rating value. In order to increase the reliability of such light sources, the processes occurring within them

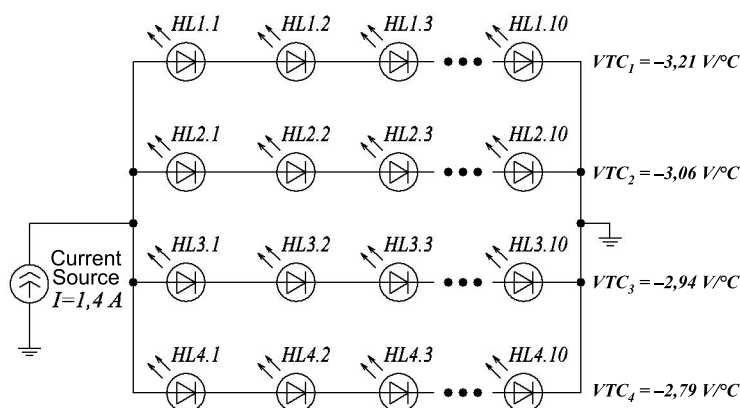


Fig. 1. LED switching diagram in the module:
 CS – current source; VTC – voltage temperature coefficient; HL – light emitting diode

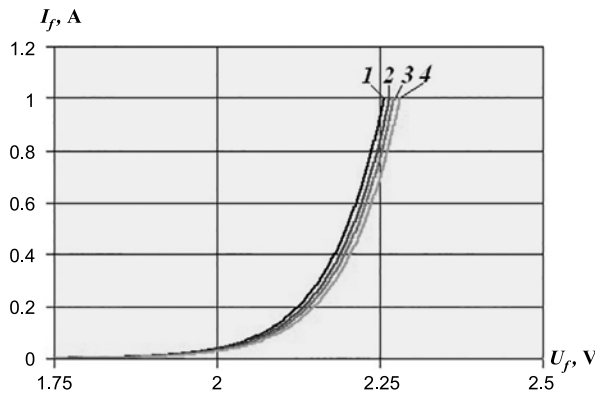


Fig. 2. VCC of each branch LED according to Fig. 1

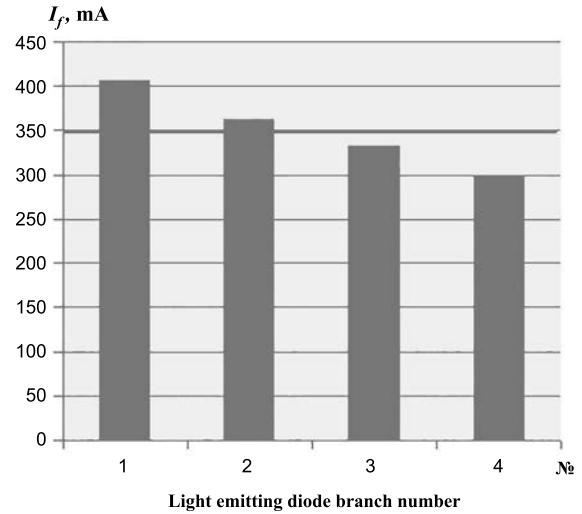


Fig. 3. Currents in parallel branches according to Fig. 1

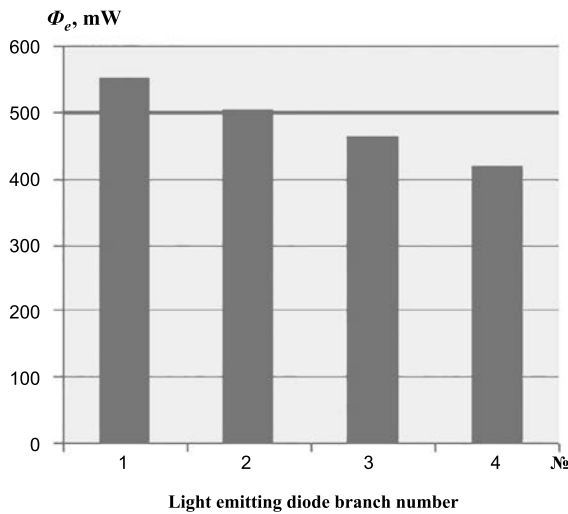


Fig. 4. Distribution of branch LED radiation flow values according to Fig. 1

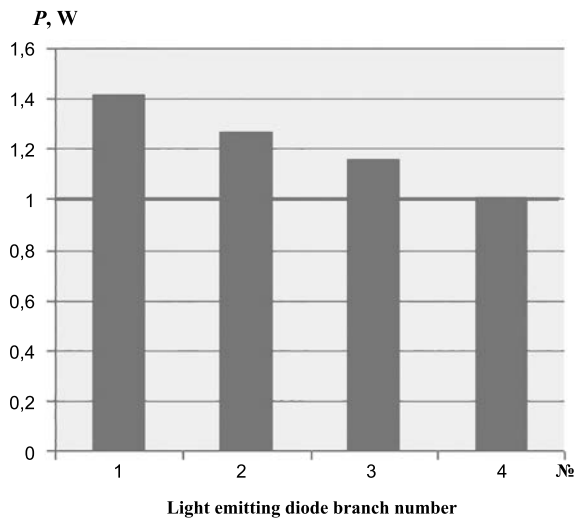


Fig. 5. Distribution of power values consumed by light emitting diodes of the branches according to Fig. 1

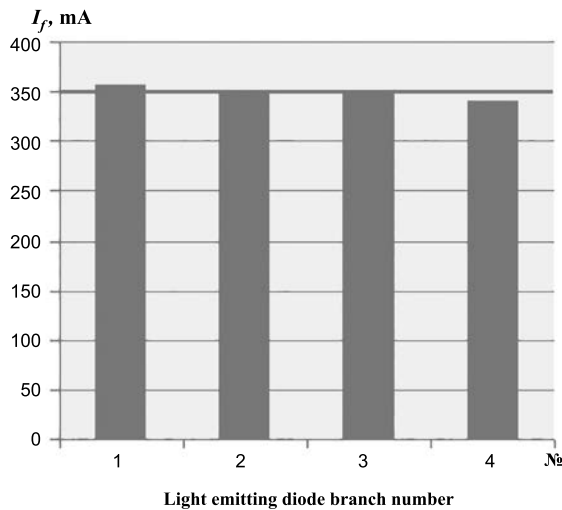


Fig. 6. Distribution of current values in parallel branches of the light-emitting diode module of the luminaire after LED selection by VTC values with accuracy of $\pm 1\%$

should be investigated, including what happens with variation of the LED electric and thermal parameter values. One of the key electric LED parameters, which manufacturers do not consider in grouping LEDs, is the voltage temperature coefficient (VTC). Therefore, there is a need to research processes within LED light sources of a luminaire in the context of a variation of VTC values of separate LEDs.

Standard LED models included in some electric circuit simulation programs are simplified and cannot form a basis for creating appropriate models of a luminaire with LEDs [1]. To solve this problem, we have developed a LED model in the *Multisim* environment [2, 3], which makes it possible to take into consideration the dependence of the radiation flow and voltage-current characteristic

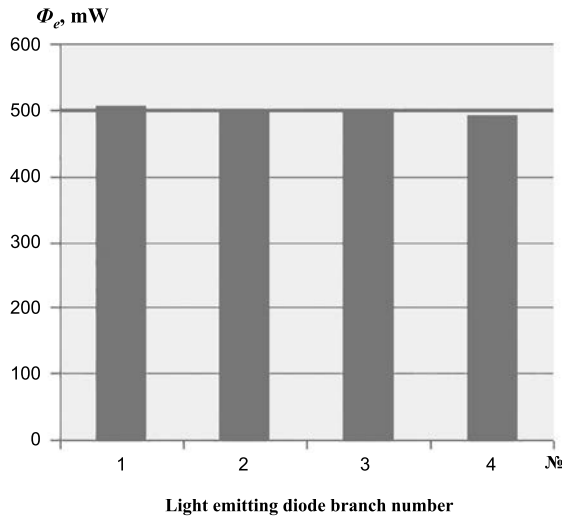


Fig. 7. Distribution of LED radiation flow values after LED selection by VTC values with accuracy of $\pm 1\%$.

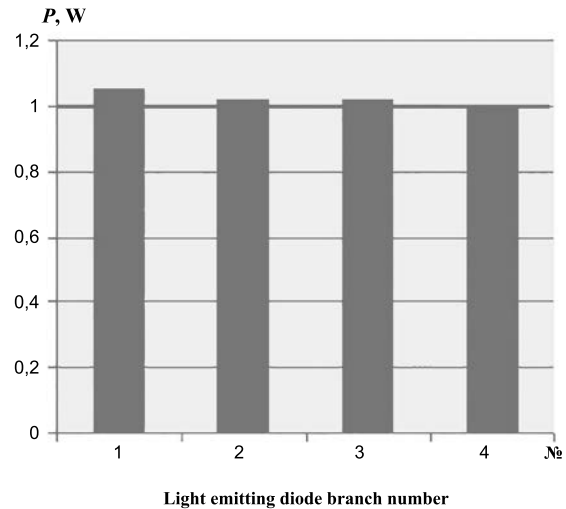


Fig. 8. Distribution of LED power values after their selection by VTC values with accuracy of $\pm 1\%$.

(VCC) of the LED on the temperature of its semiconductor structure (SCS) [4, 5]. Based on the developed model, a model of a luminaire LED module of 50 W has been created. It consists of forty LEDs *Cree XT-E Royal Blue LED* connected in series parallel (Fig. 1).

For this LED model, rated values for forward current, power and radiation flow are equal to 350 mA, 1 W and 500 mW respectively, and permitted VTC variation within one bin amounts to $\pm 7\%$ of the certified value of 3 mV/°C. For LEDs of each of four parallel LED module branches, its own VTC value is set within a deviation of admissible limits (see in Fig. 1 on the right).

The LED VTC value spread of each parallel branch leads to a difference of their VCC. To determine the degree of LED VCC difference between the different branches, a simulation of these VCC at the above-mentioned VTC value variation and at SCS temperature $T_j = 85^\circ\text{C}$ was made in the *Multisim* environment (Fig. 2).

It can be seen from Fig. 2 that in case of a VTC value spread within $\pm 7\%$ from the rated value of 3 mV/°C, the VCC of each branch of LEDs differ significantly. Voltage difference U_f of LEDs with $\text{VTC}_1 = -3.21\text{mV}/^\circ\text{C}$ and $\text{VTC}_4 = -2.79\text{mV}/^\circ\text{C}$ with LED current $I_f = 1\text{ A}$ amounts to 50 mV.

The LED VCC difference of each branch leads to the fact that in different parallel branches I_f are different. As it can be seen from Fig. 3, I_f of the first branch LEDs is 405 mA (significantly more than the rated current of 350 mA), and I_f of the fourth

branch of LEDs is 300 mA (50 mA less than the rated current).

These results are indicative of inefficient LED use in the luminaire.

According to Fig. 4, the maximum spread of the radiation flow values Φ_e is equal to 130 mW, which is more than the maximum permissible deviation of $\pm 10\%$.

Variation of LED Φ_e values between separate parallel branches leads to a difference in their luminous fluxes as well, which adversely affects the light characteristics of the luminaire [6, 7].

And based on Fig. 5, it appears that the values of power P consumed by LEDs in branches № 1, 2 and 3, are significantly higher than the rated value of 1 W. This operating mode can cause overheating in the specified branch of separate LEDs, which considerably reduces the reliability of the luminaire as a whole.

In order to align currents of the luminaire LED module's parallel branches, one should select LEDs by VTC values.

Simulation of the processes taking place in the luminaire LED module (Fig. 1) in case of variation of LED VTC values in each parallel branch within $\pm 1\%$ from the rated value of 3 mV/°C showed that after LED selection by VTC values, I_f (Fig. 6), Φ_e (Fig. 7) and P (Fig. 8) values in each parallel branch of the LED module aligned and became almost equal to the rating values of 350 mA, 500 mW and 1 W accordingly.

Thus selection of LEDs by VTC values when constructing luminaire LED modules allows:

- Raising the reliability of the luminaire, due to the fact that all its LEDs operate in a mode close to the rated;
- Reducing costs for cooling due to alignment of the thermal operation modes of the LEDs;
- Reducing the number of LEDs in the luminaire at an invariable value of its luminous flux due to more effective use of every LED.

REFERENCES

1. *Kapitonov S.S., Bepalov N.N., Kapitonova A.V., Ashryatov A.A.* Research of a standard light emitting diode model in the Multisim environment // SWorld Collection of scientific works. Issue 4 (37). Volume 1. Odessa: KUPRIENKO SV, 2014, pp. 73–75.
2. *Kapitonov S.S., Bepalov N.N., Kapitonova A.V., Ashryatov A.A., Kilmamyatov Denis R.* Development of a light emitting diode electric model in the Multisim environment // Scientific-and-technical bulletin of Povolzgye region. Kazan: Scientific-and-technical bulletin of Povolzgye region Open Company 2015, Issue 1, pp. 99–102.
3. *Kapitonov S.S., Bepalov N.N., Kapitonova A.V., Ashryatov A.A.* Features of creation of electric model of a light emitting diode // Theoretical and applied questions of science and education: Collection of scientific works based on materials of International scientific and practical conference. Tambov: Consulting company Yukom Open Company, 2015, pp. 83–85.
4. *Kapitonov S.S., Kapitonova A.V.* Research of a light emitting diode forward voltage dependence on temperature // Scientific almanac. Tambov: Consulting company Yukom Open Company, Issue 5 (7), 2015, pp. 135–138.
5. *Kapitonov S.S., Kapitonova A.V., Ashryatov A.A.* Research of a powerful light emitting diode characteristics temperature dependence // Materials of the XIIth All-Russia scientific and technical conference “Problems and perspectives of development of domestic light engineering, electrical engineering and power engineering” with international participation within the IIIrd All-Russia lighting forum with international participation. Saransk: Self-employed person Afanasyev V.S., 2015. pp. 335–338.
6. *Kapitonov S.S., Kapitonova A.V.* Simulation of temperature dependence of a powerful light emitting diode radiation flow // New university, series “Engineering sciences”. Ioshkar-Ola: Colloquium Open Company, Issue 3–4. 2015, pp. 47–50.
7. *Kapitonov S.S., Kapitonova A.V.* Simulation of radiation characteristic of a light emitting diode in the *Multisim* environment // Scientific almanac. Tambov: Consulting company Yukom Open Company, Issue 4 (6), 2015, pp. 196–200.



Nikolai N. Bepalov,
Ph.D. Graduated from the Novosibirsk Electrotechnical Institute in 1974. Head of the department “Electronics and Nano-electronics” of the Mordovia State University of N.P. Ogaryov



Sergei Kapitonov,
Ph.D. Graduated from the Mordovia State University of N.P. Ogaryov in 2013. A senior lecturer of the Chair “Electronics and nano-electronics” of the Mordovia State University of N.P. Ogaryov



Anastasiya V. Kapitonova,
an engineer. Graduated from the Mordoviya State University of N.P. Ogaryov in 2013. A post-graduate student of the Chair “Light sources” of the Mordovia State University of N.P. Ogaryov

INVESTIGATION OF HEAT TRANSFER TYPES IN AN AUTOMOBILE FOG LAMP WITH COMPUTATIONAL FLUID DYNAMIC ANALYSIS

K. Furkan SÖKMEN¹, Nurettin YAMANKARADENİZ², and Salih COŞKUN²

¹Uludag University

²Bursa Technical University

E-mail: furcan.sokmen@btu.edu.tr

ABSTRACT

This study investigated the temperature distribution and heat transfer in an automobile fog lamp. First, a mesh independent solution was obtained. The results were compared with the literature and validated with test results. Measurements were taken from five different points by using thermocouple. Tests were applied for two hours at 24 °C. For thermal analysis, ANSYS CFX 12.1 was employed. Air flow inside the fog lamp was assumed as steady, incompressible, laminar and three-dimensional. Thermophysical property variations, buoyancy and radiation effects were taken into consideration. The radiation effect is an important heat transfer type to be considered in the temperature distribution on the lenses of automotive lighting systems. The radiation effect can have a negative influence on the lens due to the selection of unsuitable material. Despite the complexity of the bulb geometry and its non-isothermal surface conditions, general flow and heat transfer characteristics did not change.

Key words: automotive lighting, head lamp, laminar natural convection, radiation, conjugate analysis, computational fluid dynamics (CFD)

1. INTRODUCTION

Automotive lighting systems such as headlamps and rear lamps are not only for night vision and vision quality [1,2]. Lighting systems are also important for travel and driver safety [2,3]. A general

study of automotive lighting systems was carried out by Bauer, [4]. A number of thermal problems in automotive lighting systems have arisen as a result of the development in halogen bulb (H1, H3, H4) [5], HID (high-intensity-discharge) [6] and LED [7] technologies. In particular, some material problems in the lighting systems were caused by the increase in bulb power. Thermal problems are seen more commonly in fog lamps than in headlamps because of the smaller volume of fog lamps and the high power of the bulbs which are used in them. The temperature distribution and profile of air flow in fog lamps were investigated by Fischer using an H11 bulb in 2005 [8]. A similar study was done on headlamps by Sokmen et al [9].

The temperature load and distribution in lighting systems were researched by Wulf [10] and he determined that temperature distribution was an important factor in the development of lighting systems and bulb technology. Wulf addressed the reasons why thermal analysis was needed. The first was concerned with the cost reduction demanded by automobile manufacturers because of the more complex design parameters. The second reason was that cost reduction depended on plastic material usage.

Bulbs used in automotive lighting systems have a short cylindrical geometry and are filled with halogen gas. When electrical power is applied to the tungsten filament inside the bulb, the bulb surface temperatures increase rapidly and non-isothermally. Heat transfer and air flow characteristics from the long horizontal cylinder have been researched

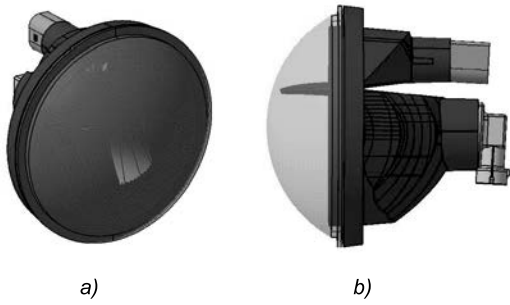


Fig. 1. Sample fog lamp used in this study: a) isometric view; b) right side view

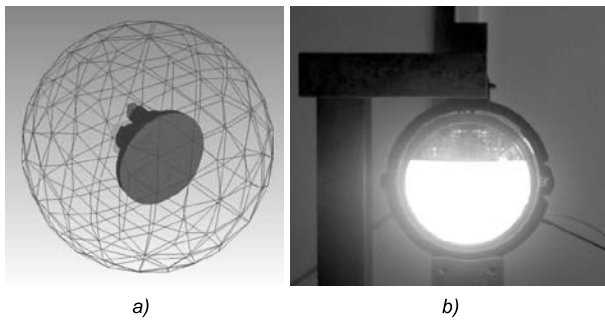


Fig. 3. Test conditions: a) in the mesh data; b) in the experiment

in [11–17] and well-known correlations have been applied in [18–20]. Cases of internal heat generation and constant heat flux have been studied in [21–24]. Complex three-dimensional systems and some numerical investigations were examined, but as they were not compared with any experimental data, these studies had some difficulties in determining flow information [25].

This study focused on temperature distribution and the influence of heat transfer type on the components in a fog lamp. Furthermore, using CFD (computational fluid dynamics) together with CAD (computer aided design) procedures, air flow characteristics around an H8 bulb were determined. To this aim, the primary temperature distribution and the temperature of points on the lens surface were obtained and validated via test results. Temperature distribution and heat transfer types

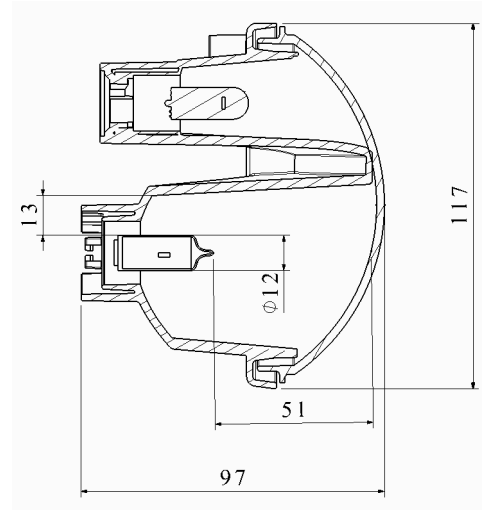


Fig. 2. Technical drawing of the fog lamp, left side view

in the fog lamp were compared with previous results obtained from the literature.

2. MATERIAL AND METOD

2.1. Geometry and modelling

Fig. 1 shows the sample fog lamp (OEM design by Automotive Lighting), which was used in this study

An H8 bulb was used in the fog lamp as a heat source. The power applied to the tungsten filament was 43 W. The materials of the fog lamp components included the lens, made of PMMA (polymethylmethacrylate), and the housing and reflector (two components in a single part) made of PC/ABS (polycarbonate/acrylonitrile butadiene styrene). Fig. 2 shows a technical drawing of the fog lamp from the left side view.

2.2. Experimental Study

The sample fog lamp analysis was set up in the full load condition and the mesh data can be seen in Fig. 3 (a). Experiments were conducted at 24 °C for two hours to reach a steady condition, Fig. 3 (b).

Table 1. Experimental apparatus and specifications

Test equipment	Trade mark	Operating range	Deviation range
Thermometer	APPA-50	-40 °C / +204 °C	+/-2,2 °C
Thermocouple	Standart (K Type)	-100 °C / +400 °C	+/-0,1 °C
Thermal camera	FLIR SC620	-40 °C / +500 °C	+/-2 °C

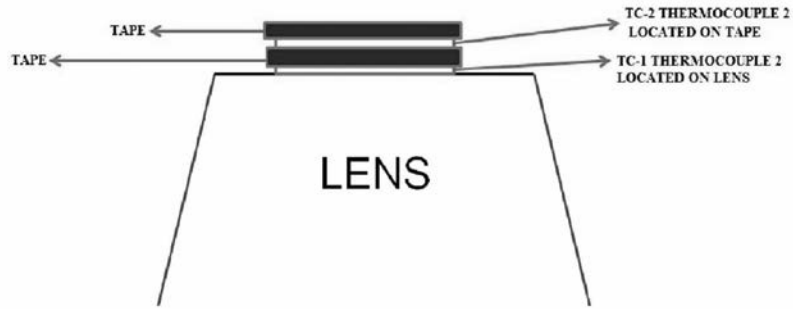


Fig. 4. Validation of thermocouple measurements

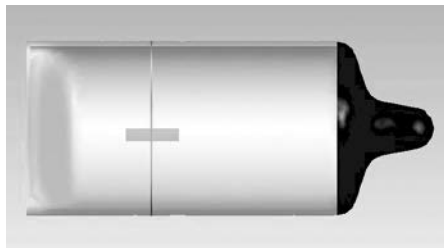


Fig. 5. Middle section calculated Ra number

The test equipment used in this study and the measurement ranges are given in Table 1.

In this study, five thermocouples were used for temperature measurement. An APPA digital thermometer, which can read values from two different thermocouples, was also used. The thermocouples were positioned on the critical surface points of the fog lamp. First, a thermocouple was situated on the lens with adhesive tape for calibration. Then, another was placed on the adhesive tape to measure the adhesive tape error rate. Thermocouple located on the lens measured the temperature of the lens surface as 50.3 °C, Fig. 4. The thermocouple located on the tape measured the temperature as 50.1 °C. As there was only a 0.2 °C difference between temperatures of the lens surface and the tape, the effect of the adhesive tape was disregarded. Five ther-

mocouple measurements were taken and recorded every half hour. The analysis was carried out under steady-state conditions and the test results obtained are given in Table 2.

2.3. Computational study

The importance of the CFD (computational fluid dynamics) tool in the automotive industry was mentioned by [26]. Kobayashi and Tsubokura also pointed to the effect of CFD application in the automotive industry [27]. A commercial CFD code of ANSYS CFX 12.1 [28] was used in this study to determine the temperature distribution of the fog lamp. A geometrical model of the fog lamp was designed and simplified using CATIA V5 R19. The mesh structure was created in ICEM CFD. All analysis and computations were run with ANSYS CFX 12.1. A coupled multiple element and fully implicit solver were employed by ANSYS using the finite volume method. The SIMPLEX algorithm was used to calculate pressure and the Rhie-Chow interpolation was applied to evaluate velocity. The assumed analysis was laminar, incompressible, steady natural air convection and three-dimensional. The momentum equation was used with a source term for buoyancy calculations.

Table 2. Test results of surface temperatures

	1 st Test Results	2 nd Test Results	3 rd Test Results
	T, °C	T, °C	T, °C
Point-1	104,12	104,02	104,08
Point-2	98,201	98,115	98,198
Point-3	80,021	80,111	80,03
Point-4	86,23	86,21	86,25
Point-5	81,03	81,05	81,12

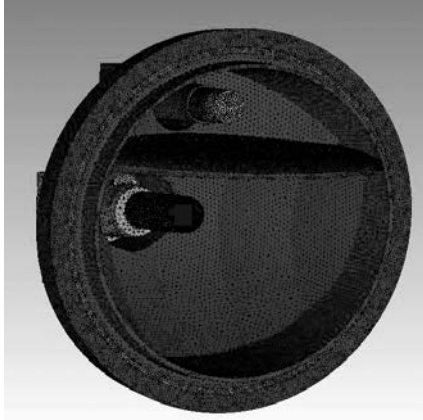


Fig 6. Mesh structure of interior fog lamp and its components

$$S_{M,buoy} = (\rho - \rho_{ref}). \tag{1}$$

The Boussinesq model was used to evaluate density difference in this equation. Rayleigh (Ra) and local Nusselt (Nu) number was calculated using a middle section of the filament, as shown in Fig. 5.

$$Ra_D = \frac{g\beta\Delta T D^3}{\nu^2} Pr = GrPr. \tag{2}$$

Here, ΔT is the difference between the bulb's surface temperature and the ambient temperature, and β is the coefficient of the volumetric thermal expansion; β was calculated by using Equation (3).

$$\beta = \frac{1}{T_f}. \tag{3}$$

T_f is the film temperature and was calculated using Equation (4).

$$T_f = \frac{T_a + T_s}{2}. \tag{4}$$

Here, T_a is defined as ambient temperature and T_s as bulb surface temperature. The Ra number is derived from the Gr (Grashof) number and the Pr (Prandtl) number. In this study, the Ra and Gr numbers were calculated as 9086 and 13264, respectively. The local Nu (Nusselt) number was calculated by Equation (5).

$$Nu = \frac{h \cdot D}{k}. \tag{5}$$

The Monte Carlo model was used to evaluate the radiation effect of the fog lamp. The Monte Carlo model is a technique for calculating radiation between the fluid and solid part in ANSYS CFX. This model assumes approximately 2.5–5 billion photons according to the volume in the vehicle lighting system. Each photon is sent to the solid parts directly. Some photons pass through the transparent solid parts, depending on the wavelength of the photon. Another method is the discrete transfer model for radiation effect. The discrete transfer model has been used in some radiation problems, but with limited success by [27]. There is a good comparison between the two models in the study [29]. Another study determined that the Monte Carlo model could be used successfully for a wide range of applications, especial-

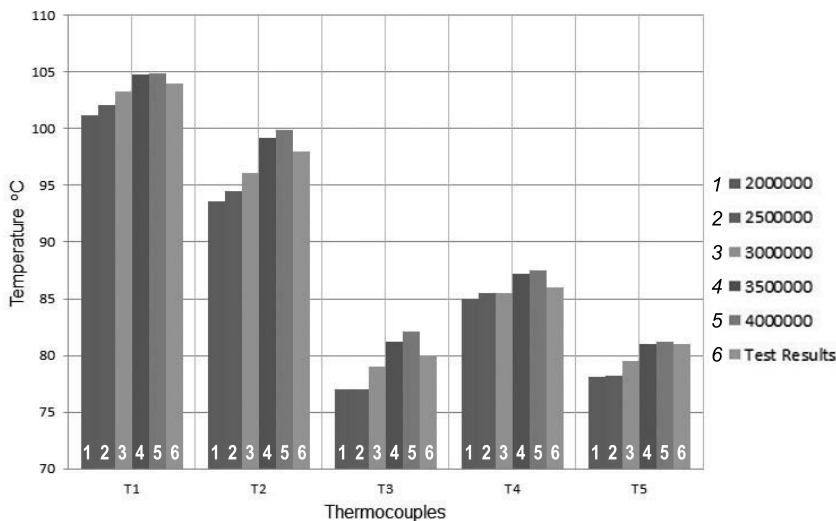


Fig 7. Comparison of temperature values for various mesh numbers with test results

Table 3. Comparison of final temperature values for various mesh numbers with test results

	Mesh Number Results					Test Results
	2 million	2,5 million	3 million	3,5 million	4 million	
	T, °C	T, °C	T, °C	T, °C	T, °C	T, °C
Point-1	101,203	102,11	103,32	104,82	104,94	104
Point-2	93,568	94,482	96,058	99,211	99,852	98
Point-3	76,985	77,021	78,985	81,251	82,15	80
Point-4	84,985	85,498	85,502	87,201	87,523	86
Point-5	78,102	78,256	79,520	81,025	81,215	81

Table 4. Comparison of final temperature values for various mesh numbers with test results

Mesh Number >		2 million	2,5 million	3 million	3,5 million	4 million
Error Rate	Point-1	-2,76 %	-1,86 %	-0,66 %	0,79 %	0,89 %
	Point-2	-4,74 %	-3,72 %	-2,02 %	1,22 %	1,85 %
	Point-3	-3,92 %	-3,87 %	-1,29 %	1,54 %	2,62 %
	Point-4	-1,19 %	-0,59 %	-0,58 %	1,38 %	1,74 %
	Point-5	-3,71 %	-3,51 %	-1,86 %	0,03 %	0,26 %

ly with semi-transparent or transparent solid models such as [30].

The mesh data of the sample fog lamp is given in Fig. 6. The Delaunay mesh structure was used for the model. All solid surfaces assumed no-slip velocity as a boundary condition. Power of 43 W was applied to the bulb’s filament as a volumetric heat sources. The emissivity coefficient for the aluminum-coated surface was assumed to be 0.1. Mesh numbers of 2, 2.5, 3, 3.5 and 4 million were run for the mesh independent solution. The temperature values of the analysis can be seen compared with the test results in Fig. 7 and Table 3. The most proximate values to the test results were obtained between the 3.5 and 4 million mesh numbers (Table 3). For the fog lamp analysis, the mesh num-

ber of 3.5 million was used in this study. The maximum difference between the test results and analysis results was detected as 1.54 % (at measurement Point 3, see Table 4) and the minimum difference was detected as 0.03 % (at measurement Point 5, see Table 4) for the 3.5 million mesh number.

3. RESULTS AND DISCUSSION

This study was generally focused on temperature distribution and heat transfer types in the fog lamp and the heat transfer around the H8 bulb. All results of the mesh independent solution were observed and compared with the test results. The temperature distribution of the lens is given in Fig. 8 (b). As seen from Figs. 8 (b) and 8(c), the high tempe-

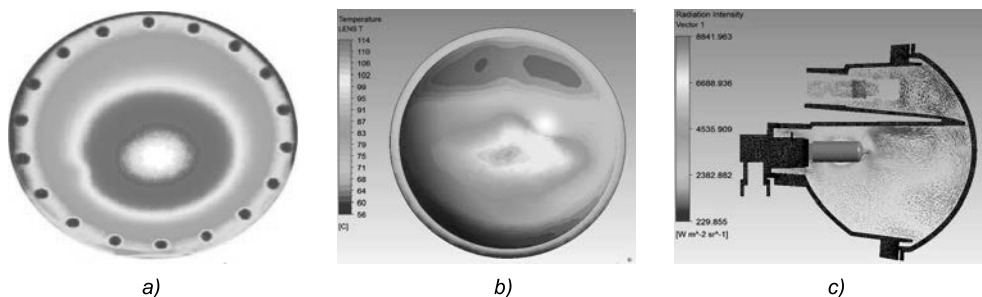


Fig. 8. a) Langebach et al. [31] Ra= 2101; b) Temperature distribution on lens; c) Temperature distribution of internal air

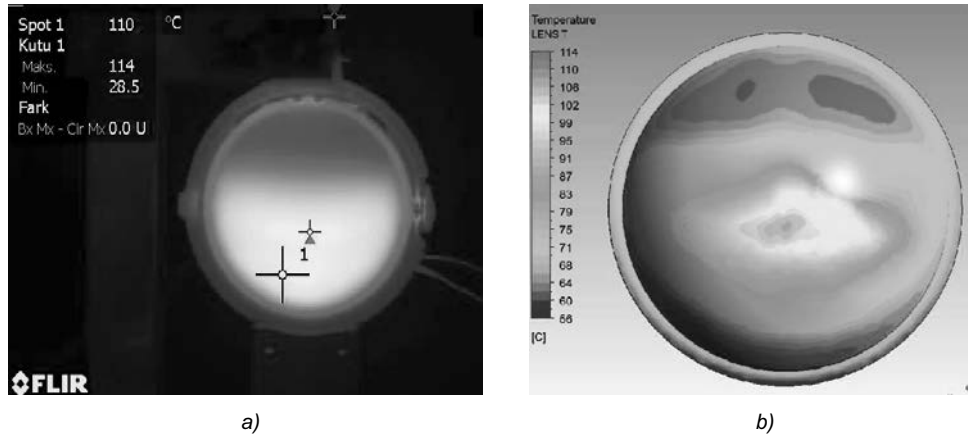


Fig. 9. a) Thermal camera picture during test; b) Temperature distribution on lens with Ansys CFX 12.1

temperature area of the lens is directly opposite the H8 bulb. The same temperature distribution was observed by [31] using a thermal camera. They determined that the Ra number affected the high temperature field on the lens. The results of their study demonstrated that the hot spot location occurred opposite the bulb axis at a low Ra number and the convection effect was increasingly reduced. The location and the temperature of the hot spot are defined by the pure radiant heat transfer for the low Ra number. A higher Ra number can change the flow characteristics and remove the high temperature field above the bulb axis or upper side of the lens. Fig. 8 (a) illustrates the temperature distribution on the lens at $Ra = 2101$ in [31] study in. Sokmen et al. investigated temperature distribution in a headlamp using an H4 bulb with a power of 75 W [8]. The Ra number was determined as 12904, and the convective heat transfer was more effective than the radiation heat transfer [9]. Their results confirm those of [31]. Thus, the hotspot

area did not occur directly opposite the H4 bulb because of the effective convection heat transfer. The heated air rose directly above the bulb, reached the ceiling of the reflector and flowed directly toward the lens. Therefore, the hotspot area occurred above the bulb axis on the lens in [9]. In this study, an H8 bulb was used with a power of 43 W and the Ra number was determined as 9086. It was expected that a high temperature area would occur above the bulb axis because of this high Ra number; however, the expectation was frustrated by the results. Despite the high Ra number and the findings of other researches [9, 32], the radiation effects were more effective than convection in this study, so the high temperature area occurred directly opposite the bulb, as seen in Fig. 8 (b). These results may have resulted from the geometry of the fog lamp. The volume of a fog lamp is smaller than that of a head lamp. Therefore, the heated air reaches the fog lamp component in a shorter time. Consequently, hot air can reach the lens more effectively, Fig. 8 (c).

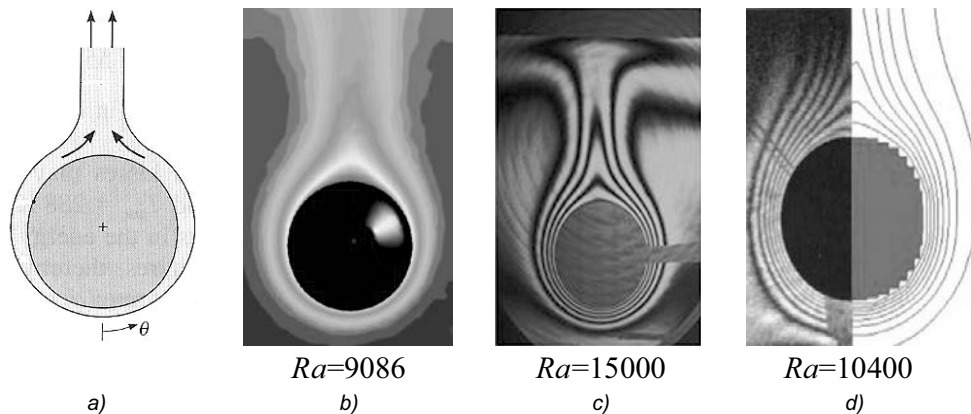


Fig. 10. a) General view [28]; b) Numerical prediction for short cylindrical bulb with variable surface temperature in bulb cavity [This study]; c) Interference photograph of temperature field around long isothermal cylinder located underneath an adiabatic ceiling [33]; d) Interference photograph for the long isothermal cylinder (left hand side) and numerical prediction (right hand side) in isothermal cubical enclosure [25]

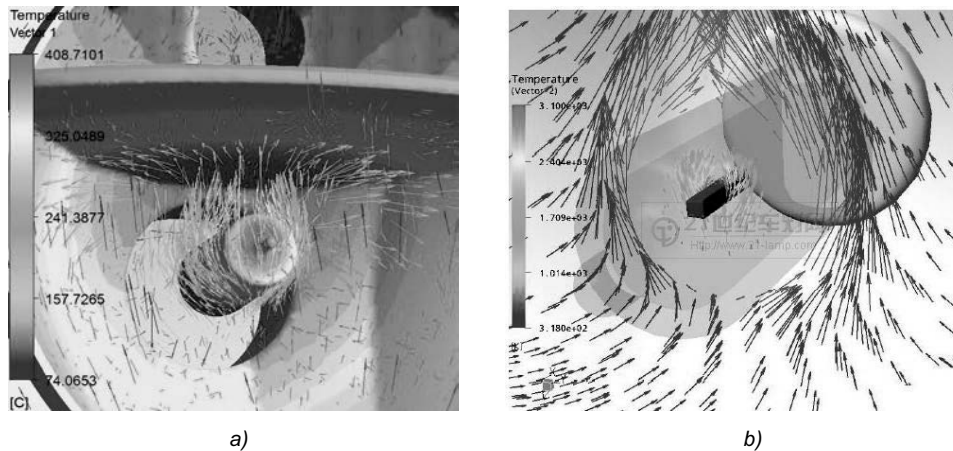


Fig. 11. Temperature distribution: a) around the H8 bulb in this study; b) in the Fischer study [8]

The thermal camera measurement results and the temperature distribution of the mesh independent solution for this study are given in Fig. 9 (a) and (b), respectively.

The H8 bulb was considered as a small cylinder in this study. The general view of a long horizontal isothermal cylinder is shown in Fig.10a [18, 25, 33], can be compared to the temperature spread from the bulb in this study shown in Fig 10 b. Fig. 10 c shows the section located beneath an adiabatic ceiling [33] and Fig. 10 d illustrates a cylinder in an isothermal cube [25].

In Fig. 10, the hot air plume from the bulb rises around $\theta = 90^\circ$ for all cases. The Ra numbers of Figs. 10 c and 10d were given, respectively, as 15000 and 10400. The Ra number of this study was 9086.

The temperature plots of the H8 bulb are given in Fig. 11 a. Approximately the same plot distribution was found by Fischer in 2005, as seen in Fig. 11 b. Hot air rising from the cylinder reaches the ceiling in Fig. 11 a the same as is seen in Fig. 11 b. In this study, the radiant heat exchange was computed by a ray-tracing method solved with a Monte-Carlo scheme. A similar study was done by Ashjaee et al. [33] but they used an adiabatic ceiling. The upper side is supposed to be the hottest field on the reflector because of the rising hot air. When the hot air strikes the upper side of the reflector, it is symmetrically divided into two separate hot air streams, as seen in Fig. 11 a. The same division was seen in [8] as shown in Fig. 11 b.

The symmetrical division of hot air was also seen in the study of [33], Fig.10c. The diameter of the volumetric heat source cylinder was 1.5 mm in [33] but in this study, the volumetric heat source

diameter was 1.2 mm. The distribution of the [33] study proved that there was no effect on free convection heat transfer due to the adiabatic ceiling. Isothermal cylinders were examined by Newport et al. in 2001 in an enclosure environment. The symmetrical division of hot air was not seen in that study [25], Fig.10d. The hot air distribution in their study is similar to that of the general application [18], Fig. 10 a.

The local Nu number was calculated in two acceptance using Equation (5) and the distribution of the local Nu number is given in Fig. 12. First acceptance was average temperature from middle section of the filament and internal air, because of difficulties to calculate each point around section (Fig.5). Second acceptance was point to point temperature distribution around middle section of the filament and internal air. Both acceptances were compared with examples in the [9, 34–36]. All curves in Fig. 12 show a similar tendency and the local Nu number increases directly proportional with the Ra number, as stated in the [37–39]. As a result of the research shown in Fig. 12, the effects of complex bulb geometry and non-isothermal surface conditions were not seen in the general air flow trend and heat transfer characteristics. However, influence of the boundary layer, which started at $\Theta = 0^\circ$ and finished at $\Theta = 180^\circ$, was seen on the local Nu number, Fig. 12. The local Nu number had a maximum value at $\Theta = 0^\circ$ and decreased with the increasing of Θ [18]. In this study, the local Nu number increased slightly after $\Theta = 0^\circ$.

Distribution of the Nu number can be related to the thickness of the thermal boundary layer around the cylinder. The thickness is the least at the bottom of the cylinder ($\Theta = 0$); therefore,

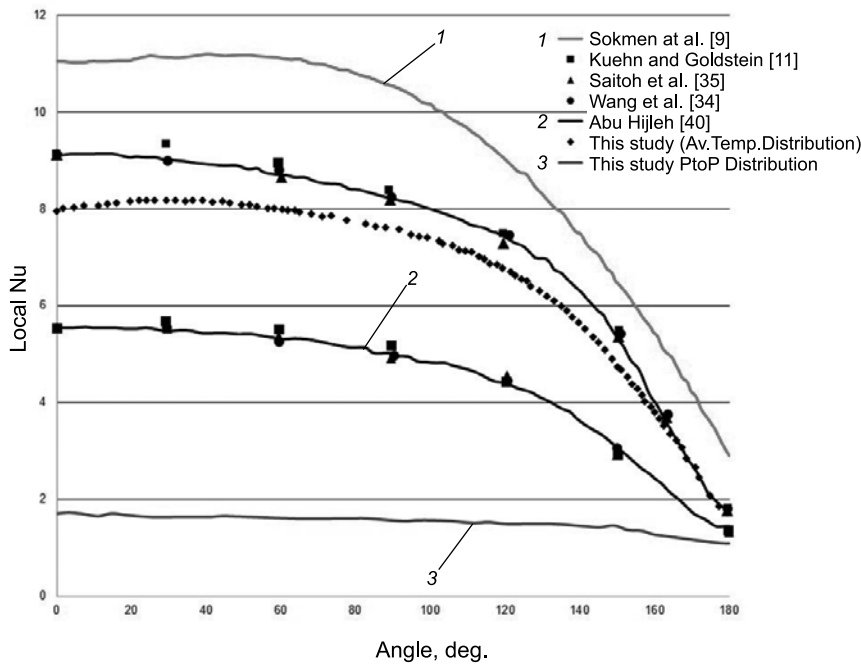


Fig. 12. Local Nusselt number distribution around half of the cylindrical bulb in comparison with examples in the literature

temperature change is the highest at $\Theta = 0$, so the maximum heat transfer is seen at this point in [38]. Heat transfer value for middle section of the filament is maximum at $\Theta = 0$ same with [34, 35, 38] for point to point temperature distribution in this study, Fig. 12. Ra number changed 10^3 to 10^5 in [34, 35]. Ra number changed between 6,5 and 81 for point to point temperature distribution in this study.

Average temperature distribution of the local Nu number was comparable with [37] but heat transfer was not maximum at the bottom of the bulb ($\Theta = 0$). Heat transfer had a maximum value at approximately $\Theta \approx 25^\circ$ in average temperature distribution around section, Fig. 12. The curve can be perceived as being horizontal at $\Theta \approx 25^\circ$, similar to Eckert and Soehngen's in findings of $\Theta \approx 40^\circ$ ($Gr = 26300$) and 50° ($Gr = 42050$) in [41]. The maximum heat transfer value was approximately at $\Theta \approx 40^\circ$ in [9] but the H4 bulb used in the was thicker than the H8 bulb. The Gr number was 13264 and the Ra number was 9086 for average temperatures in this study. Atmane et al. examined the natural convection around a horizontal heated cylinder and found similar outcomes at $\Theta \approx 100^\circ$ [39], for which the Ra was between 34363 and 53495. Grafstronningen and Jensen' study observed this situation, in which the maximum heat transfer was seen at $\Theta = 0$, at a Ra number of 10^7 [37] but the same si-

tuation was not seen by Reymond et al. [37], at the Ra number of 10^6 .

Moreover, it was determined that heat transfer was not maximum at $\Theta = 0$, but it was maximum at the top of the cylinder at about $\Theta = 150^\circ$ in [25] or $\Theta \approx 160^\circ$ in [36]. 2008. Heat transfer declines sharply towards 180° , but it did not decline in this study or in the other studies in Fig. 12.

In this study, the local Nu number increased directly proportional with the Ra number. As seen from Figure 12, all the other studies increased in a similar trend. In the present study, Ra number is between 6,5 and 81 (average Ra number: 41,74), Nu number was between 1,95 and 1,34 (average Nu number: 1,74) and Pr number is 0,7 in point to point temperature distribution. Ra number was 9086 and the local Nu number was between 8.24 and 2,69 (average Nu number: 7,16). The temperature of the cylinder surface was higher than [33–35, 41] but lower than [9]. The heat transfer type was similar to that around the H4 bulb in Sokmen et al. 2014' study but some differences can be seen, such as the maximum heat transfer rate angle, the radiation effect on the lens and point to point calculated Ra number, Nu number distribution. The most important difference between [9] and this study was the radiation effect on the lens. This situation caused thermal stratification inside the bulb, especially on the lens. Roychowdhury et al. study

determined that the pattern of flow influenced the heat transfer rate significantly [13]. Moreover, the complex geometry of the bulb, asymmetrical bulb geometry, three-dimensional natural flow and high temperature of the bulb surface can cause turbulence and increased heat transfer in an enclosure geometry. Subsequently, because of this, the radiation effect is greater on the parameters in a small geometry than in a larger one.

4. CONCLUSIONS

In this study, the temperature distributions on surfaces, heat transfer type around the bulb and the radiation effect in an automotive fog lamp were researched using mesh independence computationally under full load condition. To this aim, first, a mesh independent solution was obtained, and then, the results were compared and validated with the test results. According to the results of the analysis, the temperature field and heat transfer type estimations were compared with data in the literature and the following conclusions were obtained.

The CFD is a significant tool for calculating the radiation and conjugate effects for closed geometries such as those of automobile lighting systems. Heat transfer type, hotspot areas, radiation effects and condensation problems can all be determined and applied by using CFD.

The data of the mesh independent solution and mesh statistics are very important for obtaining reliable results. A comparison of these data demonstrated that the mesh independent solution could eliminate tests. The mesh statistics obtained giving almost the same fog lamp volumes could be used for other fog lamp analyses.

The radiation effect is an important heat transfer type to be considered in the temperature distribution on the lenses of automotive lighting systems. In the literature, similar results have been obtained and should be considered in the analysis and design of automotive lighting systems such as fog lamps.

Despite the complex bulb geometry and non-isothermal surface conditions, general flow in the internal volume and heat transfer characteristics did not change and were shown to maintain ideal flow conditions over the long isothermal cylinder.

The three-dimensional nature of the flow can be affected by complex or asymmetrical bulb geometry and can cause turbulence and thermal increase.

The high temperature of the tungsten wire affects the local Nu number distribution around the bulb.

The radiation effect can have a negative influence on the lens due to the selection of unsuitable material. Therefore, further studies examining ways of decreasing the effects of radiation (e.g., black top application on the bulb, etc.) should be carried out.

It is recommended that these studies be focused on heat transfer from bulbs having asymmetrical geometry such as those with a volumetric heat source and heat transfer from the bottom and top surfaces of the cylinder.

REFERENCES

1. Derlofske, J.V., Bullough, J.D., Gribbin, C. Comfort and visibility characteristics of spectrally tuned high intensity discharge forward lighting systems. *European Journal of Scientific Research*, 2007. 17 (1), pp.73–84.
2. Khanh, T.Q. Lighting Quality for Automotive Lighting Quality, *Light & Engineering*, 2014. 22, Issue: 4, pp. 59–63
3. Honeywill, T. Simulation sees. *Automotive Engineer*. December, 2007, pp. 32–33.
4. Bauer, H. *Automotive Electric/Electronic Systems Lighting Technology*. Editor-in-Chief: Horst Bauer Bosch GmbH Stuttgart, 1999.
5. Wulf, J and Reich, A. Temperature loads in headlamps. *SAE World Congress and Exhibition Detroit*, 2002. DOI:10.4271/2002-01-0912.
6. Sivak, M., Schoettle, B., Flannagan, M.J. Mercury-free HID lamps: glare and colour rendering. *Lighting Research Technology*, 2006, 38 (1), pp. 33–40.
7. Jang, S and Shin, W.S. Thermal analysis of LED arrays for automotive head lamp with a novel cooling system. *IEEE Transactions on Device and Materials Reliability*. 2008, 8 (3), pp. 561–564.
8. Fischer, P., Radiative Heat Redistribution and Natural Convection Flow inside an Automotive Fog Lamp. *ISAL 2005 Symposium*, Germany, Darmstadt, 2005.
9. Sokmen, K.F., Pulat, E., Yamankaradeniz, N., Coskun, S. Thermal Computations of Temperature Distribution and Bulb Heat Transfer in an Automobile Headlamp. *International Communication Heat and Mass Transfer*, 2012. DOI: 10.1007/s00231-013-1229-5 to be published in: *Heat and Mass Transfer*.
10. Wulf, J. (Calculation of temperature loads in headlamps. *SAE International Congress and Exposition Detroit*, 1998. page: 980315 doi:10.4271/980315).

11. Kuehn, TH and Goldstein, RJ. Numerical solution to the Navier-Stokes equations for laminar natural convection about a horizontal isothermal circular cylinder. *International Journal of Heat and Mass Transfer*, 1980, 23 (7), pp. 971–979.
12. Clemes, SB., Hollands, KGT., Brunger, AP. Natural convection heat transfer from long horizontal isothermal cylinders. *ASME Journal of Heat Transfer*, 1994, 116 (1), pp. 96–105.
13. Roychowdhury, DG., Das, SK., Sundararajan, T. Numerical simulation of natural convective heat transfer and fluid flow around a heated cylinder inside an enclosure. *Heat and Mass Transfer*, 2002, 38 (7–8), pp. 565–576.
14. Ambrosini, D., Paoletti, D., Spagnolo, GS. Study of free-convective onset on a horizontal wire using speckle pattern interferometry. *International Journal of Heat and Mass Transfer*, 2003, 46 (22), pp. 4145–4155.
15. Yamamoto, S., Niiyama, D., Shin, BR. A Numerical method for natural convection and heat conduction around and in a horizontal circular pipe. *International Journal of Heat and Mass Transfer*, 2004, 47 (26), pp. 5781–5792.
16. Corcione, M. Correlating equations for free convection heat transfer from horizontal isothermal cylinders set in a vertical array. *International Journal of Heat and Mass Transfer*, 2005, 48 (17), pp. 3660–3673.
17. Molla, Md M., Hossain, Md A., Paul, MC. Natural convection flow from an isothermal horizontal circular cylinder in presence of heat generation. *International Journal of Engineering Science*, 2006, 44 (13–14), pp. 949–958.
18. Incropera, FP and DeWitt, DP. *Fundamentals of Heat and Mass Transfer*. 4th Ed., page:540., Istanbul, (In Turkish), 2001.
19. Kreith, F and Bohn, MS. *Principles of Heat Transfer*, sixth ed., Brooks/Cole, California, 2001. pp.317–318.
20. Cengel, YA. *Heat and Mass Transfer*. Guven Bilimsel Kitabevi, Izmir. (In Turkish), 2011.
21. Quereshi, ZH and Ahmad, R. Natural convection from a uniform heat flux horizontal cylinder at moderate Rayleigh numbers. *Numerical Heat Transfer*, 1987, 11 (2), pp. 199–212.
22. Molla, Md M., Paul, SC., Hossain, Md A. Natural convection flow from a horizontal circular cylinder with uniform heat flux in presence of heat generation. *Applied Mathematical Modelling*, 2009, 33 (7), pp. 3226–3236.
23. Demir, H. Experimental and numerical studies of natural convection from horizontal concrete cylinder heated with a cylindrical heat source. *International Communications in Heat and Mass Transfer*, 2010, 37 (4), pp. 422–429.
24. Cheng, CY. Natural convection boundary layer flow of fluid with temperature-dependent viscosity from a horizontal elliptical cylinder with constant surface heat flux, *Applied Mathematics and Computation*, 2010, 217 (1), pp. 83–91.
25. Newport, DT., Dalton, TM., Davies, MRD., Whelan, M., Forno, C. On the Thermal interaction between an isothermal cylinder and its isothermal enclosure for cylinder Rayleigh number of order 10^4 . *ASME Journal of Heat Transfer*, 2001, 123 (6), pp. 1052–1061.
26. Shih, TIP. Application of CFD in the automotive industry: Where do we want to be and how to get there? Final Report for NSF Grant CTS-0001794 East Lansing, MI, 2001.
27. Kobayashi, T and Tsubokura, M. CFD application in automotive industry, in: E.H. Hirschel et al. (Eds.), 100 Vol. Of Notes on Numerical Fluid Mechanics NNFM 100, Springer, Heidelberg, 2009. pp. 285–295.
28. ANSYS CFX 2012 version 12.1, user manual, www.ansys.com/products/icemcfd.asp.
29. Henson, JC and Malalasekera, WMG. Comparison of the discrete transfer and monte carlo methods for radiative heat transfer in three-dimensional, nonhomogeneous, scattering media. *Numerical Heat Transfer Part A Applications*, 1997, 31 (1), pp. 19–36.
30. Ji, Y., Cook, MJ., Hanby, VI., Infield, DG., Loveday, DL., Mei, L. CFD modelling of double-skin façades with venetian blinds. in *Proceedings of the IBP-SA Building Simulation*, 2007. pp. 1491–1498.
31. Langebach, J., Senin, S., Karcher, Ch.. Experimental study of convection and radiation interaction in a headlight model using pressure variation. *Experimental Thermal and Fluid Science*, 2007. pp. 32521–528.
32. http://203.158.253.140/media/eBook/Engineer/Heat%20And%20Mass%20Transfer/Handbook%20of%20Heat%20Transfer/35558_04.pdf (Accessed in 13 August 2012).
33. Ashjaee, M., Eshtiaghi, AH., Yaghoubi, M., Yousefi, T. Experimental investigation on free convection from a horizontal cylinder beneath an adiabatic ceiling. *Experimental Thermal and Fluid Science*, 2007, 32 (2) pp. 614–623.
34. Wang, P., Kahawita, R., Nguyen, TH. Numerical computation of the natural convection flow about

a horizontal cylinder using splines. Numerical Heat Transfer Part A Applications, 1990, 17 (2), pp. 191–215.

35. Saitoh, T., Sajik, T., Maruhara, K. Benchmark solutions to natural convection heat transfer problem around a horizontal circular cylinder. International Journal of Heat and Mass Transfer, 1993, 36 (5), pp. 1251–1259.

36. Razavi, SE., Barar, F., Farhangmer, V. Characteristics-Based finite-volume solution for natural convection around a horizontal cylinder. Journal of Applied Sciences, 2008, 8 (10), pp. 1905–1911.

37. Reymond, O., Murray, DB., O'Donovan, TS. Natural convection heat transfer from two horizontal cylinders. Experimental Thermal and Fluid Science, 2008, 32 (8), pp. 1702–1709.

38. Grafsonningen, S and Jensen, A. B.A.P. Reif, PIV investigation of buoyant plume from natural con-

vection heat transfer above a horizontal heated cylinder. International Journal of Heat and Mass Transfer, 2011, 54 (23–24), pp. 4975–4987.

39. Atmane, MA., Chan, VSS., Murray, DB. Natural convection around a horizontal heated cylinder: The effects of vertical confinement. International Journal of Heat and Mass Transfer, 2003, 46 (19), pp. 3661–3672.

40. Abu-Hijleh BAK Natural convection heat transfer from a cylinder with high conductivity permeable fins. ASME J Heat Transfer, 2003, 125(2), pp. 282–288.

41. Kreith F, Bohn MS Principles of heat transfer, 6th edn. Brooks/Cole, California, 2001, pp 317–318.

42. Kuehn TH, Goldstein RJ Numerical solution to the Navier-Stokes equations for laminar natural convection about a horizontal isothermal circular cylinder. Int J Heat Mass Transfer, 1980, 23(7) pp. 971–979.



K. Furkan SÖKMEN,

Assoc. Professor at Bursa Technical University. He graduated Uludağ University Mechanical Engineering Department. He has a more than 12 years experience as thermal engineer in Automotive Lighting (Magnetti Marelli Group) Company and Fiat Auto Sp A. He has a more than 20 years in CFD, heat transfer and thermodynamic. This study was done by manuscript team for Magnetti Marelli Group in Sökmen' Ph.D. thesis



Salih COŞKUN,

Assoc. Prof. at Vocational School of Technical Science, Uludag University. He graduated Uludağ University Mechanical Engineering Department. He has a more than 20 years experience in heat transfer and thermodynamic



Nurettin YAMANKARADENİZ,

Dr. at Vocational School of Technical Science, Uludag University. He graduated Uludağ University Mechanical Engineering Department. He has a more than 10 years experience in HVAC System and thermodynamic

NEW POWERFUL ULTRA-VIOLET AND VIOLET RADIATING DIODES

Lev M. Kogan¹, Alexander. N. Kolesnikov², and Andrei N. Turkin³

¹OPTEL Scientific-design centre Open Company, Moscow

²OPTRON Open Society, Moscow

³Moscow State University of M.V. Lomonosov, Moscow

E-mail: levkogan@mail.ru

ABSTRACT

This is a report on the development of new powerful UV radiating diodes (UVRD) with a radiation peak wavelength of $\lambda_{\max} = 360\text{--}390$ nm, radiation flux 0.6–1.5 W and axial radiant intensity up to 9.5 W/sr. The article also describes the development of new powerful violet radiating diodes (VRD) with $\lambda_{\max} = 390\text{--}410$ nm, radiation flux up to 2.7 W and axial radiant intensity to 12 W/sr. The devices are produced with radiation angles of $2\theta_{0.5} = (60 \pm 3)^\circ$ and $(11 \pm 1)^\circ$.

Keywords: UV radiating diode, violet radiating diode, spectrum, radiant flux, radiant intensity, angle of radiation, wavelength

INTRODUCTION

UVRDs and VRDs are applied in tasks such as air cleaning, metal failure detection, glue hardening, in medical science, for room and water disinfection, for document and banknote authenticity checks, in photolithography and in other fields. The scope of these applications can be expanded in particular by increasing the radiation flux Φ_e as well as of UVRD and VRD axial radiant intensity I_e .

In the past, the OPTEL Scientific-design centre Open Company developed and now manufactures UVRDs with $\Phi_e = 45\text{--}270$ mW [1]. UVRDs and VRDs by *SemiLEDs* Company of the C3535 type have Φ_e values not less than: 60 mW at $\lambda_{\max} = 365\text{--}375$ nm and forward current $I_f = 350$ mA; 560

mW at $\lambda_{\max} = 380\text{--}390$ nm and $I_f = 500$ mA; 650 mW at $\lambda_{\max} = 390\text{--}410$ nm and $I_f = 500$ mA [2].

RADIATING CRYSTAL AND STRUCTURE OF THE DIODES

Crystals by *SemiLEDs* Company of types *EV-D80T-U* and *EV-U80T-U2.09*×2.09 mm in size were

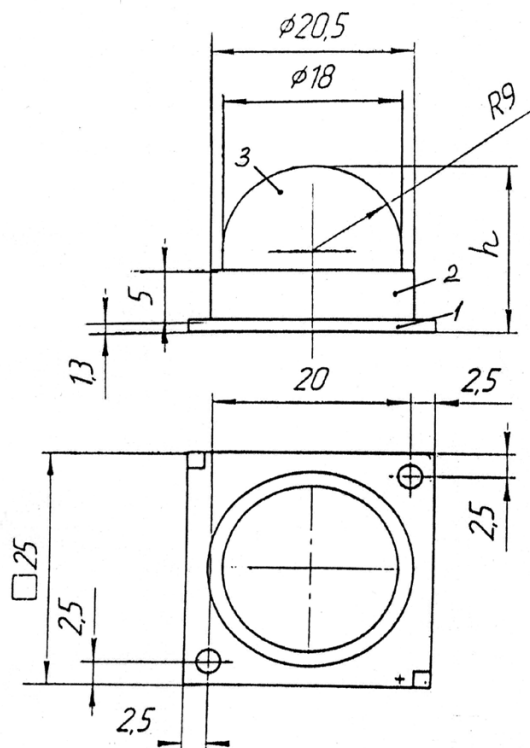


Fig. 1. Structure of UV and violet radiating diodes:
1 – printed-circuit board, 2 – reflector, 3 – polymeric lens

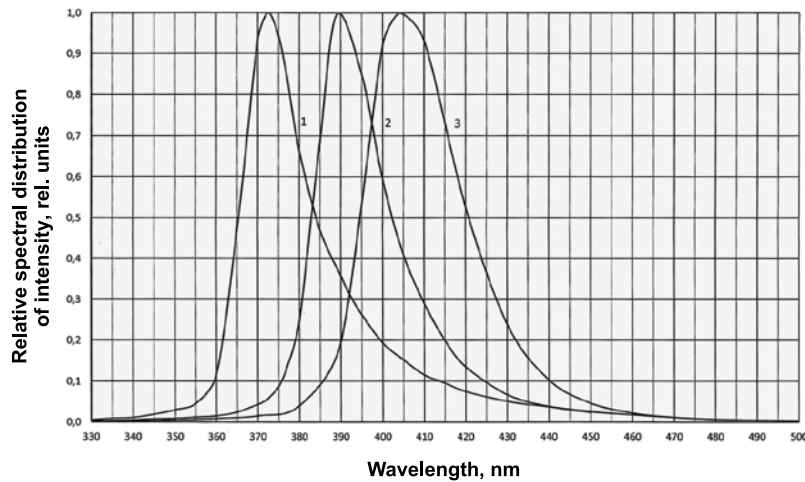


Fig. 2. Typical relative spectra of UV (1, 2) and violet (3) radiating diodes

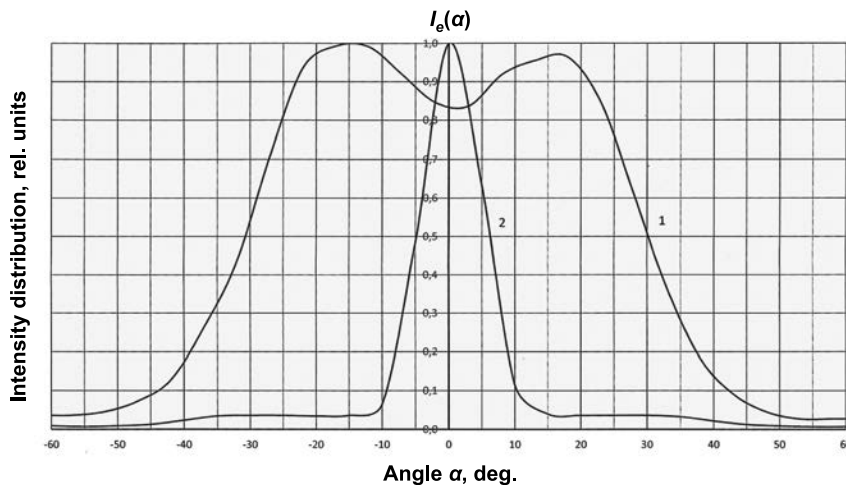


Fig. 3. Typical radiation indicatrices of UV and violet radiating diodes with radiation angle of $2\theta_{0.5} \approx 60^\circ$ (1) and 11° (2)

used on *p-n* heterostructure basis in the *InGaAlN* system (*p-n* heterojunction size is 1.93×1.93 mm)¹. The crystal was mounted on a special printed-circuit board on a copper basis, on which a ceramic reflector of crystal lateral radiation was installed, and then a transparent polymeric lens 18 mm in diameter with a relative refractive index of 1.56 with a hemispherical dome (Fig. 1) was formed. The height of the device *h* amounted to 17 mm maximum (to provide a radiation angle of $2\theta_{0.5} \approx 60^\circ$), or 22 mm ($2\theta_{0.5} \approx 11^\circ$). The electric circuit of the diode was insulated from the case. Thermal resistance between *p-n* junction and the case

amounted to $5-7$ °C/W. The diode was studied using a radiator.

METHODS AND RESULTS OF THE MEASUREMENTS

Measurement of the spatial distribution I_e of the UVRDs and VRDs was carried out in the photometric measurement system (*C*, γ) using a goniophotometer, including a rotary mechanism and photodiode FD-288 with a calibrated aperture diaphragm of 6 mm diameter. Distance from the diode to the photodetector was 4.0 m. The spectral sensitivity of the FD-288 photodiode within wavelength interval of (225–455) nm was determined with an error of no more than 3.5 % (verification test of the VNIIOFI).

UVRD and VRD Φ_e calculation was performed according to the measured values I_e with zone so-

¹ Heterostructure of the vertical type has a multilayered quantum well, a light reflecting layer at the substrate boundary, a diffusive light-output surface and a substrate of copper alloy with high heat conduction. It provides a high radiation generation and output efficiency.

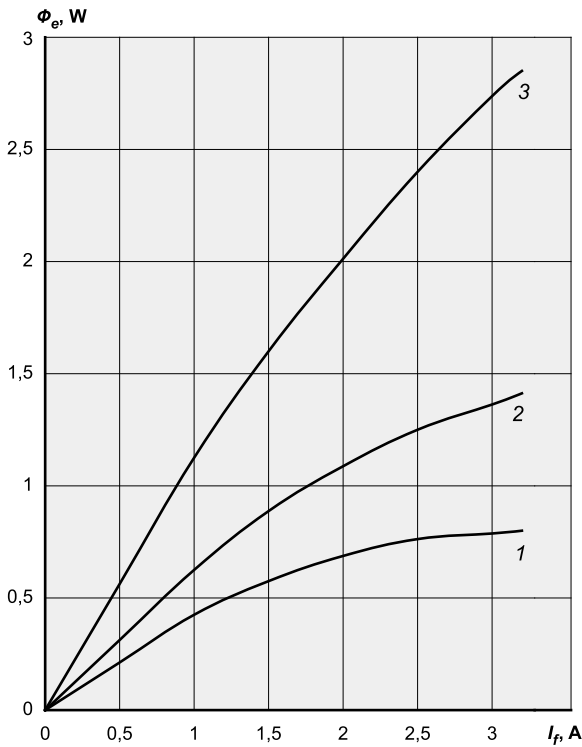


Fig. 4. Typical radiation flux Φ_e dependences on forward current I_f for UV and violet radiating diodes with radiation angle of $2\theta_{0.5} \approx 60^\circ$ and $\lambda_{\max} = 360\text{--}380$ nm (1), $380\text{--}390$ nm (2) and $390\text{--}410$ nm (3) accordingly

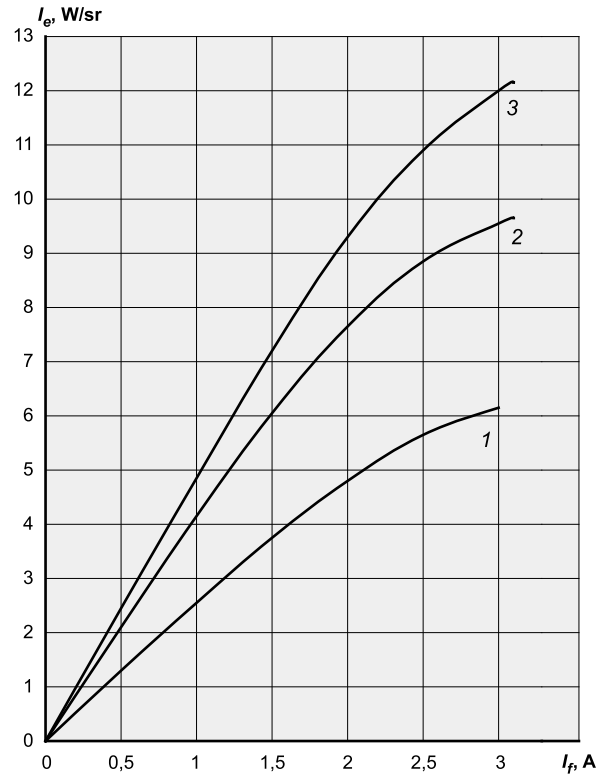


Fig. 5. Typical axial radiant intensity I_e dependences on forward current I_f for UV and violet radiating diodes with radiation angle of $2\theta_{0.5} = 11^\circ$ and $\lambda_{\max} = 360\text{--}380$ nm (1), $380\text{--}390$ nm (2) and $390\text{--}410$ nm (3) respectively

lid angle values corresponding to the angle areas 5° in width (in accordance with the standard GOST 17677–82, appendix 6). In doing so, I_e calculation was carried out based on the measured values of photocurrent of the photodiode working in a short circuit mode, with due regard for UVRD and VRD spectrum measured using MDR-2 double monochromator with a light measuring lamp SIRSH 6–100 calibrated by the VNIIOFI as the source with known radiance spectral distribution.

Typical spectra of UVRDs with $\lambda_{\max} = 360\text{--}390$ nm, and of VRDs with $\lambda_{\max} 390\text{--}410$ nm are given in Fig. 2. The half-width of UVRD and VRD radiation bands were (20 ± 1) nm and (26 ± 1) nm respectively.

Typical indicatrices of UVRD and VRD radiation with $2\theta_{0.5} \approx (60 \pm 3)^\circ$ and $(11 \pm 1)^\circ$ are given in Fig. 3, and Φ_e typical dependences on I_f for UVRDs and VRDs with $2\theta_{0.5} = 60^\circ$ are presented in Fig. 4.

As it can be seen, Φ_e of UVRDs reaches 0.7 W ($\lambda_{\max} = 360\text{--}380$ nm, $I_f = 2.5$ A) and 1.4 W ($\lambda_{\max} = 380\text{--}390$ nm, $I_f = 3$ A). And the radiation external quantum efficiency η_{ext} is equal to 9 % and 18 % at $I_f = 2.5\text{--}3.0$ A respectively.

VRD Φ_e reaches 2.7 W ($\lambda_{\max} = 390\text{--}410$ nm, $I_f = 3$ A), which corresponds to $\eta_{\text{ext}} = 29\%$ at $I_f = 3.0$ A, $\eta_{\text{ext}} = 33\%$ at 2 A and $\eta_{\text{ext}} = 36\%$ at 1 A.

Typical axial I_e dependences on UVRD and VRD I_f with $2\theta_{0.5} = 11^\circ$ are given in Fig. 5. As it can be seen, axial I_e of UVRDs reaches 5.5 W/sr ($\lambda_{\max} = 360\text{--}380$ nm, $I_f = 2.5$ A) and 9.5 W/sr ($\lambda_{\max} = 380\text{--}390$ nm, $I_f = 3$ A), and axial I_e of VRDs is equal to 12 W/sr ($\lambda_{\max} = 390\text{--}410$ nm, $I_f = 3$ A). High values of axial I_e make it possible to use UVRDs and VRDs effectively when they are distant from the illuminated object.

The UVRDs and VRDs under consideration can be effectively used in a pulse electric mode with pulse I_f to 10 A and average I_f to 1 A. In this case, pulse Φ_e and I_e increase approximately three times. UVRD Φ_e with $2\theta_{0.5} = 60^\circ$ in a pulse reaches 3–4 W, and UVRD axial I_e with $2\theta_{0.5} = 11^\circ$ reaches (15–25) W/sr. VRD Φ_e with $2\theta_{0.5} = 60^\circ$ in a pulse reaches 7.5 W, and VRD axial I_e with $2\theta_{0.5} = 11^\circ$ reaches 35 W/sr.

Parameters of the UVRDs and VRDs developed are given in Table 1 and 2, the analysis of which points to the fact that Φ_e and I_e grow with λ_{\max} increase in the spectral intervals considered. But

Table 1. Photometric and electric parameters of UV radiating diodes with *p-n* junction temperature of $(25 \pm 10)^\circ\text{C}$

Type	I_f , A	U_f , V, no more than	λ_{\max} , nm	$2\theta_{0.5}$, °	Φ_e , W		I_e , W/sr	
					not less than	Typical value	not less than	Typical value
Y-124UVD-370-1 Y-124UVD-385-1	2.5 3.0	4.0	360-380 380-390	60 ± 3	0.6 1.3	0.7 1.4	0.5 1.0	1.0 1.5
Y-124UVD-370-2 Y-124UVD-385-2	2.5 3.0	4.0	360-380 380-390	11 ± 1	0.15 0.6	0.2 0.7	5.0 9.0	5.5 9.5

Table 2. Photometric and electric parameters of violet radiating diodes with *p-n* junction temperature of $(25 \pm 10)^\circ\text{C}$

Type	I_f , A	U_f , V, no more than	λ_{\max} , nm	$2\theta_{0.5}$, °	Φ_e , W		I_e , W/sr	
					not less than	Typical value	not less than	Typical value
Y-124VD-400-1 Y-124VD-400-2	3.0 3.0	4.0 4.0	390-410 390-410	60 ± 3 11 ± 1	2.5 1.0	2.7 1.5	2.0 11.0	2.5 12.0

within lesser λ_{\max} (360–370 nm), these parameters are sufficiently high.

The operation speed of UVRD and VRD is characterised by radiation pulse increase and decrease time at 0.1–0.9 levels within 20–30 ns interval.

Thus, it is shown that there is a possibility to obtain high Φ_e and I_e values of UVRDs and VRDs (to 2.7 W and to 12 W/sr) values accordingly².

The authors are grateful to I.T. Rassokhin and A.L. Gofshtein-Gardt for their help in the work.

REFERENCES

1. Galchina N.A., Kogan L.M., Kolesnikov A.A., Portnyagin J.A. Powerful ultra-violet radiating diodes // Svetotekhnika. 2010, # 3, pp. 35–37.
2. Turkin A. New products in the light emitting diode range of *SemiLEDs* Company // Modern electronics. 2015, # 4, pp. 2–5.
3. Kogan L., Galchina N., Gofshtein-Gardt A., Kolesnikov A. Radiating diodes of infra-red interval // Semiconductor light engineering. 2014, #5, pp. 48–49.

² Earlier [3], for IR radiating diodes with $\lambda_{\max} = (850 \pm 20 \text{ nm})$, Φ_e to 3.3 W and axial I_e to 8.5 W/sr were obtained



Lev M. Kogan,
Dr. of Technical Sc.,
graduated from MPEI
in 1956, Scientific Head
of OPTEL Scientific-design
centre Open Company



Alexander N. Kolesnikov,
engineer-physicist,
graduated from MEPhI in
1971, leader metrologist
of OPTRON Open Society



Andrei N. Turkin,
Ph.D. in phys. – math.,
graduated from physical
faculty of MGU
by M.V. Lomonosov
in 1995, senior
teacher at physical
faculty semiconductor
chair of MGU
by M.V. Lomonosov

COMPARISON OF RESULTS OF COMPUTER SIMULATIONS FOR THE ESCAPE ROUTE LIGHTING INSTALLATION

Andrzej Pawlak

Central Institute for Labour Protection – National Research Institute, Warsaw
E-mail: anpaw@ciop.pl

ABSTRACT

The purpose of the study was to determine the performance accuracy of the simulation of escape route lighting installations using the most popular programs supporting the lighting design – DIAUX and RELUX and possible errors associated with illuminance measurement of emergency escape lighting. In order to complete the projects we have selected five emergency lighting luminaires with LED sources with different light curves and the values of the luminous flux. Calculations in both programs have been made for a corridor with dimensions of $22 \times 2 \times 2.28$ m, and based on the most accurate possible calculation grid, and only on direct light from luminaires. Lighting requirements have been determined in accordance to the provisions of the standard EN1838: 2013 Lighting applications – Emergency lighting for escape routes with a width of 2 m. Based on the analysis of the results of computer simulations and measurements, we made conclusion that both programs supporting emergency escape lighting design, despite some defects, properly calculate the emergency escape lighting.

Keywords: escape route lighting, program supporting the lighting design DIALUX and RELUX, escape lighting luminaire, EN1838: 2013

1. INTRODUCTION

In case there is sudden and prolonged lack of basic lighting, buildings cannot be vacated safely, especially if many people are present, and the ongoing

activities cannot be completed while observing the necessary safety principles. All escape routes must be visible and clearly marked. For the determination of evacuation routes are applied safety signs, which can be internally or externally illuminated. Externally illuminated signs are made of photoluminescent materials and require appropriate conditions for exposure. As shown conducted research [1], to achieve the required luminance values of the surface sign are very important: the chemical composition of the material, from which made a sign, exposure time and value of illuminance on material surface of sign before disappearance of general lighting, and the spectral distribution of excitation source. For lighting of escape routes are used suitable luminaires. These luminaires are designed to allow people to safely vacate rooms – hence they are called escape lighting luminaires. For reliable operation of emergency lighting, additional sources of electricity are used to supply power to selected general lighting luminaires or special luminaires installed for this



Fig. 1. Image showing the Zumtobel luminaire (Emergency lighting catalogue ZUMTOBEL)

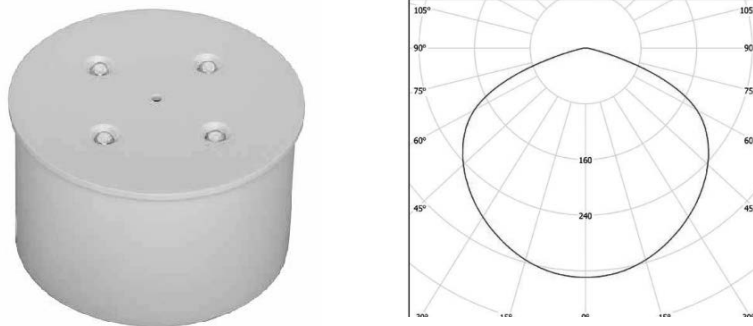


Fig. 2. Image showing the Amatech luminaire (Discret N) and its luminosity curve [Emergency lighting systems. Catalogue 2105. AMATECH – AMABUD]

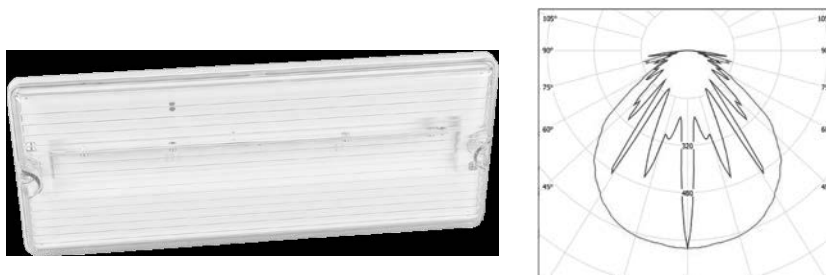


Fig. 3. Image showing the Amatech luminaire (Alfa III) and its luminosity curve (Emergency lighting systems, catalogue 2105, AMATECH – AMABUD)

very purpose. According to regulations currently in force in Poland, automatically activated emergency lighting should be installed in every facility, in which the loss of power may put human life and health at risk, seriously endanger the environment and cause serious damage in property. Hence, emergency lighting systems are directly connected to the safety of people. Consequently, their technical parameters (related to illumination and electricity), and most importantly their operating efficiency, are strictly prescribed in standards. The requirements specified in standards stipulate minimal values that emergency lighting systems should satisfy [2]. Unfortunately, there are still many buildings with improperly operating escape lighting systems, which may be the result of, for instance, incorrect execution of design, incorrect execution of installation works or lack of maintenance.

2. OBJECT OF STUDY

2.1. Escape lighting luminaires

Five various types of escape lighting luminaires were selected for the study, with emergency and mains power supply, i.e. with their own sources of emergency power supply, that satisfy the times specified in the standard PN-EN1838:2013, af-

ter B, which illuminance whose value is 0.25 lx and 0.5 lx is achieved on the escape band after 5 seconds and, respectively 0.5 lx and 1 lx after 60 seconds [3]. These requirements can be satisfied, most of all, by luminaires with LED sources.

The first type is a luminaire by Zumtobel, Oriled 2/1W LED760 (Fig. 1.), already installed on a corridor wall. These luminaires have two 1 W LED sources. The remaining luminaires to be studied were selected from the following products of: Amabud-Amatech, Hybryd, Awex and TM Technology, the four leading producers of emergency lighting luminaires from Poland. The main parameters taken into account when selecting these luminaires were the luminosity curve, the luminous flux value and the number / power of LED sources. Following the analysis of technical data, luminaires of the first two named producers were chosen, which are:

- DISCRET N, 4 x 1 LED, AT, DW1/4/4/AS/1H/ produced by AMATECH (Fig. 2);
- ALFA III, AT, AL3/4/4/AS/1H produced by AMATECH (Fig. 3);
- HERKULES-P ROAD AT 1J LED5 produced by HYBRYD (Fig. 4);
- KWADRA SIDE N AT 1J LED3 produced by HYBRYD (Fig. 5).

All these luminaires are designed to operate in emergency mode for one hour.

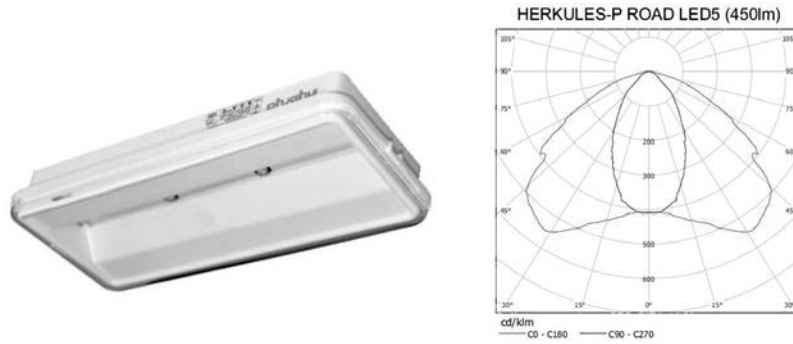


Fig. 4. Image showing the Hybrid luminaire (Herkules) and its luminosity curve (Emergency Lighting Luminaires' 2015, catalogue HYBRYD)

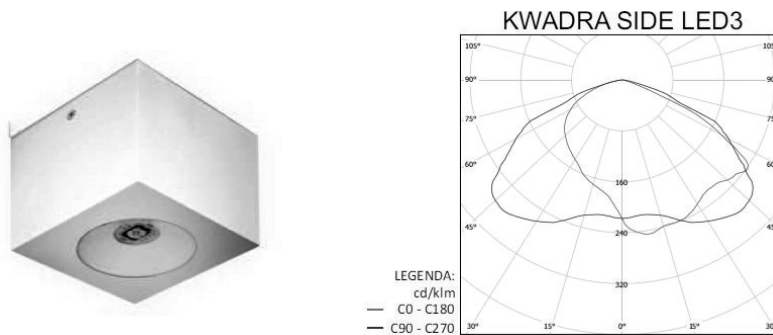


Fig. 5. Image showing the Hybrid luminaire (Kwadra Side) and its luminosity curve (Emergency Lighting Luminaires' 2015, catalogue HYBRYD)

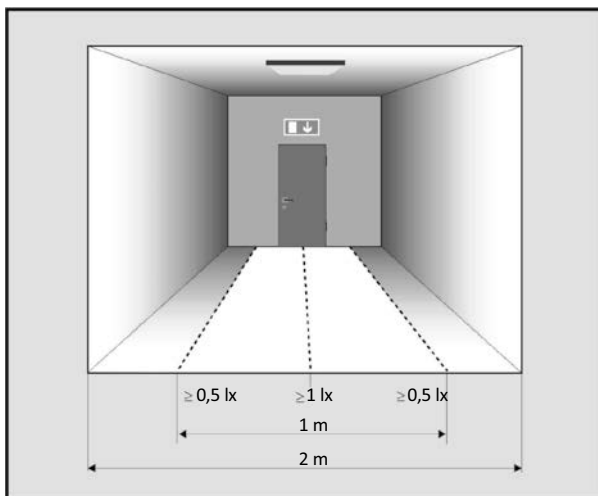


Fig. 6. Normalized escape route [4]

2.2. The examined room

A corridor whose dimensions are 22 x 2 x 2.28 m was selected for the study. Zumtobel luminaires were installed on one wall at the height of 0.58 m in relation to the floor and with a distance of 4.4 m between the luminaires (2.2 m from shorter walls). The remaining luminaires were installed on the wall

at the height and with distances between the luminaires that satisfy requirements of the standard.

3. ILLUMINATION RELATED REQUIREMENTS

Pursuant to illumination related requirements specified in the standard for escape band's up to 2 m wide, the illuminance may not be lower than 1 lx at any point along the centre line. At the same time, the illuminance should be at least 0.5 lx (Fig. 6.) in the central band that covers at least half of the escape route width.

4. ESCAPE LIGHTING DESIGNS

DIALUX and RELUX, two, most popular in Poland commercial programs aiding the design of lighting were selected for the purpose of creating designs of escape lighting. In both programs the most accurate available calculation grid was selected, containing 4096 points (128 x 32). In both programs an option using only the indirect constituent was selected, for which the co-operation of reflected light was not taken into account – satisfying

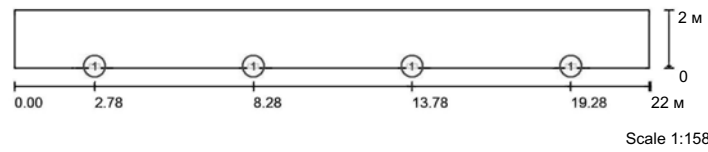


Fig. 7. Layout plan of Amatech luminaires in DIALUX

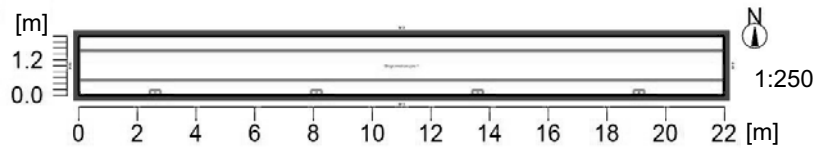


Fig. 8. Layout plan of Amatech luminaires in RELUX

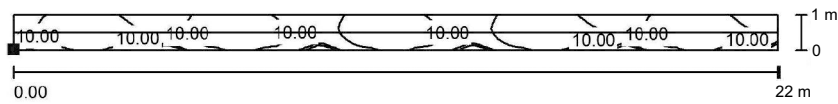


Fig. 9. The determined distributions of illuminance of luminaires by Zumtobel obtained in DIALUX

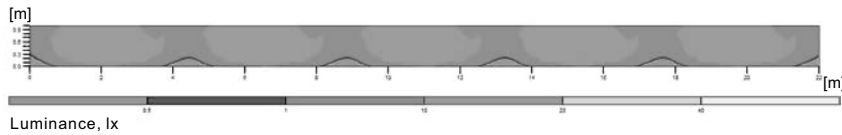


Fig. 10. The determined distributions of illuminance of luminaires by Zumtobel obtained in RELUX

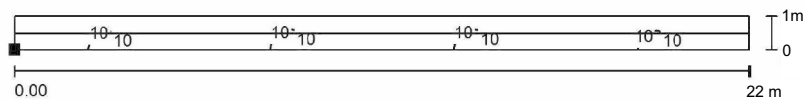


Fig. 11. The determined distributions of illuminance of luminaires by Amatech (Discret N) obtained in DIALUX

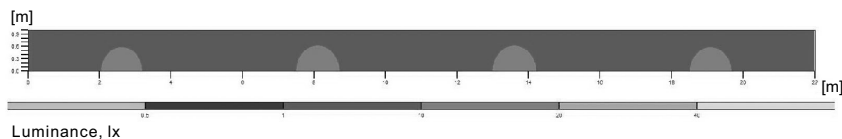


Fig. 12. The determined distributions of illuminance of luminaires by Amatech (Discret N) obtained in RELUX

the requirements for the designed emergency lighting. Moreover, the lighting designs assumed zero value coefficients of reflection of the walls, the ceiling and the floor, and a conservation (maintenance) coefficient equal to 0.77 (a value suggested by both programs).

The escape lighting designs were made for a corridor whose dimensions are 22 x 2 x 2.28 m. Thus, a central escape band 22 x 1 m and a centre line, 22 m long, placed in the middle of this band, were assumed in both programs for the purpose of calculating the illuminance.

Due to the fact that luminaire layout plans in various designs don't have significant differences, Fig. 7 shows an example of location of ALFA III luminaires by Amatech in DIALUX software, while Fig. 8 displays such locations in RELUX.

5. RESULTS OF ESCAPE LIGHTING DESIGNS

Figs. 9–18 show the determined distributions of lighting in the form of counter lines for the completed designs. Table 1 shows the values of minimal

Table 1. A list of results of values illuminance of escape lighting obtained from computer simulation

Type of luminaires / producer	Program supporting the lighting design	The centre line of an escape route			The central band of an escape route		
		E_{max} , lx	E_{min} , lx	E_{max} / E_{min} , lx	E_{max} , lx	E_{min} , lx	E_{max} / E_{min} , lx
ORILED2/1W LED760 ZUMTOBEL	DIALUX	14.0	2.94	4.76: 1	19.0	0.13	146: 1
	RELUX	14.6	1.5	9.73: 1	19.8	0.0	—
DISCRET N, 4 x 1 LED, AT AMATECH	DIALUX	10.78	1.94	5.56: 1	12.0	1.85	6.49: 1
	RELUX	10.5	1.5	7.0: 1	11.7	1.4	8.36: 1
ALFA III, AT, AL3/4/4/AS/1H AMATECH	DIALUX	6.0	1.32	4.55: 1	16.0	1.04	15.38: 1
	RELUX	5.8	0.8	7.25: 1	16.7	0.7	23.86: 1
HERKULES-P ROAD AT LED5 HYBRYD	DIALUX	28.0	2.8	10: 1	30.0	2.48	12.1: 1
	RELUX	20.8	0.5	41.6: 1	21.2	0.4	53: 1
KWADRA SIDE N AT 1J LED3 HYBRYD	DIALUX	10.5	1.89	5.56: 1	13.0	1.48	8.78: 1
	RELUX	11.1	0.6	18.5: 1	12.8	0.3	42.67: 1

Values marked in bold italic type satisfy the standard’s requirements.

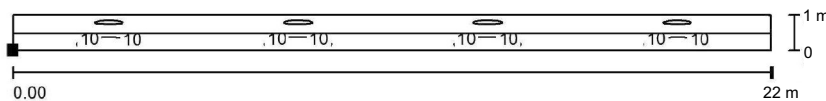


Fig. 13. The determined distributions of illuminance of luminaires by Amatech (ALFA III) obtained in DIALUX

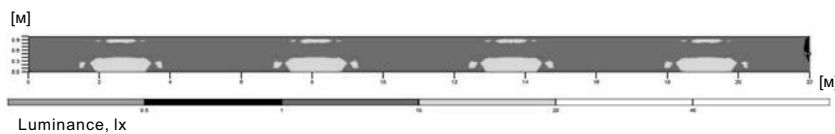


Fig. 14. The determined distributions of illuminance of luminaires by Amatech (ALFA III) obtained in RELUX

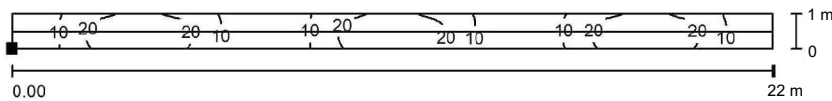


Fig. 15. The determined distributions of illuminance of luminaires by Hybryd (Herkules) obtained in DIALUX

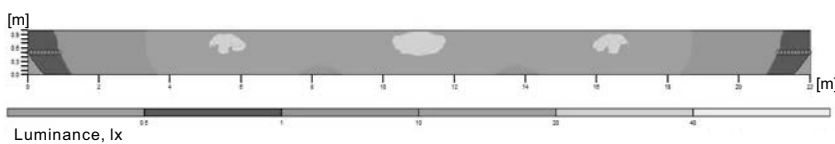


Fig. 16. The determined distributions of illuminance of luminaires by Hybryd (Herkules) obtained in RELUX

and maximal illuminance, obtained from computer simulation, for the centre line and the central band of the escape route. The table also speci-

fies the determined relations of the maximal value to the minimal value of illuminance for both measurement areas.

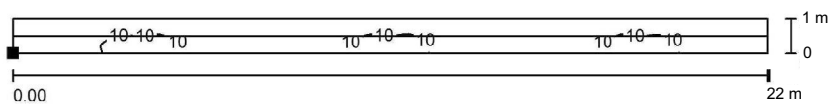


Fig. 17. The determined distributions of illuminance of luminaires by Hybryd (Kwadra Side) obtained in DIALUX

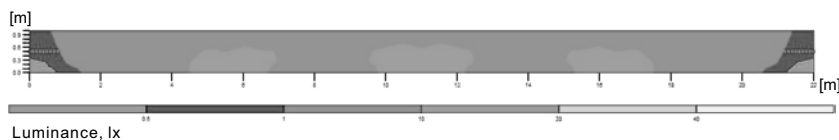


Fig. 18. The determined distributions of illuminance of luminaires by Hybryd (Kwadra Side) obtained in RELUX

6. THE EXAMINATION OF CORRECTNESS OF COMPUTER SIMULATIONS

6.1. Impact of reflectance coefficient values

In order to examine the impact of the obtained results on assuming non-zero values of coefficient of reflection of all surfaces in the room, for both programs the option of calculations with indirect constituent was applied. In the first variant the values of coefficients of reflectance of the walls, the ceiling and the floor were applied, whereas in the second variant these values were applied, respectively: 50 %, 70 % and 20 %. On the basis of simulations in both programs for the five studied types of escape lighting luminaires, it was found that the obtained values of minimal and maximal illuminance in the centre line and in the central band of escape route did not differ in any of the calculated cases by even a hundredth of a lx and were identical to the values presented in Table 1. Based on this, it can be stated that the selection of the option that applies a direct constituent for escape lighting calculations "automatically" resets reflectance coefficients.

6.2. Influence of the number of calculation grid points

The influence of the assumed number of calculation grid points on measurement results was also examined. Despite the modification of the declared number of points in RELUX, e.g. from 128×32 to 43×3 , the obtained measurement results did not change. However, in DIALUX, with the same modification of the number of points, the same illuminance results were obtained for the centre line

in the escape route, but different values were obtained for the central band (Table 2).

6.3. Conclusions from the examination of correctness of computer simulations

While decreasing the number of calculation points in DIALUX, for all studied luminaires:

- The value of maximal illuminance in the escape central band decreases;
- The value of minimal illuminance in the escape central band increases.

After the calculation grid was changed, in all cases but for ORILED2/1W LED760 by Zumtobel the standard's requirements were satisfied.

7. CONCLUSIONS

On the basis of the listed results a conclusion can be made that the designs of escape lighting with Zumtobel luminaires, made in both programs, fail to satisfy the requirements of the standard with regard to the minimal illuminance in the escape route's central band. Naturally, these designs could have been made correctly but, as mentioned in the beginning, the height and location of luminaires were predetermined by the existing escape lighting system.

In the case of Discret N luminaires made by Amatech, the escape lighting designs made in both programs satisfy all parameters specified in the standard.

The same regularity was identified for ALFA III luminaires by Amatech and Herkules-P Road and Kwadra Side luminaires made by Hybryd, namely that for designs made in DIALUX all parameters required by the standard are met, whereas in the case of designs made in RELUX the standard's re-

Table 2. A list of results of illuminance values of escape lighting obtained from computer simulation in DIALUX with two values of calculation grid

Type of luminaires / producer	Number of points where calculations are made – DIALUX	The centre line of an escape route			The central band of an escape route		
		E _{max} , lx	E _{min} , lx	E _{max} / E _{min} , lx	E _{max} , lx	E _{min} , lx	E _{max} / E _{min} , lx
ORILED2/1W LED760 ZUMTOBEL	128 x 32	14.0	2.94	4.76: 1	19.0	0.13	146: 1
	43 x 3	14.0	2.94	4.76: 1	15.0	0.44	34.1: 1
DISCRET N, 4 x 1 LED, AT AMATECH	128 x 32	10.78	1.94	5.56: 1	12.0	1.85	6.49: 1
	43 x 3	10.78	1.94	5.56: 1	11.0	2.02	5.45: 1
ALFA III, AT, AL3/4/4/ AS/1H AMATECH	128 x 32	6.0	1.32	4.55: 1	16.0	1.04	15.38: 1
	43 x 3	6.0	1.32	4.55: 1	14.0	1.48	9.46: 1
HERKULES-P ROAD AT LED5 HYBRYD	128 x 32	28.0	2.8	10: 1	30.0	2.48	12.1: 1
	43 x 3	28.0	2.8	10: 1	29.0	2.9	10: 1
KWADRA SIDE N AT 1J LED3 HYBRYD	128 x 32	10.5	1.89	5.56: 1	13.0	1.48	8.78: 1
	43 x 3	10.5	1.89	5.56: 1	12.0	1.74	6.9: 1

Values marked in bold italic type satisfy the standard's requirements.

requirements are not met. These are not significant variances when related to the standard's requirements and can be eliminated in a simple way, e.g. by changing the distance between the luminaires. However, the idea behind the simulation was, first of all, to compare the results obtained in both programs. Hence, the same input parameters and the height of installation and location of luminaires were applied in both programs.

However, following the comparative analysis of illuminance results for the same areas obtained in DIALUX and RELUX a conclusion can be made that:

- In five cases (with the exception of Oriled luminaire by Zumtobel) the illuminance results obtained in RELUX fail to satisfy the requirements (for three out of four examined luminaires). However, the illuminance values determined in DIALUX are correct in all cases;

- By rule, in all examined cases the failure to meet standard requirements with respect to illuminance is related to the failure to meet the requirement of the relation of maximal illuminance to minimal illuminance;

- In the majority of cases, 16 out of 20, the illuminance values determined in DIALUX are higher than the ones determined in RELUX;

- In 14 cases out of 20, the differences between illuminance values were slight – up to 2 lx, while the maximal differences of 7.2 and 8.8 lx only applied to one luminaire – Herkules-P Road made by Hybryd.

Conclusions from the use of DIALUX and RELUX software:

- The use of the escape lighting module in DIALUX is more intuitive and convenient than in RELUX;

- The technical data of luminaires applied in the designs (taken from a data base) in both programs have different parameters, e.g. the luminous flux or luminous efficacy; luminaire sizes are specified in RELUX, while the luminosity curves specified in DIALUX are presented more clearly;

- The drawing of the room with counter lines provided in the calculation results in RELUX is much more legible than the analogous drawing in DIALUX;

- In the results calculated in RELUX, in two instances results of simulation are given, of which

one is rounded to single digits, which affects the determined value of the relation of the maximal and minimal illuminance;

- Only the results of calculations in RELUX specify the standard requirements, while the requirements concerning the minimal illuminance are given in an inaccurate manner (applies to the centre line);

- The results of calculations in DIALUX do not specify the minimal illuminance along the middle line – this value should be calculated.

8. SUMMARY

Both programs aiding the design of escape lighting have certain disadvantages and strong points and, consequently, a unanimous decision on selecting the better program cannot be made. The designs made in RELUX can be considered more restrictive or "safer" only because of the lower values of illuminance obtained in that software. However, it is unknown at this stage whether these illuminance values translate into real values.

ACKNOWLEDGEMENTS

This paper has been prepared on the basis of the results of a research task carried out within the

scope of the second stage of the National Programme "Improvement of safety and working conditions" supported in 2014–2016 – within the scope of state services and statutory activity – by the Ministry of Labour and Social Policy. The Central Institute for Labour Protection – National Research Institute is the Programme's main co-ordinator.

REFERENCES

1. WANDACHOWICZ, K., ZALESINSKA, M. Analysis of the excitation parameters of photoluminescent low-location lighting materials (pl), PRZEGLĄD ELEKTROTECHNICZNY2008. V84, #8, pp.118–121.
2. PAWLAK, A. Principles of operation of emergency lighting systems (pl), PRZEGLĄD ELEKTROTECHNICZNY2015. V91, #7, pp.62–66.
3. EN1838: 2013 Lighting applications – Emergency lighting.
4. PAWLAK, A. Poradnik Technika Świetlna'09, Tom 2, Oświetlenie awaryjne. PKOŚ SEP, Warszawa 2013. pp.141–156
5. Emergency lighting systems. Catalogue 2105. AMATECH – AMABUD.
6. Emergency Lighting Luminaires' 2015. Catalogue HYBRYD.
7. Emergency lighting catalogue ZUMTOBEL.



Andrzej Pawlak

is an assistant in Central Institute for Labour Protection – National Research Institute. He graduated from Warsaw Technical University in 1987, where he received Master of Science in Electrical Engineering, specialty lighting technology. At present time, he works on method of determining photobiological safety of contemporary light sources. He performs also measurement and assessment of risk from optical radiation and lighting. He is a member of Polish Committee on Illumination. He is the author of several dozen technical papers and conference lectures

METHODS AND DEVICES FOR QUICK EVALUATION OF OPTICAL RADIATION ENERGY EFFICIENCY UNDER PHOTOCULTURE CONDITIONS

Vladimir N. Kuzmin and Sergei E. Nikolaev

TKA Scientific and Technical Enterprise Open Company, St.-Petersburg
E-mail: kvnlight@mail.ru; lab@tkaspb.ru

ABSTRACT

The article describes a method of measuring energy efficiency of a flux of optical radiation sources under photoculture conditions, and presents a spectrophotometer developed in TKA Scientific and Technical Enterprise Open Company.

Keywords: photon flux density of photosynthesis, phytoluminaires, artificial source of daylight, light spectral distribution, energy efficiency, plants

INTRODUCTION

It is known that almost all energy on the earth surface comes directly or indirectly from the Sun. Plants convert this energy to a useable form through photosynthesis.

Historically, it has been accepted that measurements of photosynthetic active radiation (PAR) are somewhat subjective, because there are disagreements in scientific opinion on the concept of PAR and its quantitative description.

When studying the influence of optical radiation on plants, it is important to consider that in physiological processes (photosynthesis, forming pigments, growth, photomorphogenesis and so forth), only that part of radiation which is absorbed by vegetable tissues participates. At the end of the 19th century, Kliment Timiryazev set a task for plant physiologists to find out what part of sunlight falling on a leaf was used by it. Keith J McCree (*Agric. Meteorol.*, 10:443, 1972) determined that the correlation between plant photosynthesis and

the number of photons is stronger than with irradiation energy. This thesis is based on the fact that photosynthesis is quantitatively proportional to the number of photons absorbed by the leaves, and is only caused by light within a certain wave length interval. McCree noted that light spectral distribution used in photosynthesis varies significantly in different studies. He also stated that to compare photosynthesis speed values it is important that all experiments used the same criteria.

Studies have shown [1, 2] that radiation spectral range can be conditionally divided into intervals according to its influence on physiological processes: more than 1000 nm is a thermal exposure, used when designing irradiating lighting installations (ILI); 700–750 nm (long-distance red) has a strongly pronounced regulatory effect and in small amounts (several percent) should be a part of the general radiation; 600–700 nm (red) is the area of maximum photosynthetic effect, chlorophyll synthesis and photoperiodism; 500–600 nm (green) is not necessary for plant photosynthesis, but due to its high penetrating effect it is useful for photosynthesis of optically dense leaves and of dense plant seeds; 400–500 nm (dark blue) provides absorption by caratinoids, the second photosynthetic peak, growth and formative effects; 320–400 nm plays a regulatory role in plant development, so this radiation makes sense in small amounts (several percent) of the general radiant flux; 280–320 nm (UV-B). This radiation is harmful for most plants; less than 280 nm (UV-C) causes plant death.

DEVELOPMENT OF THE MEASUREMENT TECHNIQUE

A solution to the problem of measurement is necessary when plants are grown in an artificial irradiation environment. Plants grown using the photoculture method with radiant energy of electric lamps do not create new reserves of energy on earth but only transform the radiant energy of the lamps into chemical energy of the plants. The higher the plant absorption factor of artificial radiation, the less electric energy is needed to grow a unit of vegetative product and hence the greater the value artificial irradiation of plants has to the national economy.

The spectral composition of artificial sources is determined by the lamp types used and by their combination, filter transmission, protection materials, etc. This complexity was very vividly revealed with the introduction of new source types, significantly different by their spectral composition.

Conventionally, a green leaf can be considered a plain optical colour light filter, transmitting and reflecting radiant energy according to the laws of optics. Unlike transparent glass optical filters, a leaf is a muddy light-diffusing environment, which greatly complicates the measurement of radiant energy that the leaf transmits, reflects and absorbs. Spectral curves of transmission and reflection of radiant energy by leaves of most cultures showed that their spectral properties are similar. As a rule, the greatest portion of radiation reflection and transmission is in the green part of the spectrum (550 nm). Absorption has two peaks: one in blue-violet (440 nm), and another is in red (about 660 nm) part of the spectrum.



Fig. 1. Appearance of the TKA-SPECTRUM Spectrophotometer device (PAR)

Internationally, in industry practice there have been attempts to create a uniform sensor for all plants and conditions. But serial manufacture of a uniform sensor with perfect spectral sensitivity is problematic until it isn't a spectral radiometer. In this system, intensity of incident radiation is only determined within the PAR spectral interval: the absorbing ability of plants and to radiating characteristics sources at this interval are not considered. However, it allows applying thermal radiation receivers (phyto-pyranometers) to measure plants irradiance [3].

In global industry practice, an agreement has been accepted, which allows determining and measuring PAR irradiance as an incident quantum flux within an interval from 400 to 700 nm without involving any experimental reactions of plants. In the scientific literature, the terms PAR, PPF (photosynthesis photons flux) and PPFD (photosynthetic photon flux density) have begun to be used interchangeably.

The introduction of new technologies into hot-house plant cultivation (vegetable growing, floriculture), perfection of rationing irradiation installations and of electric energy efficiency, as well as a competent combination of lighting installation versions with various types of light sources — all of this requires application of modern technological facilities ensuring measurement of optical radiation parameters with sufficient accuracy and reliability across the spectral interval.

Undertaking the project entitled “A time-effective evaluation of energy efficiency of optical radiation flux under intensive photoculture conditions”, we have developed the TKA-SPECTRUM Spectrophotometer (PAR) device together with the State Scientific Institution of Northwest Scientific Research Institute of Mechanisation and Electrification of Agriculture of the Russian Academy of Agricultural Sciences, Figs. 1, 4.

The radiance spectral concentration of light sources (or light-emitting diode modules) is determined using standard procedures and lamps with a known correlated colour temperature. This is based on determining the density of photosynthetic photon flux. To measure radiant energy, a widespread evaluation of the photon number is used.

Evaluating the efficiency of crop-growing radiation sources by photon flux requires a correlation of photon number with the quantity of sub-

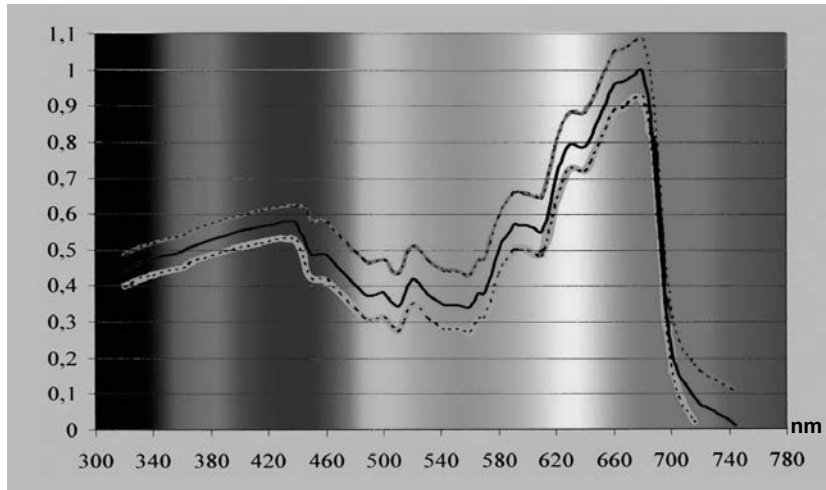


Fig. 2. Statistically average values of relative spectral efficiency of photosynthesis for various plant types based on 66 experimental results from six different authors

stance molecules capable of absorbing the flux. Theoretically, each photon can lead potential pigment molecules to a raised state, therefore, we can assume some correspondence of the incident photons to the quantity of substance molecules capable of absorbing them.

The concept of the measuring device followed on from the feature the understanding of photobiological radiation's influence on a plant. For example, photosynthesis is the most widespread photochemical reaction in nature, transforming light energy into chemical energy. Fig. 2 presents plant photosynthesis spectral efficiency diagrams.

The spectral sensitivity of the photodetectors (photo cells) manufactured don't coincide with the spectral efficiency of photosynthesis (curves are individual), therefore, it should be corrected according to the required effect. The simplest correction method is to use optical filters of coloured glass in sequence within the input device in front of the radiation receiver. To create spectral sensitivity of a square, the boundaries of which coincide with the boundaries of the spectral area, is a very complex problem from a technical point of view.

We abandoned this method due to a lack of a suitable range of glass in the series manufacture within the territory of CIS.

OPERATION PRINCIPLE OF THE DEVICE

The device's operating principle is based on a measurement of optical radiation spectral composition with subsequent mathematical pro-

cessing of the measured results. The dispersive device represents a polychromator, which registers decomposed radiation using a photodiode ruler. The device is a continuation of the serially manufactured TKA-VD Spectrocolorimeter [5]. Knowing the spectrum of the measured light source allows solving almost any task. The technological complexity and labour intensiveness are disadvantages to this.

CALCULATION PROCEDURE

The irradiance spectral concentration $E_{e,\lambda}$ is the relation of irradiance dE_e value falling on a little spectral interval $d\lambda$, to the width of this interval:

$$E_{e,\lambda}(\lambda) = \frac{dE_e}{d\lambda} \quad (1)$$

The measurement unit of $E_{e,\lambda}$ in the SI system is $W \cdot m^{-2} \cdot nm^{-1}$.

$$PPFD = \frac{1}{N_A} \int_{400nm}^{700nm} \frac{\lambda}{hc} \cdot E_{e,\lambda}(\lambda) d\lambda, [\mu mol/m^2 s] \quad (2)$$

where:

$h = 6.62606 \cdot 10^{-34} J \cdot s$ (Planck's constant);

$c = 299792458 m/s$ (light speed);

$N_A = 6.02214 \cdot 10^{17} \mu mol^{-1}$ (Avogadro number).

The spectrophotometer is a direct measuring device with output of irradiance zone values, W/m^2 . The software is divided into two parts. The metrologically significant part of the software is set by the manufacturer directly into the Program-

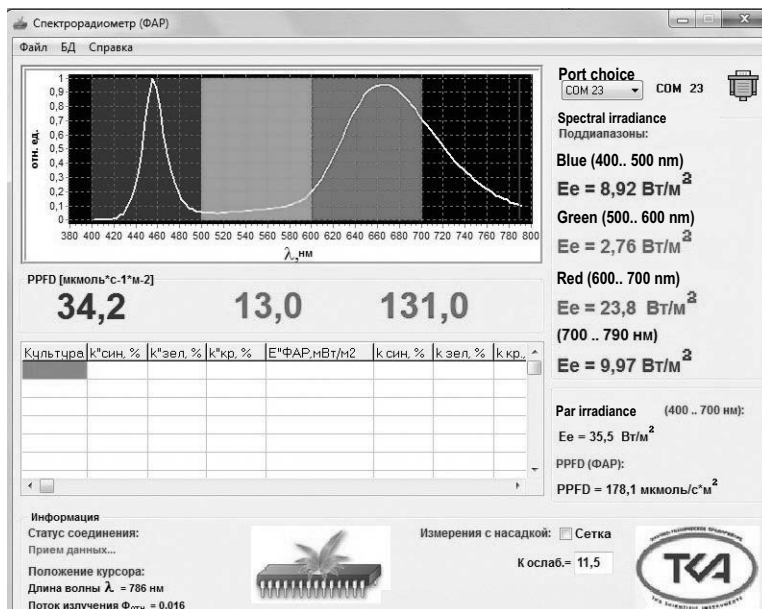


Fig. 3. Working window of the software

mable read-only memory (PROM) of the microcontroller. The interface part of the software is introduced into a personal computer and serves to display the received data both in tabulated, and in graphic form, as well to store measurement results, Fig. 3. It also allows transforming both zone and general PPF from W/m² into μmol/m²/s. Due to the increased energy consumption of irradiation, frequently studies focus on the energy efficiency aspect. For agricultural installations, radiation sources and irradiators with higher spectral efficiency are used. For research, an operator can create a database of normalized tables for irradiated cultures and calculate the deviation factor of the culture spectrum, spectral energy capacity, irradiance energy capacity and full energy capacity [6].

$$E_{blue} = \sum_{400}^{500} E_i; E_{green} = \sum_{500}^{600} E_i; E_{red} = \sum_{600}^{700} E_i. \quad (3)$$

$$E_{PAR} = E_{blue} + E_{green} + E_{red} \quad (4)$$

$$k_{blue} = \frac{E_{blue}}{E_{PAR}} \cdot 100; k_{green} = \frac{E_{green}}{E_{PAR}} \cdot 100; \quad (5)$$

$$k_{red} = \frac{E_{red}}{E_{PAR}} \cdot 100.$$

An example of calculating light source energy efficiency for different cultures is given in Table 1. Spectrum deviation factor:

$$K_S = \sqrt{\frac{1}{3} \sum_{i=1}^3 (k_i - k_i^n)^2}, \quad (6)$$

where k_i and k_i^n are relative values of real and normalised zone irradiance for a specified culture in the i^{th} spectral interval respectively.

Spectral energy capacity ε_λ :

$$\varepsilon_\lambda = MAX \left\{ \frac{k_{blue}^n}{k_{blue}}, \frac{k_{green}^n}{k_{green}}, \frac{k_{red}^n}{k_{red}} \right\} \quad (7)$$

Table 1

Culture	k_{blue}^n , %	k_{green}^n , %	k_{red}^n , %	E_{PAR}^n , mW/m ²	k_{blue} , %	k_{green} , %	k_{red} , %	K_s , ref	$\varepsilon_{\lambda, ref}$	$\varepsilon_{E, ref}$	ε , ref
Tomato	15	17	68	100	28	41	31	26.55	2.19	2.9	6.35
Cucumber	17	40	43	150	28	41	31	9.42	1.39	1.93	2.68

Irradiance energy capacity ε_E :

$$\varepsilon_E = \frac{E_{PAR}}{E_{PAR}^n} \quad (8)$$

Full energy capacity ε :

$$\varepsilon = \varepsilon_\lambda \cdot \varepsilon_{PAR} \quad (9)$$

The calculated values are displayed on the screen and can be transferred into Microsoft Excel. This capability allows raising measurement accuracy without use of additional facilities, as only requirements for operator quality are increased. Calculating results in Excel, rather than in a specialised package using a programming language, can promote wider application of the technique. It makes it possible to research radiation sources, to make decisions on their features and on methods of their application, and also allows minimising the negative exposure of these radiations.

To evaluate ILI performance it is important to analyse efficiency, which in addition to energy consumption indicators, should also take into account irradiation quality determined by uniformity level of the radiation absorbed energy distribution over the surface or the scope of environment of the irradiated object.

CONCLUSIONS

The spectrophotometer has performed well when analyzing light-emitting diode hothouse photolamps and their Chinese analogues. This research was carried out by the Laboratory of phytolight (FitoLabb.ru). Spectral composition and



Fig. 4. Working moment of the measurements

PPFD parameters determine the efficiency of one lamp over another for a plant and its quick growth. Comparison of the two types of light sources: sodium lamps and light-emitting diode luminaires was performed by measuring the following parameters: efficiency of the source spectrum and PPF to power consumption ratio, W, as well as spectrum composition. The obtained results are sufficient to determine luminaire number and their suspension point locations.

Finally, it should be noted that when determining the metrological characteristics of the irradiance measurement channel, a photometric metrological database was used. Quality control of crop-growing lamps and of useful irradiance under production conditions should be carried out using devices with spectral sensitivity correspondent to the spectral efficiency of the photosynthesis, or by using spectral devices.

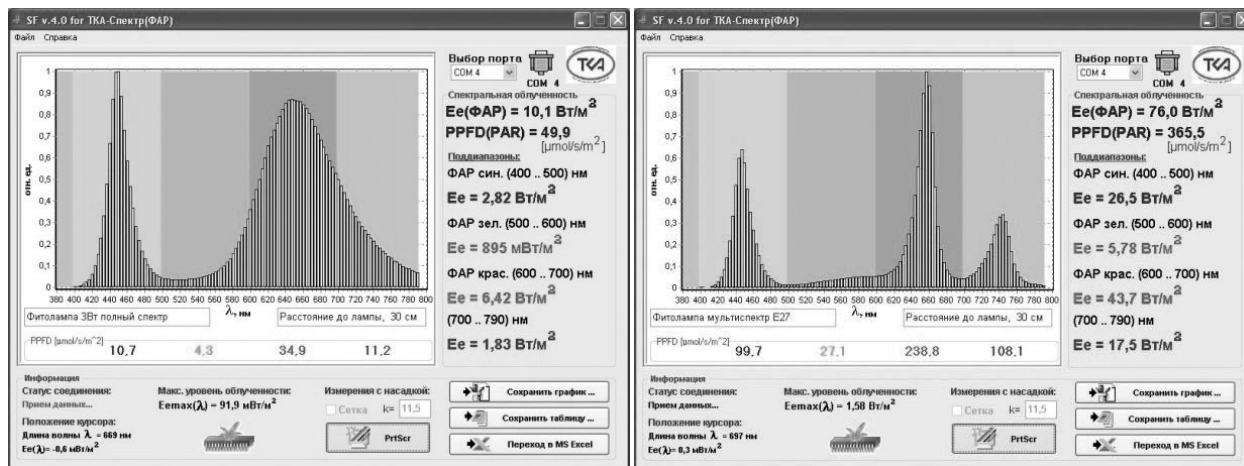


Fig. 5. Comparison of phytolamp parameters (3W socket E27), full spectrum and multispectrum at a distance of 0.3 m

When carrying out such measurements, in order to calibrate the devices, light measuring lamps with known radiation exergy intensity values are necessary. Calculation of radiation exergy intensity of reference lamps, the luminous flux and luminous intensity of which are determined with a set chromatic temperature of the incandescent filament, is easy and does not require additional photometric measurements [4].

The TKA enterprise continues research to determine changes of material properties under the influence of light together with other scientific organisations and LED luminaire production laboratories. Work is in progress to improve the quality of the described device together with the users. A new version of the software has been written for quick analysis of source radiation spectra (Fig. 5).

The purpose of this article is to develop dialogue between manufacturers, consumers of lighting products, metrological service engineers and research laboratories to jointly develop needed solutions in the following fields: measurement techniques; measurement metrological provision; development and upgrading of new devices for crop producers. We are looking to cooperate with interested specialists.

REFERENCES

1. Reference book on light engineering / Under editorship of Yu.B. Aizenberg. The 3rd revised edition. Moscow: Znak. 972 p., 2006.
2. Sarychev G.S. Irradiating lighting installations / G.S. Sarychev. Moscow: Energoatomizdat, 1992. 242 p.
3. V. Yu. Kazenas. Biophotometric control of plant irradiation // Transactions of the first international lighting conference. St.-Petersburg, 1993, pp. 97–98.
4. Sventitsky I.I., Obynochny A.N. A method of measurement of optical radiation exergy [OR] for plant growing // Power supply and energy saving in agriculture. P. 1. Moscow, VIESH, 2003, pp. 260–266.
5. Antonov V.V., Kruglov O.V., Kuzmin V.N.. Devices for measurement of optical parameters and characteristics of light emitting diodes // Semiconductor light engineering. #3. 2010, pp. 26–31.
6. Rakutko S.A., Sudachenko V.N., Markova A.E. Evaluation of optical radiation application efficiency in photoculture based on energy capacity value // Fruit and berry growing of Russia, 2012, #33, pp.270–278.



Vladimir N. Kuzmin,

Dr. of Sc., Prof. HE is graduated from the Kishinevsky State University in 1971, specialising in optics and spectroscopy. At present, he is Deputy General Director on optics and photometry of the TKA scientific and technical enterprise. Fields of scientific interest include development and research of methods and devices to measure parameters and characteristics of optical radiation sources



Sergei E. Nikolaev

Graduated from the Northwest State Correspondence Technical University in 2001, speciality – design and technology of radio-electronic facilities. At present, he is a Head of the optoelectronic devices design laboratory of the TKA scientific and technical enterprise. Development of devices for measurement of parameters and characteristics of optical radiation sources and production technology are in field of his scientific interests

EXPERIMENTAL STUDY OF HOW LIGHTING PATTERNS AFFECT OPTICAL MINISTICKS CHARACTERISTICS

Sergei A. Golubin^{1,2}, Alexei N. Lomanov¹, Vladimir S. Nikitin²,
Valery M. Komarov¹, and Ernst I. Semenov¹

¹Rybinsk State Aviation Technological Academy (RSATU)

²Tenzosensor LLC, Rybinsk

E-mail: 707gsa@mail.ru

ABSTRACT

The article suggests the design of a digital optical ministick based on a poroelastic polymeric element and common receiver optical pattern. The article describes arrangement and operation principle of the optical ministick and its advantages as compared with conventional switching devices. The experimental studies were conducted to determine the characteristics of the developed ministicks.

Keywords: optical ministick, robotics control, switching device, poroelastic polymeric element, experimental study

The increasing complexity of modern robotics, its expanding functionality due to complex manipulators requires the use of compact and multi-functional input devices. One of such input devices is ministicks – two-axis mini joysticks. A ministick is a two-axis mini joystick controlled by a finger unlike conventional joysticks controlled by the entire hand. Fingers move 5–7 times faster than a hand, which allows for quicker and more accurate control actions. A small size allows you to place several ministicks on the panel or control arm.

Resistive principle-based conventional ministicks have several disadvantages: difficult manufacturing, short life, gradual change in their operation characteristics.

NPP Tenzosensor LLC with the specialists of Rybinsk State Aviation Technical University named after P.A. Soloviev involved has develo-

ped an optical ministick design considered in the [1] and [3]. In comparison with existing counterparts, the optical ministick has the following distinctive features: simple design, manufacturability for mass production, high reliability due to the absence of mechanical contact and deformable resistive elements. The optical ministick is notable for noiseless operation, fire and explosion safety, injury safety, light weight and versatility (functions can be reprogrammed [2]).

Ministick appearance is shown in Fig. 1.

Fig. 2 shows a schematic diagram of the optical ministick, which consists of the housing 2 placed on the board 1 and poroelastic element 4 made integral with the control arm 3. There is a light receiver (photodiode, photoresistor) 6 and at least one light source (LED, laser) 7 connected to the microprocessor on the board 1 under the poroelas-



Fig. 1. Optical ministick

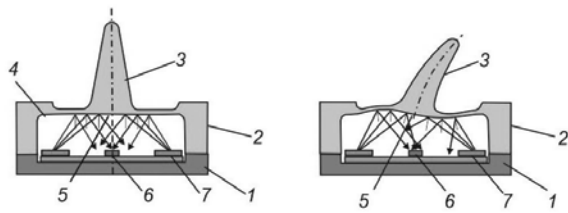


Fig. 2. Optical ministick: 1 – circuit board; 2 – housing; 3 – control arm; 4 – poroelastic element, 5 – light-reflecting surface, 6 – photoelectric converter (photo-diode, photoresistor); 7 – light source (LED, laser).

tic element 4. The poroelastic element 4, an elastic polymeric material piece, contains a light-reflecting or light-absorbing surface 5 located above the light source 6 and photoelectric converters 7. The poroelastic element is made of elastic material in the form of a plate with control arm 3 resting on the optical ministick housing 2 elements attached to the board 1.

The operation principle of the optical ministick is reflecting the light from the light-reflecting surface of the polymeric poroelastic element deformed by the arm depending on the direction and pressure degree.

The following lighting patterns of the ministick are developed:

- Ministick with a common receiver and three light emitters;
- Ministick with a common receiver and four light emitters arranged transversely towards the arm deflection;

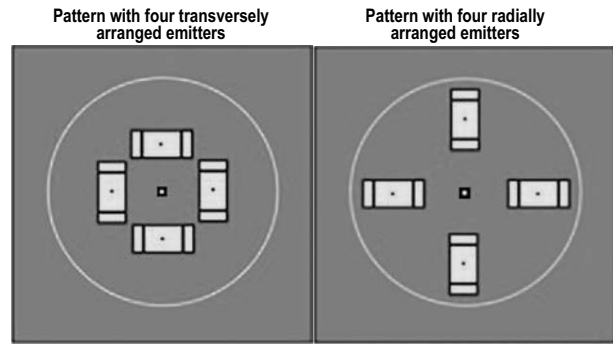


Fig. 3. Patterns of the ministicks with 4 light emitters

- Ministick with a common receiver and four light emitters arranged radially;
- Ministick with a common receiver and six light emitters.

Differences between the ministicks with four radially arranged emitters and four transversely arranged emitters are shown in Fig. 3.

The goal of the experimental study is to determine how the ministick optical pattern affects its transfer function – dependence of the ministick useful signal on the deviation of the control arm.

The ministick useful signal is two numeric values corresponding to the deviation values of the ministick arm with respect to the *X* and *Y* coordinates. Output signal units of measurement are ministick microcontroller ADC readings, which correspond to the relation of ministick photoelectric converters voltages to the ADC reference voltage. The photoelectric converters voltages are determined by the intensity of the reflected light impinging on them,

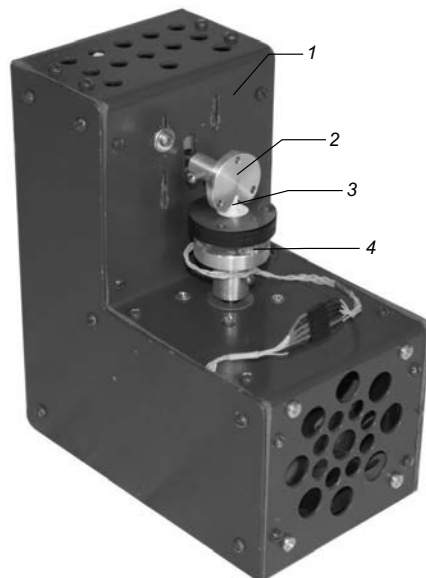


Fig. 4. Multipurpose test bench: 1 – bench body, 2 – deviation element, 3 – ministick, 4 – turning base

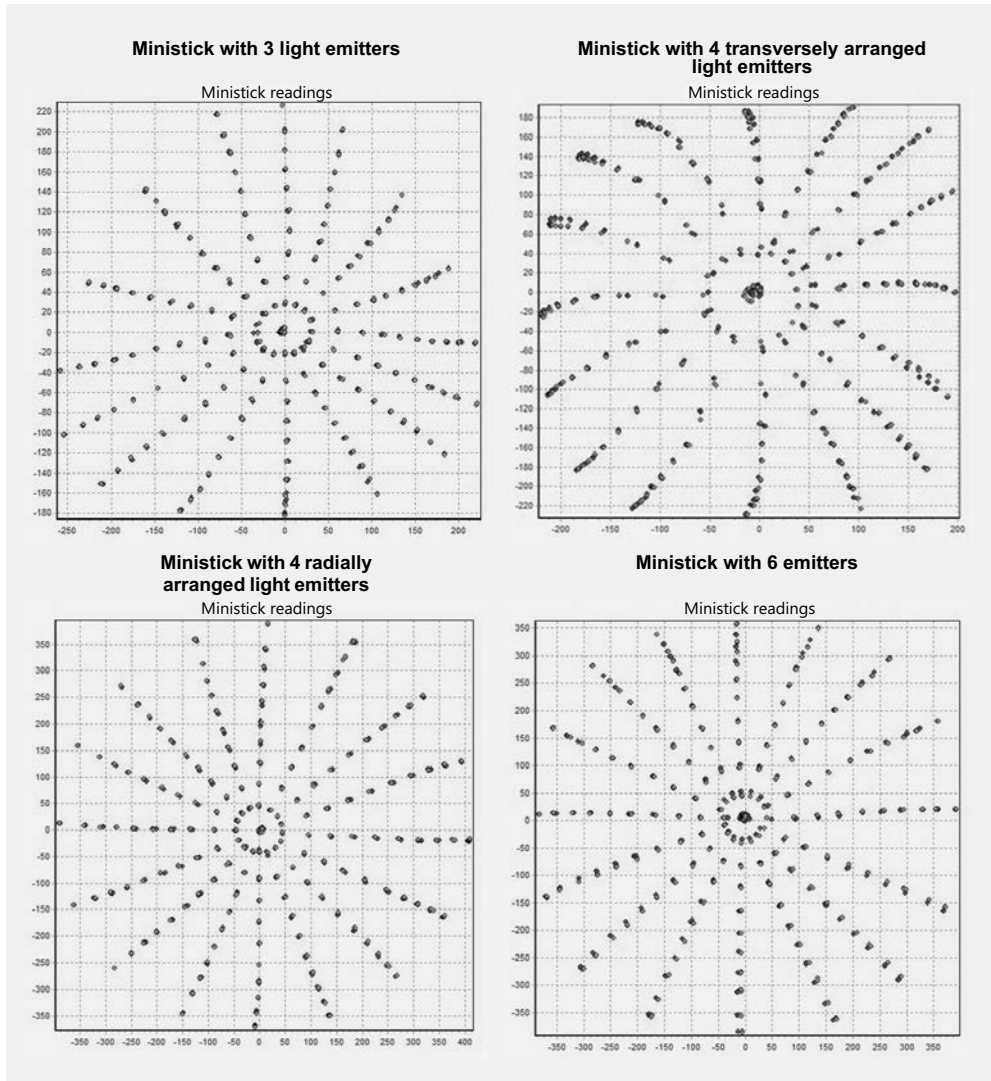


Fig. 5. Ministick readings beam diagrams

which depends on the value of the ministick control arm deviation.

The experiment method is to record the ministick readings in the X- and Y-directions at the points with specified value of the ministick arm deviation from the central position and direction of such deviation defined by the ministick body turning angle.

To study dependence of the ministick signals on the value of the ministick arm linear deflection and ministick turning angle (transfer function) a multipurpose test bench for ministick characteristics computer-aided study was developed. The bench (Fig. 4) includes a turning base 4 with fixed ministick 3 and the deviating element 2 that deviates the ministick arm from the central position strictly to the left or to the right. The base turning and arm deflection are induced with stepper

motors. To ensure accurate positioning and setting the initial position the motor shafts are equipped with absolute digital encoders (angle sensors) with turning angle error not exceeding 0.35° .

To ensure adequacy of the lighting patterns comparison experiment the ministick samples were made with the following common parameters:

- Poroelastic element – of the same size and shape;
- Light emitters – KP-3216F3C LEDs manufactured by Kingbright;
- Photoreceiver – PIN-photodiode PD15–21B/TR8 manufactured by Everlight;
- Metering device – 12-bit analog-to-digital converter integrated into the microcontroller HT46R02B manufactured by Holtek.

Ministick readings were measured under the following conditions:

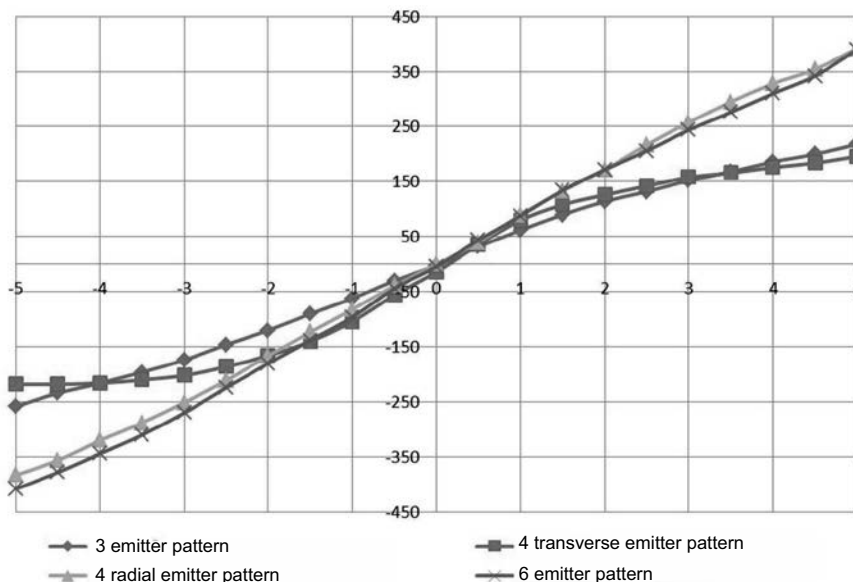


Fig. 6. The transfer function of ministicks with different X-direction patterns (with ministick turning angle of 0°)

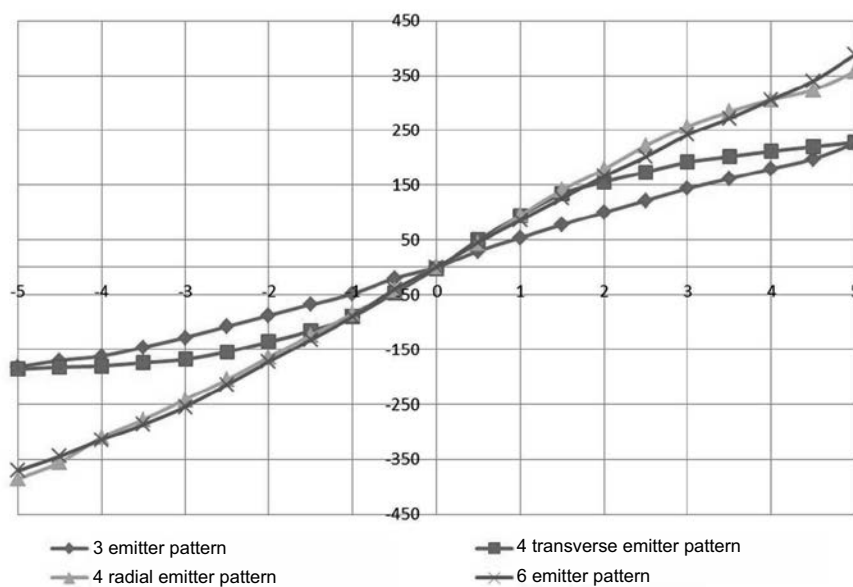


Fig. 7. The transfer function of ministicks with different Y-direction patterns (with ministick turning angle of 90°)

- Limits of ministick arm deviation from the center: $-5..+5$ mm, with a pitch of 0.5 mm;
- Deviation direction: to the left (from +5 mm to -5 mm) to the right (-5 mm to +5 mm);
- Ministick turning angle: from 0° to 157.5° with a pitch of 22.5° ;
- Number of reading measurements: 5, followed by averaging the obtained values.

On completion of the tests, the bench testing program automatically constructs a beam diagram. The beam diagram shows the results of the ministick useful signal measurements in the form

of points with X and Y coordinates corresponding to the numerical values of the ministick output signal. The measurement results obtained at the arm deviation to the right are shown by rectangle dots, to the left – by triangle dots. The beam diagram allows to visually assess the quality of the ministick output signal: signal amplitude, accuracy, linearity, hysteresis.

The beam diagrams of the studied ministicks are shown in Fig. 5.

Results of studying the transfer function of ministicks with different lighting X-direction patterns

Table 1. Quality parameters of the studied ministicks signal

Type of a ministick lighting pattern	with 3 light emitters	with 4 transversely arranged light emitters	with 4 radially arranged light emitters	with 6 light emitters
X-direction range of values (amplitude)	476	414	775	798
Y-direction range of values (amplitude)	408	414	742	758
Max. spread of values	<0.5 %	<0.5 %	<0.5 %	<0.5 %
Max. X-direction nonlinearity	5.83 %	13.25 %	2.40 %	2.45 %
Max. Y-direction nonlinearity	5.91 %	14.27 %	4.75 %	3.23 %
Max. X-direction hysteresis	0.84 %	4.35 %	1.16 %	0.75 %
Max. Y-direction hysteresis	0.99 %	2.42 %	1.75 %	1.06 %

(turning angle is 0°) are shown in Fig. 6. Results of studying the transfer function of ministicks with different lighting Y-direction patterns (turning angle is 90°) are shown in Fig. 7. The diagrams are superimposed to compare them.

The quality of the real ministick useful signal is evaluated in terms of:

- Accuracy – spread of values at a certain arm deviation;
- Nonlinearity – deflection of the studied ministick transfer function curve from the straight line;
- Hysteresis – difference between the values of the output signal with the same arm deviation values, but with different directions.

To assess the readings accuracy we use a root-mean-square deviation value of the measured readings at the point with specified arm deviation. The relative value δ was calculated as follows

$$\delta = |RMSD/\Delta X|, \quad (1)$$

where the δ is a relative deviation of the ministick readings with respect to this coordinate, RMSD is a root-mean-square deviation of the ministick readings with respect to this coordinate, ΔX is a range of values (amplitude) of the transfer function with respect to this coordinate.

To assess the nonlinearity using the least squares method we construct an approximating func-

tion of the straight line $X=kx+b$. Then the nonlinearity N_L is calculated as follows

$$N_L = |X - X_{ESTIM}|/\Delta X, \quad (2)$$

where the X is an actual value of the ministick readings with respect to this coordinate at a given point;

X_{ESTIM} is the value calculated using the approximating function;

ΔX is a range of values (amplitude) of the transfer function with respect to this coordinate.

Hysteresis G of the readings is estimated as follows:

$$G = |X_R - X_L|/\Delta X, \quad (3)$$

where the X_R is a value of the ministick readings with respect to this coordinate at a given point when the arm is moved to the right;

X_L – when the arm is moved to the left;

ΔX is a range of values (amplitude) of the transfer function with respect to this coordinate.

The results are shown in Table 1.

CONCLUSIONS:

1. Selected poroelastic element-based optical ministick patterns allow designing operational and highly efficient devices.

2. The maximum range of the ministick arm deviations is ± 5.0 mm, which is within an optimal range of the fingers deviation amplitude of about 12–20 mm.

3. Ministick blind zone does not exceed 0.5 mm with respect to all coordinates.

4. The ministick made with a common receiver and six light emitter pattern has the best useful signal characteristics: high signal amplitude, transfer function symmetry, low nonlinearity (at most 3.3 %), low hysteresis (at most 1.1 %).

5. The ministick made with a common receiver and four radially arranged light emitters pattern yields to the ministick with six emitters insignificantly in terms of useful signal characteristics. It has high signal amplitude, transfer function symmetry, low nonlinearity (less than 5 %), low hysteresis (less than 2 %).

6. The ministick made with a common receiver and three light emitter pattern has output signal low hysteresis, but its transfer function is asymmetric, nonlinear, and the signal amplitude is 1.7 times lower than that of the ministick with six light emitters.

7. The ministick made with a common receiver and four transversely arranged light emitters pattern has the worst characteristics: high nonlinearity, low amplitude, high hysteresis.

Thus, the following ministick lighting patterns are recognized as the best ones:

- 6 emitter pattern;
- 4 radially arranged light emitters pattern.

The transfer function of the optical ministicks with these lighting patterns complies with the main requirements to complex robotics, manipulators and aircraft controls.

The lighting pattern of the ministick with 3 emitters can be used for polymorphic switches [6]

and for applications where high precision is not required.

The lighting pattern of the ministick with 4 transversely arranged light emitters is the worst of those studied and is not recommended for use.

ACKNOWLEDGEMENT

Applied scientific researches and experimental developments are performed with governmental financial support represented by the Russian Ministry of Education and Science. A unique identifier of applied researches and experimental developments is RFMEFI57914X0087.

REFERENCES:

1. Golubin S.A., Komarov V.M., Lomanov A.N., Nikitin V.S., Semenov E.I. Study of optical ministicks characteristics // *Svetotekhnika*, 2015, No. 6, pp.17–20.
2. Golubin S.A., Nikitin V.S., Belov R.B. Digital optical ministicks for robotics control // *Telecommunications*. 2015. No. 11.
3. Golubin S.A., Komarov V.M., Lomanov A.N., Nikitin V.S., Semenov E.I. Experimental study of optical ministicks characteristics with a common emitter // *P.A. Soloviev RSATU bulletin*. 2015. No. 1
4. Nikitin V.S., Belov R.B. Leverless control // *Science and Life*. 2012. No. 12.
5. Optical joystick: invention application 2013112435 Russian Federation. No. 2013112435/08: applied on 19/03/2013: published by 27/09/2014.
6. Electrical circuits switching method and polymorphic switch used for that: patent 2455678 Russian Federation. No. 2011101226/08: applied on 13/01/2011: published by 10/07/2012.

STUDY OF CHARACTERISTICS OF VCSEL-BASED OPTICAL MINISTICKS

Sergei A. Golubin^{1,2}, Alexei N. Lomanov¹, Vladimir S. Nikitin²,
Valery M. Komarov¹, and Ernst I. Semenov¹

¹Rybinsk State Aviation Technological Academy (RSATU)

²Tenzosensor LLC, Rybinsk

E-mail: 707gsa@mail.ru

ABSTRACT

The article suggests the results of experimental study of a digital optical ministick based on a poroelastic polymeric element and optical circuit with common VCSEL. It also describes design and function of the optical ministick, as well as methods and equipment for studying the ministick transfer function. The experimental studies were conducted to determine the characteristics of the developed ministick.

Keywords: optical ministick, robotics control, switching device, poroelastic polymeric element, VCSEL-laser, experimental study

Control of robotic equipment, aircrafts and complex manipulators requires precision, reliable and compact input devices. Ministick – a two-axis mini joystick – is an efficient input device. Ministick is manipulated with fingers unlike traditional joysticks controlled by the entire hand. Finger manipulations are 5–7 times faster than hand movements and allows for much quicker generation of control actions. Small size of ministicks allows for placing them on a control panel or handle in a compact manner.

Most of the existing ministicks are based on resistive sensor elements. The disadvantages of this approach include short life and gradual deterioration of operation characteristics due to resistive layer rubbing.

In cooperation with the specialists from Rybinsk State Aviation Technical University named after P.A. Soloviev NPP Tenzosensor LLC developed an optical ministick, which is shown in Fig. 1. In previously developed ministick optical circuits described in [1–3], as light emitters LED chips are used, which have wide scattering angle. In the studied ministick design vertical-cavity surface-emitting laser (VCSEL) was used as a light emitter.

Fig. 2 shows a schematic diagram of the optical ministick, which consists of the housing 2 placed on the board 1 and poroelastic element 4 made integral with the control arm 3. Light emitter (VCSEL) 6 and at least one light receiver (photodiode, photoresistor) 7 connected to the microprocessor are installed on the board 1 under the poroelastic element 4. The poroelastic element 4, an elastic polymeric material piece, includes a light-reflecting or light-absorbing surface 5 located above



Fig. 1. Optical ministick

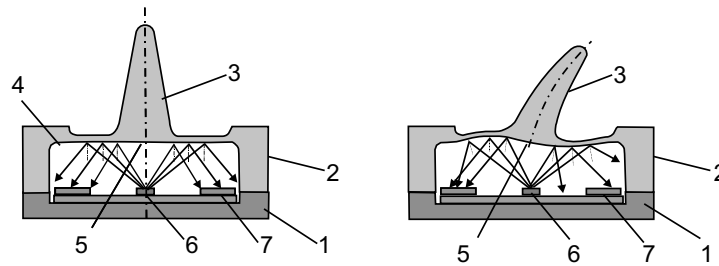


Fig. 2. Design of optical ministick: 1 – printed circuit board; 2 – housing; 3 – control arm; 4 – poroelastic element, 5 – light-reflecting surface, 6 – light source (VCSEL); 7 – photoelectric converter (photodiode, photoresistor)

the light source 6 and photoelectric converters 7. The poroelastic element is made of elastic material in the form of a plate with control arm 3 resting on the elements of optical ministick housing 2 attached to the board 1.

The operating principle of the optical ministick is based on the effect of light reflection by the light-reflecting surface of the polymeric poroelastic element deformed by an arm depending on the direction and pressing force.

As compared to conventional ministicks, optical ministick has many advantages: simple design, manufacturability for mass production, high reliability due to the absence of mechanical contact and deformable resistive elements, noiseless operation, fire and explosion safety, injury free operation, light weight and versatility (functions can be reprogrammed [3]).

The goal of the experimental study of ministick transfer function is to determine the correlation be-

tween the ministick useful signal and the amount of control arm deflection.

The ministick useful signal is a combination of two numeric values corresponding to the amount of ministick arm deflection along *X* and *Y* coordinate axes. Units of measurement of the output signal are the ADC readings of the ministick microcontroller which correspond to the ratio of ministick photoelectric converters voltages to the ADC reference voltage. The photoelectric converters voltages are determined by the intensity of the reflected light impinging on them, which depends on the amount of the ministick control arm deflection.

The experiment method is to record the ministick readings along *X* and *Y* axes at the points with given amount of ministick arm deflection from the central position and direction of such deflection, which is determined by turning angle of the ministick body.

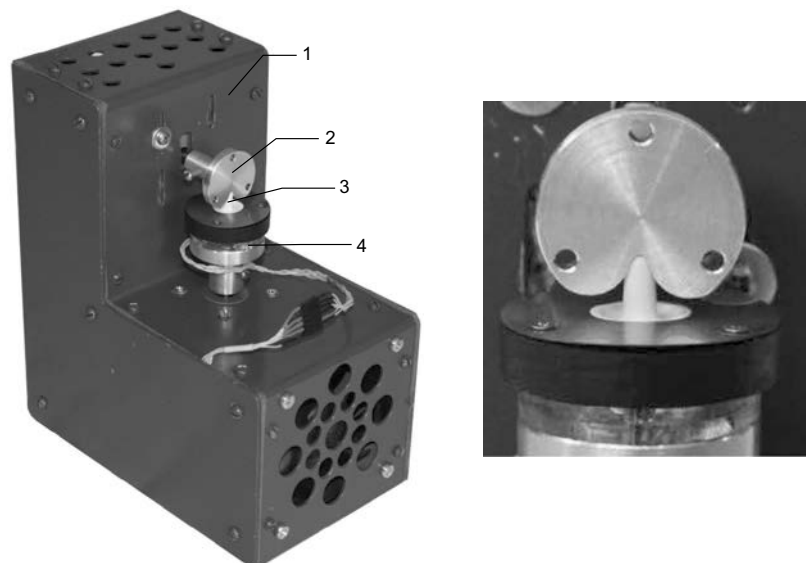


Fig. 3. Test bench: 1 – bench body, 2 – deflecting element, 3 – ministick, 4 – turning base

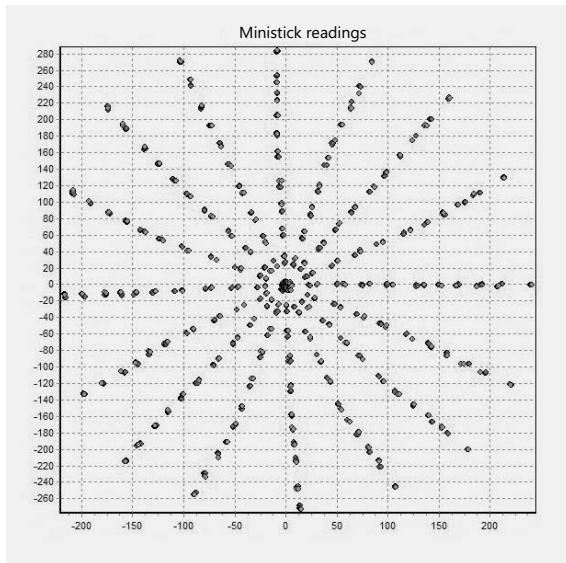


Fig. 4. Ministick transfer function along X axis (with ministick turning angle 0°)

In order to study the correlation between the ministick signals and the amount of ministick arm linear deflection and ministick turning angle (transfer function), a test bench for computer-aided studying the ministick characteristics was developed. The bench (Fig. 3) includes a turning base 4 with fixed ministick 3 and the deflecting element 2 which deflects the ministick arm from the central position strictly to the left or to the right. Base turning and arm deflecting are driven by stepper motors. To ensure accurate positioning and initial position setting the motor shafts are equipped with absolute digital encoders (angle transducers) with turning angle error not exceeding 0.35° . Ministick readings were measured under the following conditions:

- Limits of ministick arm deflection from the center: $-5..+5$ mm, with pitch 0.5 mm;
- Deflecting directions: to the left (from $+5$ mm to -5 mm) to the right (-5 mm to $+5$ mm);
- Ministick turning angle: from 0° to 157.5° with pitch 22.5° ;
- Number of reading measurements: 5, followed by averaging the values obtained.

On completion of the tests, the bench-testing program automatically draws a beam diagram. The beam diagram shows the results of the ministick useful signal measurements in the form of points with X and Y coordinates corresponding to the values of the ministick output signal. The obtained results of measurement for right deflection of the arm are shown by red dots, and left deflection –

by green dots. The beam diagram provides visualization of the ministick output signal quality for further evaluation of the following characteristics: amplitude, accuracy, linearity and hysteresis

The beam diagrams of the studied ministick are shown in Fig. 4.

The results of studying transfer function of the ministick along X axis (turning angle 0°) and Y axis (turning angle 90°) are shown in Fig. 5.

The quality of the real ministick useful signal is evaluated through the following parameters:

- Amplitude – the range of values of ministick transfer function when the control arm is deflected within the limits set ($-5..+5$ mm);
- Resolution – number of values of the ministick output signal per unit deflection of the ministick control arm;
- Accuracy – spread of values for a given value of arm deflection;
- Nonlinearity – deviation of transfer function curve of the studied ministick from the straight line;
- Hysteresis – difference between the values of the output signal, when the arm deflection values are the same, but directions are different.

Amplitude of the ministick output signal was calculated using equation:

$$\Delta X = X_{max} - X_{min},$$

where ΔX – range of values (amplitude) of transfer function along this coordinate axis, X_{max} – maximum value of transfer function along this coordinate axis, X_{min} – minimum value of transfer function along this coordinate axis.

Resolution of ministick output signal was calculated using equation:

$$R = \frac{\Delta X}{\Delta L},$$

where ΔL – range of values of the control arm deflection in mm, ΔX – range of values (amplitude) of transfer function along this coordinate axis.

To estimate the readings accuracy we use a root-mean-square deviation of the measured readings at a given value of arm deflection. The percentage value δ was calculated as follows

$$\delta = |RMSD / \Delta X|, \quad (1)$$

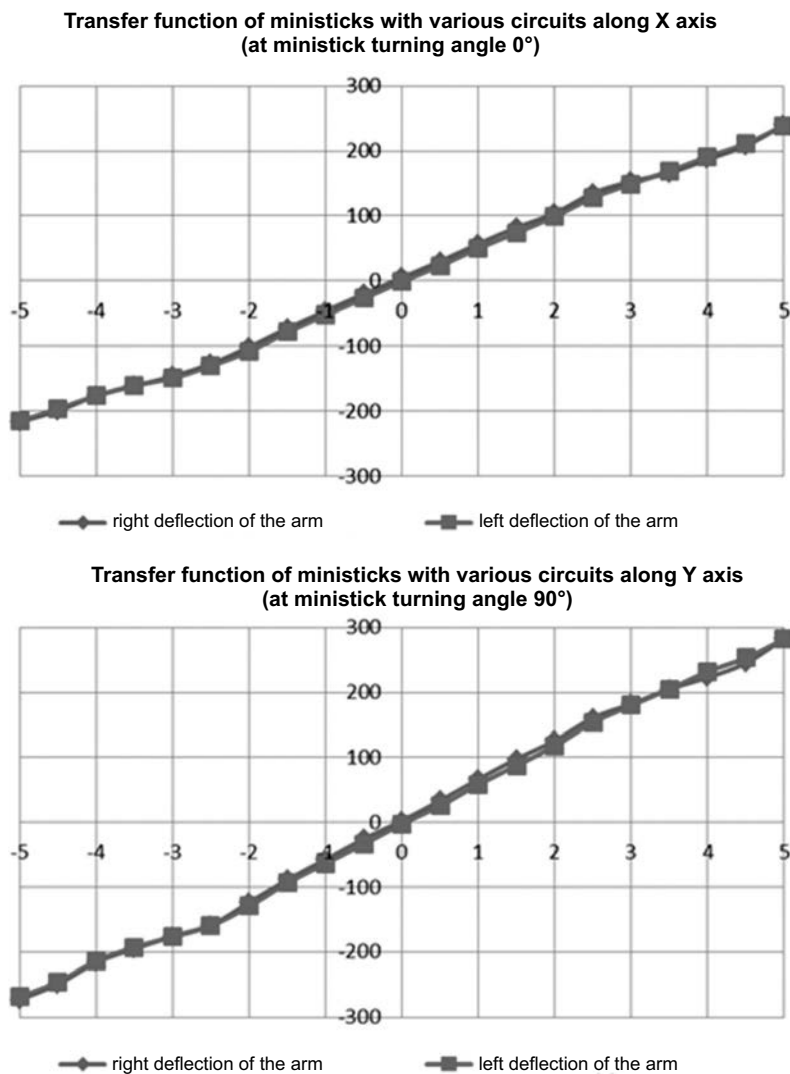


Fig. 5. Graphs of transfer function of the ministick along X and Y axis

where δ – percentage deviation of the ministick readings along this coordinate axis, RMSD – root-mean-square deviation of ministick readings along this coordinate axis, ΔX – range of values (amplitude) of transfer function along this coordinate axis.

For evaluation of nonlinearity using least square method we draw linear approximating function $X=kx+b$. Then, nonlinearity N_L was calculated using equation

$$N_L = |X - X_{calc}| / \Delta X, \tag{2}$$

where X – actual value of ministick readings along this coordinate axis at a given point;

X_{calc} – the value calculated using the approximating function;

ΔX – range of values (amplitude) of transfer function along this coordinate axis.

Hysteresis G of the readings is estimated as follows:

$$G = |X_{right} - X_{left}| / \Delta X, \tag{3}$$

where X_{right} – value of ministick readings along this coordinate axis at a given point, when control arm is deflected to the right;

X_{left} – the same for control arm deflection to the left;

ΔX – range of values (amplitude) of transfer function along this coordinate axis.

The results of calculating the signal quality parameters of the studied ministick are shown in Table 1.

Based on the results obtained, a 3D-surface diagram was drawn (Fig. 6) showing ministick readings along coordinate axes X and Y as a function of an-

Table 1. Signal quality parameters of the studied minystick

Parameter	Value
Range of values along X axis (amplitude)	454
Range of values along Y axis (amplitude)	550
Resolution along X axis, values per mm	45.4
Resolution along Y axis, values per mm	55
Max. spread of values	<0.5 %
Max. nonlinearity along X axis	3.43 %
Max. nonlinearity along Y axis	3.41 %
Max. hysteresis along X axis	1.05 %
Max. hysteresis along Y axis	1.3 %

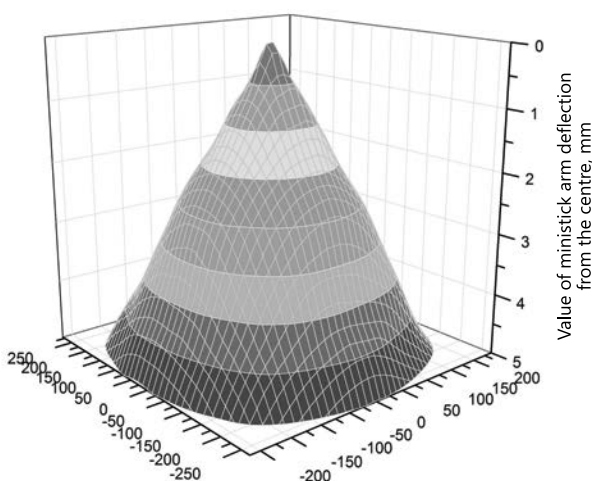


Fig. 6. 3D-surface diagram of correlation between minystick readings and value of minystick arm deflection

gle and amount of deflection of the minystick control arm.

CONCLUSIONS:

1. The optical circuit of the minystick based on poroelastic element and VCSEL allows developing workable and highly efficient devices.
2. The maximum range of the minystick arm deflection is ± 5.0 mm, which is within the optimal range of finger movements, which amplitude of deflection is about 12–20 mm.
3. The studied minystick features sufficiently high amplitude of output signal – up to 550 values along one axis (for example, for EasyPoint Joystick Position Sensor based on Hall-effect the amplitude of output signal equals to 256 values).

4. Maximum resolution along X axis is equal to 55 values per mm, and along Y axis – 45.4 values per mm. It means that sensitivity of the minystick is 0.02 mm along X axis and 0.025 mm along Y axis.

5. Transfer function of the studied optical minystick is linear and symmetrical throughout the entire range of control arm deflection values which is from –5.. to +5 mm. Nonlinearity does not exceed 3.5 % for each axis.

6. Minystick blind zone does not exceed 0.5 mm along all coordinate axis.

7. Maximum value of hysteresis is 1.3 % of the range of transfer function values.

Thus, the transfer function of the optical minystick complies with the basic requirements on complex robotics, manipulators and aircraft controls. Application of hybrid matrices of VCSEL and pin-photodiodes allows developing high-quality digital ministicks.

REFERENCE:

1. Golubin S.A., Komarov V.M., Lomanov A.N., Nikitin V.S., Semenov E.I. Experimental study of characteristics of common emitter optical ministicks // RSATU Bulletin 2015. No. 1
2. Golubin S.A., Komarov V.M., Lomanov A.N., Nikitin V.S., Semenov E.I. Study of characteristics of optical ministicks // Svetotekhnika (Russian), 2015, No. 6, pp.17–20.
3. Golubin S.A., Nikitin V.S., Belov R.B. Digital optical ministicks for control of robotic technology systems // Telecommunications 2015. No. 11.

4. Nikitin V.S., Belov R.B. Controlling without control arms // Science and Life, 2012. No. 12.

5. Optical joystick: application for an invention 2013112435 Russian Federation. No. 2013112435/08; submitted: 19.03.2013; Published: 27.09.2014.

6. Electrical circuits switching method and polymorphic switch used for that: patent 2455678 Russian Federation. No. 2011101226/08; submitted: 13.01.2011; Published: 10.07.2012.

ACKNOWLEDGMENT

Applied scientific researches and experimental developments are carried out with governmental financial support represented by the Russian Ministry of Education and Science. A unique identifier of applied researches and experimental developments is RFMEFI57914X0087.



Sergey A. Golubin, post-graduate of Federal State-Financed Educational Institution of Higher Professional Education «P. A. Solovyov Rybinsk State Aviation Technical University» (RSATU). He is graduated

from RSATU in 2013. At present, he is a systems engineer in Tenzosensor LLC



Aleksey N. Lomanov, Ph.D. and associate professor in Federal State-Financed Educational Institution of Higher Professional Education (RSATU). He is graduated from Rybinsk State Aviation Technological

Academy (now RSATU) in 2003. He has much experience in electrical engineering, microcontroller systems, industrial control and thin-film technologies, works in RSATU since 2003. At present, he is the dean of Faculty of radioelectronics and computer science



Vladimir S. Nikitin, Ph.D. and CEO&founder of Tenzosensor LLC. Inventor and idea man, leading expert in the field of R&D organization and performance, strategy development, organization of project

team work. Miscellaneous expert in the field of Physics, Chemistry, Electronics, Material Sciences, highly qualified designer and

programmer, possesses a great experience of working at executive positions. He has 24 patents, 5 certificates for PC software products, 100+ published works in scientific and popular editions; author of the book Technologies of the Future (Tekhnosfera publishing house, 2010)



Valery M. Komarov, Ph.D. and full professor of Federal State-Financed Educational Institution of Higher Professional Education «P. A. Solovyov Rybinsk State Aviation Technical University»

(RSATU). Graduated from Rybinsk Aviation Technological Institute (now RSATU) in 1972, got an academic degree in 1980. He has more than 40 years' experience in designing microprocessor systems and technological control systems. Works in RSATU from 1977. He has 49 author's certificates, 60+ published works



Ernst I. Semyonov, Ph.D., Prof., graduated from Rybinsk Evening Aviation Technological Institute (RSATU) with a degree in Radio Engineering.

Area of expertise: light film manufacturing process control, automatics, radio electronics, microelectronics, computer engineering

CONTENTS

VOLUME 24

NUMBER 1

2016

LIGHT & ENGINEERING

(SVETOTEKHNİKA)

Chao-Ming FU (傅昭銘)

An Interview with professor Chao-Ming Fu at LED Forum 2015

Peter Bodrogi, Tran Quoc Khanh, D. Stojanovic, and Yandan Lin

Intercultural Colour Temperature Preference of Chinese and European Subjects Living in Germany

Can Cengiz, Mikko Maksimainen, Marjukka Puolakka, and Liisa Halonen

The Effects of High Luminance Objects on Peripheral Target Detection in Mesopic Conditions

Natalya V. Bystryantseva, Yelena I. Lekus, and Nikolai V. Matveev

The Domestic School of Light Design: Strategy and Tactics

Yuliya Revsina and Dmitry Shvidkovsky

Illumination of Classical Architecture Memorials in Search of Authenticity

Sergei A. Aleksandrov

Sports Illumination of Ski Tracks in the Territory of the Rosa Khutor Freestyle Centre

Amrita Bhattacharjee and Saswati Mazumdar

A Study of the Suitability of LED Light Sources over Conventional Light Sources in a Museum Environment

Sebastian Słomiński

Selected Problems in Modern Methods of Luminance Measurement of Multisource LED Luminaires

Georgy V. Boos and Andrei A. Grigoryev

New Approach in the Determination of Qualitative Characteristics of Outdoor Illumination Installations

Ko Jae-jun and Kim Chung-hyeok

Ensuring the Safety of Ballast Compatible LED, as an Alternative Type of Fluorescent Lamp, in Korea

Tagir A. Akhmyarov, Alexander V. Spiridonov, and Igor L. Shubin

New Solutions for Translucent Structures

Filiz Açari Erbil and Leyla Dokuzer Öztürk

An Experimental Investigation of Mirror Lighting

CONTENTS

VOLUME 24**NUMBER 2****2016**

LIGHT & ENGINEERING

(SVETOTEKHNIKA)

A.T. Ovcharov and Yu.N. Selyanin

Solatube® Technology: Prospects in Architecture and Construction of Russia

Rajesh Sarkar and Saswati Mazumdar

Studies and Experiments for Determination of Degradation of Paintings of Museum Art Galleries Caused by Artificial Light Sources

N. V. Matveev, V. T. Prokopenko, N. P. Sapunova, and D. A. Friedman

Research of Influence of Light Organ Performances on a Psychophysiology of the Person

Hongyi Cai and Linjie Li

How LED Lighting May Affect Office Ergonomics: The Impact of Providing Access to Continuous Dimming Controls on Typing and Colour-Matching Tasks Performance

O. V. Kryukov and A.V. Serebryakov

Modern Systems of External Illumination of Compressor Stations

Aniruddha Mukherjee and Amit Soni

Effect of Rise in Ambient Temperature on the Life of Light Emitting Diodes

Biswadeep Gupta, Aparajita Dutta Bakshi, and Biswanath Roy

Development and Validation of Dynamic Conductance Based Wattage Independent Model for Magnetic Ballast Driven Non-Retrofit CFLs

V.A. Levchenko, O. A. Popov, S. A. Svitnev, and P. V. Starshinov

Electric and Emission Characteristics of a Transformer Type Lamp with a 16.6 mm Diameter Discharge Tube

S.P. Arapova, S.Yu. Arapov, and A.G. Tyagunov

Polygraph Hybrid Laboratory Light Source, Spectrally Near Standard CIE Sources Type “D”

Irfanud Din and Hoon Kim

Energy-Efficient Optical Power Control for Data Rate and Illuminance Provision in Visible Light Communication

K. Sindhubala and B. Vijayalakshmi

Survey on Noise Sources and Restrain Techniques in Visible-Light Communication

K. Sindhubala and B.Vijayalakshmi

Experimental Indoor Visible-Light Communication System Using Solar Panel Receiver in the Presence of Ambient Light Noise

N. N. Dergunova, I.N. Koshin, and T.A. Rozhkova

«Technology» of Recovery from the Crisis or «NIIS by A. N. Lodygin» New Startup

CONTENTS

VOLUME 24**NUMBER 3****2016**

LIGHT & ENGINEERING
(SVETOTEKHNKA)

Vol. 24, No.3, 2016 is devoting to the selected high quality papers from the partnership of Light&Engineering Journal from CHINA, which are focused in the scope of the journal.

Lan WANG

Exploration of Literary and Artistic Cultural Values of Large-Scale Landscape Lighting Engineering

Qiang MAI

Analysis of the Design and Reliability of a New Type of Intelligent LED Illumination Control System

Xiaoqiang ZHANG and Weiping ZHANG

A Novel High Efficiency LED Driver with a High Power Factor and Low Output Ripple

Hao YANG, Jianan ZHAO, Wenhao ZHU, Yingtong DOU, and Jianguo YU

Progress of Wireless Network Signal Transmission Technology Based on LED Visible Light Communication Technology

Dan LIU, Renqiang XIE, Xiaozhen JIANG, and Jie ZHU

Application of LED-Based Visible Light Communication in Logistics Transportation

Yancheng JI, Junma LI, Guoan ZHANG, and Zhanghua CAO

Extraction of Characteristic of Frequency Response Curves in LED Visible Light Communication Systems

Wei LIAO and Yan XU

Design of a Novel UAV Based on Short-Distance LED Visible Light Communication Technology

Yu JING and Yaan LI

Design of LED Visible Light Real-Time Video Transmission System Based on FPGA

Feng JIANG and Yunqing LIU

Study of an Atmosphere Detection Model Based on LED Visible Light Array Information Transmission Technology

Hongmei ZHU and Yan PIAO

Study on the Information Acquisition from Stereo Images Based on a Novel CSS3D Lighting System

Donghai JIANG, Chang LIU, and Wenqiang MA

Monitoring the Creep Rupture of Fractured Coal-Rock Mass with Crack Expansion Based on the LED Visible Light Sight Distance Measurement

Yingmei YIN, Ronghui ZHANG, and Huiqing LV

Flatness Detection of Asphalt Pavement Maintenance Based on LED Visible Light Sight Distance Measurement

Dong LIANG, Zhaojing ZHANG, Huahua XIE, and Hao JIN

Application Study on Data Mining Technology in the Image Transmission Based on LED Visible Light

Hongping PU and Kaiyu QIN

Application of LED Visible Light Communication Technology in the Airborne
Passive Location for Emergency Communication

Zhenyang FENG, Dongyan LIU, Zhengwei ZHU, and Haifeng DING

Rock Slope Monitoring Techniques Based on Semiconductor Light Source Application

Jialing LI, Min HUANG, Penghao LIANG, and Lige ZHENG

Application of a New LED Light Irradiation Technology in the Resin Repair of Dental Fluorosis

Bin REN and Chunyi CHEN

Numerical Simulation of Light Pulse Transmission in Atmospheric Turbulence

Xiaohua JIN

Application of LED-Based Array Signal Transmission Technology in the Information
Transmission of Biological Tissue

Li WANG, Hongjian HUANG, Peitao TAN, and Xiaowei ZHANG

Design of Periodical Light Compensation Equipment for Lettuce in Greenhouse Combining LED Lights

Yanping LIU

The Development Status and Countermeasures of Photovoltaic-Ecological Agriculture in China

Ya BI and Cunfa WANG

Analysis of the Access System of Photovoltaic Power Station Based on Photovoltaic
Power/Agricultural Planting Hybrid

Zhiming XU, Tieliu JIANG, and Yong LI

Optimal Design of Solar Photovoltaic Power Generation System

Jun SHI

The Development of the Photovoltaic Industry of Sichuan Province, China: Human
Capital Investment and Knowledge Innovation

Liang LIN and Xintong WU

Technological Innovation and Policy Systems for the Photovoltaic Industry
of Sichuan Province, China

Yan LI, Taozhen HUANG, Qiaoliang ZHANG, and Minghao BAI

Analysis of the Environmental Regulation Regarding the Pollution Caused by Photovoltaic Industry

Xiaoqiang ZHANG and Weiping ZHANG

Review of Equivalent Circuit Model for Photovoltaic and Li-ion Cells

Xiang DENG

Measurement and Analysis of the Innovation Efficiency of China's Photovoltaic Industry

Wei WU

The Role of the Government in the Development of the LED Industry

Yunzhe CHEN

Financial System Innovation of Large-Scale LED Enterprises in China within the Internet Economy

Dejie SUN, Wenyuan LIU, and Jie ZHANG

Dynamic Pricing of LED Components Based on Strategic Consumer Behavior within a under Competitive Environment

Shizhang PANG, Xiaofeng JU, and Hualong YANG

Analysis of the Micro-Blog Marketing Method by the Industrial and Commercial Banks of China for Large-Scale LED Enterprises

Xilong DENG

The Incentive Effect of Modes of Government Subsidies on Technological Innovation of LED Lighting Enterprises in China

Jian JIN and Jianxiang WANG

Analysis of the Current Situation and Development Trends of the LED Lighting Industry in China

Bingyun ZHENG and Sui LI

Competitive Strategy Choice of LED Optical Fiber Communication Enterprises in China: Pure or Hybrid Strategy

Mina GE and Jun FAN

Current Market Development Status and Marketing Strategy of Chinese LED Optical Fibre Illumination Enterprises

Yongbo YU, Yunchao DU, and Yuan GAO

Evaluation of the Operational Efficiency of Listed LED Lighting Industry of China Based on DEA Model

Chuantao WANG, Xiaofei CAI, and Hua QIN

Decision Game Model of Supply Chain Considering Non-Deceptive LED Lighting Counterfeits

Qiaoxia SUN

Psychological Training Programmes for Young Employees in China's New Energy Industries: a Photovoltaic Industry Case Study

Zhang LI

Operation Optimization of Photovoltaic Enterprises and Micro-Grid Agents with the Objective of Profit Maximization

Yan MAO and Yongjian LI

Study on the Behavior Oriented Incentive Mechanism of Large Lighting Fixture Manufacturers Based on the Game Theory of Incomplete Information

PARTNERS OF LIGHT & ENGINEERING JOURNAL

Editorial Board with big gratitude would like to inform international lighting community about the Journal Partners Institute establishment. The list with our partners and their Logo see below. The description of partner's collaboration you can found at journal site www.sveto-tehnika.ru

GENERAL PARTNER



BL GROUP holding



PLATINUM PARTNERS



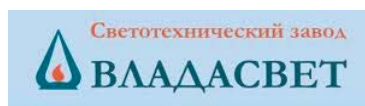
ГЛОБАЛ
ЛАЙТИНГ

GOLD PARTNERS

FAGERHULT



SILVER PARTNERS



BRONZE PARTNERS

